UNIVERSITY OF CALIFORNIA, SAN DIEGO

The Role of cGMP-dependent Protein Kinases in Bone Cell Growth and Survival

A dissertation submitted in partial satisfaction of the requirements for the degree Doctor

of Philosophy

in

Biomedical Sciences

by

Nisha Madhav Marathe

Committee in Charge:

Professor Renate Pilz, Chair
Professor Gerry Boss, Co-chair
Professor Laurence Brunton
Professor Mark Ginsberg
Professor Pamela Mellon

2011

The Dissertation of Nisha Madhav Marathe is approved and it is acceptable in quality and

form for publication on microfilm and electronically:

_____

_____

_____

_____
Co-chair

_____
Chair

University of California, San Diego

2011

DEDICATION

To my parents and my sister.

For all your love and support.

I couldn't have done this without you.

and

To my grandparents.

TABLE OF CONTENTS

LIST OF FIGURES

LIST OF TABLES

Chapter 3:

Chapter 4:

ACKNOWLEDGEMENTS

I would like to first thank my advisor, Dr. Renate Pilz, for the giving me the opportunity to do my graduate research in her lab. She has helped me through all the bumps in the road and her passion for science has been a great motivator. I can't express how much her support has meant to me. In her lab, I was able to grow both as a scientist and as a person, and I can't thank her enough for that. I also thank Dr. Gerry Boss for all his support, insights, and opportunities.

The camaraderie of all the current and former members of the Boss Pilz lab has made my graduate experience enjoyable. I appreciate the time I have spent with them; their knowledge and experience has helped guide me along the way. My time would have definitely been less enjoyable without them. I would especially like to thank Darren Casteel, Hema Rangaswami, Raphaela Schwappacher, and Tong Zhang for their invaluable support, guidance, and friendship. I would also like to take the opportunity to thank my friends and family who have been with me through every step of this journey. They have helped shape who I am and, without them, I would not have reached so far.

I also appreciate the time and guidance of my thesis committee; Drs Larry Brunton, Mark Ginsburg, and Pamela Mellon.

Chapter 2 is currently being prepared for submission for publication of the material. Marathe N, Rangaswami H, Zhuang S, Boss GR, Pilz RB. The NO/cGMP pathway mediates the osteocyte-protective effects of estrogen via differential actions of cGMP-dependent protein kinases I and II. The dissertation author was the primary investigator and author of this material.

Chapter 4, in part, is material which appears in Rangaswami H, Marathe N, Zhuang S, Chen Y, Yeh JC, Frangos JA, Boss GR, Pilz RB. Type II cGMP-dependent protein kinase mediates osteoblast mechanotransduction *J Biol Chem* 2009, 284:14796-14808. The dissertation author was the second author and investigator of this material. The remaining part of Chapter 4 is material which appears in Rangaswami H, Schwappacher R, Marathe N, Zhuang S, Casteel DE, Haas B, Chen Y, Pfeifer A, Kato H, Shattil S, Boss GR, Pilz RB. Cyclic GMP and protein kinase G control a Src-containing mechanosome in osteoblasts. *Sci Signal* 2010, 3:ra91. The dissertation author was the third investigator and author of this material.

This work was supported, in part, by the Hypertension Training Grant T32-HL007261.

VITA

2005   Bachelor of Science, Microbiology,
Immunology, and Molecular Genetics
University of California, Los Angeles
Los Angeles, California

2006   Teaching Assistant, Department of Biology
University of California, San Diego
La Jolla, California

2008-2011   Institutional Kirschstein-NRSA Research
Training Grant
University of California, San Diego
La Jolla, California

2011   Doctor of Philosophy, Biomedical Sciences
University of California, San Diego
La Jolla, California

PUBLICATIONS

Rangaswami H, Marathe N, Zhuang S, Chen Y, Yeh JC, Frangos JA, Boss GR, Pilz RB: **Type II cGMP-dependent protein kinase mediates osteoblast mechanotransduction.** *J Biol Chem* 2009.

Rangaswami H, Schwappacher R, Marathe N, Zhuang S, Casteel DE, Haas B, Chen Y, Pfeifer A, Kato H, Shattil S, Boss GR, Pilz RB: **Cyclic GMP/Protein Kinase G Control a Src-containing Mechanosome in Osteoblasts.** *Sci Signal.* 2010.

ABSTRACT OF THE DISSERTATION

The Role of cGMP-dependent Protein Kinases in Bone Cell Growth and Survival

by

Nisha Madhav Marathe

Doctor of Philosophy in Biomedical Sciences

University of California, San Diego, 2011

Professor Renate Pilz, Chair

Professor Gerry Boss, Co-Chair

Skeletal integrity is preserved by continuous bone remodeling by osteoblasts and osteoclasts. While the careful regulation between bone formation and resorption is known to be a hallmark of bone maintenance, the signaling mechanisms which drive each of these processes are incompletely understood. Estrogens and fluid shear stress are known to exert positive effects on osteoblast proliferation and osteocyte survival. Both

stimuli have been shown to rapidly increase nitric oxide (NO) production in a number of cell types, suggesting an activation of the NO/cGMP/PKG pathway. NO is involved in regulating cell survival and proliferation in different cell types.

In the first part of the dissertation, we show that estrogen-mediated osteocytes survival is regulated through the NO/cGMP pathway. Trypan blue, TUNEL, and cleaved caspase 3 staining show the inability of estrogen to protect osteocytes from etoposide-induced apoptosis in the presence of pharmacological inhibitors of NOS, soluble guanylate cyclase, and PKG, or siRNA targeting PKG. The pro-survival effects of estrogen were mimicked by a membrane-permeable analog of cGMP. We show that PKGs function in a dual mechanism to prevent apoptosis; PKGII activates Akt and ERK, and PKGIα directly phosphorylates the Bcl-2 family member, BAD. cGMP is also involved in regulating mRNA expression of pro-apoptotic genes.

The second part of this dissertation focuses on the role of PKGII in mechanotransduction. We first analyzed the effects of the NO/cGMP pathway on downstream *fos* family gene expression. We determined that *fos* genes were induced upon fluid shear stress through a NO/cGMP/PKGII mechanism activating MEK and ERK. We found that PKGII is recruited to a complex containing SHP-1, SHP-2, Src, and $\alpha_v\beta_3$ integrins in response to fluid shear stress. SHP-1 is directly phosphorylated by PKGII, and in turn, dephosphorylates and activates Src, allowing for downstream ERK signaling.

In conclusion, we reveal a integral role for NO/cGMP/PKG signaling in the maintenance of bone integrity.

Chapter 1:

Introduction

Bone Structure

Bones are comprised of a hard outer shell, known as cortical bone, with a porous interior, which is referred to as trabecular bone. Together, both parts of the bone provide a structure and protection for the body as well as a number of metabolic and storehouse functions [1]. Bones contain three main types of cells: osteoblasts, osteocytes, and osteoclasts. Osteoblasts are immature bone cells but are responsible for creating all bone tissue. They produce the osteoid— the unmineralized, organic component of the bone matrix composed mainly of type I collegen, osteocalcin, and chondroitin sulfate— which eventually mineralizes to form the bone matrix. Osteocytes are mature bone cells; they are differentiated from osteoblasts which have become trapped in the bone matrix. Osteocytes no longer produce the bone matrix but are involved in bone homeostasis. Osteoclasts are large multinucleated cells derived from monocytes and are responsible for bone resorption [2, 3].

Bone is a dynamic organ; it is constantly being formed and resorped. Bone remodeling is required to maintain the bone integrity by repairing microcracks in the bone caused weight strain and impact from movement [2]. A number of factors are known to induce bone formation resulting from osteoblast proliferation. Osteoblasts proliferate and differentiate in response to mechanical fluid shear stress [4-7], growth factors such as bone morphogenic proteins (BMPs) [8-12] and Wnts [13-16], and hormones such as estrogens [17-21] and androgens [22-25]. Bone formation is a tightly controlled process with paracrine signaling between osteoblasts and osteoclasts. For instance, osteoblasts produce Fas ligand (FasL) in response to estrogens. FasL can then bind to the Fas receptor on osteoclasts, resulting in osteoclast apoptosis [26]. Conversely,

osteoclasts release chemokines and growth factors which attract pre-osteoblasts to a newly resorped site and promote differentiation [2, 27]. Thus, both osteoblasts and osteoclasts help regulate each other to keep the process of bone formation in check.

Osteoporosis: an overview

Osteoporosis is a chronic disorder diagnosed by low bone mineral density. The disease results in increased bone fractures, most frequently in the vertebral column, hip or wrist [28]. Lifestyle choices and age, as well as genetics, impact osteoporosis risk. Poor diet, lack of exercise, taking steroid medications, family history, and low circulating estrogen or testosterone levels are all important contributors [1, 28]. As life expectancy continues to increase, the prevalence of osteoporosis is also increasing. The National Osteoporosis Foundation estimates that about 10 million individuals in the United States are currently diagnosed with osteoporosis and as many as 34 million more are at high risk for developing osteoporosis. Women have a higher risk than men of becoming osteoporotic; prevalence in postmenopausal women is four times higher than in men, with one in five women over 50 having osteoporosis [28].

Osteoporosis is caused by an imbalance between osteoblast proliferation and osteoclast resorbtion. As noted above, bone turnover is occurring constantly. However, when bone resorption outpaces bone formation, osteoporosis occurs. This can be caused by increased bone resorption, decreased bone formation, or an inadequate peak bone mass [1]. Studies have long shown that estrogens are able to help alleviate osteoporosis [29, 30]; indeed, low estrogen levels after menopause are a major cause of osteoporosis. However, the mechanism(s) by which estrogens protect against osteoporosis are largely

unknown. A more complete understanding of the estrogen-mediated prevention of osteoporosis is imperative to the development of better therapies against the disease.

Estrogens and Estrogen Receptors

Estrogens are steroid hormones which modulate reproductive development and sexual maintenance; they are also involved in neuronal development [31], neuronal protection [32, 33], hepatoprotection [34, 35], cadiovascular protection [36], osteoblast proliferation and differentiation [37], and prevention of osteoblast and osteocyte apoptosis [38]. Being hydrophobic, estrogens are able to diffuse through the plasma membrane and bind to cytosolic estrogen receptors. The receptor-ligand complex can then translocate to the nucleus and regulate gene expression, either by directly binding DNA or through interactions with transactivators or transrepressors [39]. Additionally, estrogens can also modulate extragenomic signaling cascades through interaction with membrane-bound estrogen receptors [39].

Three forms of estrogen are present in humans: estrone (E_1), estradiol (E_2, 17β-estradiol) and estriol (E_3). Of the three, the effects of estradiol are the best studied and the most relevant to osteoblastic studies. Estradiol is more prevalent and a more potent hormone than either estrone or estriol. Estradiol is produced by the adrenal cortex, adipocytes and the brain in addition to the ovaries and testes. Estrone is the least abundant, present primarily during pregnancy and in post- menopausal women and is synthesized by the ovaries [40]. Synthesized by the placenta, estriol is only produced during pregnancy [41].

Estradiol has three known receptors in ostecytes: estrogen receptor α (ERα), estrogen receptor β (ERβ) and G protein-coupled receptor 30 (GPR30). In contrast to the well-defined roles of ERα and ERβ in estradiol signaling, the contribution of GPR30 remains controversial. GPR30 binds estradiol with nanomolar affinity and can trigger rapid signaling [42] with increased adenyl cyclase activity [43]. Additionally, GPR30 knockout mice exhibit shortened femurs caused by reduced growth plate height [44] and show metabolic problems [45]. However, overexpression or knockout studies *in vivo* and in intact cells reveal inconclusive, and of contradictory, results [46, 47].

ERα and ERβ are encoded by two different genes on chromosomes six and fourteen, respectively. The structure of both receptors is similar to other nuclear receptors with two transcriptional activation domains, a DNA-binding domain and a ligand-binding domain. Three splice variants exist for ERα and five isoforms for ERβ [48]. Original gene knockouts for ERα generated by Lubahn *et al* [49] in 1993 and for ERβ generated by Dupont *et al* [50] showed reduced fertility but otherwise normal sexual development. However, the ERα knockout was created by targeting exon 2, allowing the presence of the other two splice variants of ERα to contribute to the maintenance of estrogen responses. A total ERα knockout mouse was subsequently generated by deleting exon 3, which encodes the first zinc finger of the DNA binding domain [50]. The total ERα knockout mice show overall decreased bone density [51] and both ERα knockout mice are unable to respond to mechanical stimulation, as measured by strain-induced proliferation, NO production and transcriptional response [52-54]. ERβ knockout mice show increased bone density [55]. The response of these mice to mechanical strain is

controversial with some groups reporting decreased ERK activation [52] while others report increased bone formation [56]. The double knockout mouse is sterile with normal sexual development [50] and decreased bone mineral density [57]. In the following, we will refer to ERα as ER.

The estrogen receptor must be properly posttranslationally modified to ensure successful downstream signaling. Palmitoylation occurs within the ligand binding domain at cysteine 447 on ERα [58] and at cysteine 399 on ERβ [59]. This modification is required for ER localization to specific plasma membrane domains, called caveolae, and interaction with caveolin-1 [60, 61]. In addition, phosphorylation at six sites on the ERα receptor have been reported [62]. The phosphorylation of the five serine residues have varying effects on ER-dependent transcriptional regulation [62] but phosphorylation at tyrosine 537 induces conformational changes which enhance estradiol binding and ER dimerization [63]. Src family kinases phosphorylate ERα tyrosine 537 *in vitro* [63]. It is speculated that phosphorylation at this site enhances binding to SH2 domains of other proteins. This could lead to interactions with Src or dimerization by interactions with the SH2 domain on a second ER molecule to modulate downstream signaling.

Extragenomic Estrogen Signaling

Membrane-bound ligand-free ERs are localized to caveolae —a subset of cholesterol-sphingolipid-enriched lipid rafts within the plasma membrane containing high levels of caveolin— which are centers of signal transduction. Previous reports have shown that ER interacts with a number of cellular proteins, including caveolin-1 [60], Src [64, 65], modulator of non-genomic activity of ER (MNAR) [66] and endothelial nitric

oxide synthase (eNOS) [67]. Physiological effects of these protein interactions are are increased cell proliferation and decreased apoptosis [68, 69].

Previous work has demonstrated that the extragenomic effects of estradiol mediated by membrane-bound estrogen receptors are, in part, dependent on increased NO synthesis [70-72]. Nitric oxide (NO) is a gaseous second messenger molecule generated from L-arginine by nitric oxide synthases (NOS). Among other effects, NO binds to and activates soluble guanylate cyclase (sGC), generating cGMP, an activator of a number of proteins including phosphodiesterases and cGMP-dependent protein kinases (PKGs) [73].

Furthermore, estradiol has been shown to activate extracellular signal-regulated kinases (ERKs) and Akt in a variety of cell types [74-84]. Estradiol also causes activation of protein kinase A [84] and protein kinase C [85] pathways as well as induce rapid intracellular calcium release [86], induce ion channel fluxes [87-89] and generate G-protein coupled receptor mediated second messengers such as cAMP [20, 89].

Caspase-dependent Apoptosis

Apoptosis is the process of programmed cell death and allows for natural cell turnover. It may also be triggered in response to a number of internal or external signals, such as starvation or drug treatments. Apoptosis is characterized by membrane blebbing, loss of attachment, nuclear fragmentation, chromatin condensation, chromosomal DNA fragmentation, cell shrinkage, and the formation of apoptotic bodies [3]. There are two forms of apoptosis: a caspase-dependent mechanism and a caspase-independent mechanism.

Caspases are a family of cysteine proteases with important roles in apoptosis. Upon stimulation by apoptotic factors, initiator caspases (caspases 2, 8, 9, 10) process effector procaspases (caspases 3, 6, 7) into their active form. Activated effector caspases then cleave downstream target proteins to complete cell death. Caspases are regulated posttranslationally to ensure a quick response to apoptotic stimuli.

As the cleavage activity of caspases can lead to dire consequences for a cell, caspase activation is a tightly regulated process. For intrinsic apoptotic signals, a family of apoptotic regulatory proteins, known as the Bcl-2 family, regulate caspase activation. The Bcl-2 family is categorized into three subfamilies: multi-domain anti-apoptotic proteins, multi-domain pro-apoptotic proteins, and BH3-only pro-apoptotic proteins. Together, the Bcl-2 family members are sensors of cell stress and control apoptosis based on the ratio of active pro-apoptotic proteins to active anti-apoptotic proteins. The current cell death model for the role of Bcl-2 family-mediated apoptosis suggests that the pro-apoptotic proteins, mainly the BH3-only proteins, bind and inactivate the anti-apoptotic, thereby preventing the anti-apoptotic members from exerting their survival actions and shifting the ratio toward more active apoptotic proteins [90, 91]. This allows for Bax and Bak, two pro-apoptotic proteins, to form a pore in the mitochondrial membrane and release cytochrome c from the intermembrane space into the cytoplasm. Cytochrome c then binds to and activates the adaptor protein, apoptotic protease activating factor (APAF) which, in turn, activates the initator caspase 9. Active caspase 9 can then cleave caspases 3 and 7, resulting in cell death [92].

The caspase-independent cell death (CICD) is a process that is not completely understood. It was discovered after scientists noticed that inhibition of caspases and

transgenic mice with knockouts of key apoptosis factors did not prevent apoptosis. It is suggested that mitochondrial outer membrane permeabilization (MOMP) is required but there are instances where CICD occurs without MOMP. This releases a number of factors, such as apoptosis-inducing factor (AIF), Endonuclease G, Smac/Diablo, and Htr2A/Omi. Some of these factors translocate to the nucleus and cause chromotin condensation and DNA fragmentation [93].

cGMP-dependent Protein Kinases

cGMP-dependent protein kinases (PKGs) are activated by the NO/cGMP pathway. NO is produced by nitric oxide synthases (NOS). NO then binds to the heme group of soluble guanylyl cyclase (sGC) to activate the enzyme and allow for the conversion of guanosine triphosphate to 3',5'- cyclic monophosphate (cGMP). cGMP acts as the activator for PKG. There are two isoforms of PKG; PKGI, a cytosolic isoform expressed highly in smooth muscle cells, and PKGII, a membrane-bound isoform expressed in brain. There are two splice variants of PKGI: PKGIα and PKGIβ. These isoforms share a common C-terminus and differ only in the leucine zipper region at the N-terminus. To date, there are no known differential binding partners of each of the splice variants. The PKGI knockout mouse has a reduced life span and the bone phenotype has yet to be characterized [95]. PKGII knockout mice exhibit dwarfism caused by a defect in endochondral ossification at the growth plates [94], indicating a functional role of PKGII in bone development.

The work presented in the second chapter of this dissertation will demonstrate the role of PKGs in estrogen protection from apoptosis. Importantly, we show that both PKGIα and PKGII are independently required to protect cells against an apoptotic stimuli. Both PKGs function through different mechanisms with PKGIα directly inhibiting the pro-apoptotic machinery and with PKGII activating cell survival pathways. The third chapter provides further evidence that PKGs are involved in pro-survival signaling. We use multiple apoptotic stimuli and multiple steroid hormones to validate that the pro-survival signaling is mediated via PKG. The fourth and fifth chapters of this dissertation will focus on the PKGII mediated response to fluid shear stress. We first analyze the PKGII-mediated activation of *fos* genes and ERK in response to fluid shear stress. Second, we define a mechanosome which converts the extracellular fluid shear into an intracellular signaling cascade. Finally, we begin to characterize the bone phenotype of PKGII knockout mice. The results from this study reveal an integral role of PKGII in the formation of bone.

References:

1.   *Bone Health and Osteoporosis: A Report of the Surgeon General.* Rockville, MD: U.S. Department of Health and Human Services, Office of the Surgeon General; 2004.

2.   Whitfield JF: *Growing Bone.* Second edn. Austin, TX: Landes Bioscience and Springer Science+Business Media; 2007.

3.   Alberts B JA, Lewis J, et al.: *Molecular Biology of the Cell.* 4th edn. New York: Garland Science; 2002.

4.   Jiang GL, White CR, Stevens HY, Frangos JA: **Temporal gradients in shear stimulate osteoblastic proliferation via ERK1/2 and retinoblastoma protein.** *Am J Physiol Endocrinol Metab* 2002, **283:**E383-389.

5.   Kapur S, Baylink DJ, Lau KH: **Fluid flow shear stress stimulates human osteoblast proliferation and differentiation through multiple interacting and competing signal transduction pathways.** *Bone* 2003, **32:**241-251.

6.   Taylor AF, Saunders MM, Shingle DL, Cimbala JM, Zhou Z, Donahue HJ: **Mechanically stimulated osteocytes regulate osteoblastic activity via gap junctions.** *Am J Physiol Cell Physiol* 2007, **292:**C545-552.

7.   Lee DY, Li YS, Chang SF, Zhou J, Ho HM, Chiu JJ, Chien S: **Oscillatory flow-induced proliferation of osteoblast-like cells is mediated by alphavbeta3 and beta1 integrins through synergistic interactions of focal adhesion kinase and Shc with phosphatidylinositol 3-kinase and the Akt/mTOR/p70S6K pathway.** *J Biol Chem* 2010, **285:**30-42.

8.   Yamaguchi A, Katagiri T, Ikeda T, Wozney JM, Rosen V, Wang EA, Kahn AJ, Suda T, Yoshiki S: **Recombinant human bone morphogenetic protein-2 stimulates osteoblastic maturation and inhibits myogenic differentiation in vitro.** *J Cell Biol* 1991, **113:**681-687.

9.   Tang DZ, Hou W, Zhou Q, Zhang M, Holz J, Sheu TJ, Li TF, Cheng SD, Shi Q, Harris SE, et al: **Osthole stimulates osteoblast differentiation and bone formation by activation of beta-catenin-BMP signaling.** *J Bone Miner Res* 2010, **25:**1234-1245.

10. Wang M, Jin H, Tang D, Huang S, Zuscik MJ, Chen D: **Smad1 Plays an Essential Role in Bone Development and Postnatal Bone Formation.** *Osteoarthritis Cartilage* 2011.

11.   Kim IS, Song YM, Cho TH, Kim JY, Weber FE, Hwang SJ: **Synergistic action of static stretching and BMP-2 stimulation in the osteoblast differentiation of C2C12 myoblasts.** *J Biomech* 2009, **42:**2721-2727.

12.   Thies RS, Bauduy M, Ashton BA, Kurtzberg L, Wozney JM, Rosen V: **Recombinant human bone morphogenetic protein-2 induces osteoblastic differentiation in W-20-17 stromal cells.** *Endocrinology* 1992, **130:**1318-1324.

13.   Yang Y, Topol L, Lee H, Wu J: **Wnt5a and Wnt5b exhibit distinct activities in coordinating chondrocyte proliferation and differentiation.** *Development* 2003, **130:**1003-1015.

14.   Kato M, Patel MS, Levasseur R, Lobov I, Chang BH, Glass DA, 2nd, Hartmann C, Li L, Hwang TH, Brayton CF, et al: **Cbfa1-independent decrease in osteoblast proliferation, osteopenia, and persistent embryonic eye vascularization in mice deficient in Lrp5, a Wnt coreceptor.** *J Cell Biol* 2002, **157:**303-314.

15.   Canalis E: **Growth factor control of bone mass.** *J Cell Biochem* 2009, **108:**769-777.

16.   Bodine PV, Zhao W, Kharode YP, Bex FJ, Lambert AJ, Goad MB, Gaur T, Stein GS, Lian JB, Komm BS: **The Wnt antagonist secreted frizzled-related protein-1 is a negative regulator of trabecular bone formation in adult mice.** *Mol Endocrinol* 2004, **18:**1222-1237.

17.   Komm BS, Terpening CM, Benz DJ, Graeme KA, Gallegos A, Korc M, Greene GL, O'Malley BW, Haussler MR: **Estrogen binding, receptor mRNA, and biologic response in osteoblast-like osteosarcoma cells.** *Science* 1988, **241:**81-84.

18.   Gray TK, Flynn TC, Gray KM, Nabell LM: **17 beta-estradiol acts directly on the clonal osteoblastic cell line UMR106.** *Proc Natl Acad Sci U S A* 1987, **84:**6267-6271.

19.   Ernst M, Schmid C, Froesch ER: **Enhanced osteoblast proliferation and collagen gene expression by estradiol.** *Proc Natl Acad Sci U S A* 1988, **85:**2307-2310.

20.   Levin ER: **Plasma membrane estrogen receptors.** *Trends Endocrinol Metab* 2009, **20:**477-482.

21.   Imai Y, Kondoh S, Kouzmenko A, Kato S: **Regulation of bone metabolism by nuclear receptors.** *Mol Cell Endocrinol* 2009, **310:**3-10.

22.   Krum SA: **Direct transcriptional targets of sex steroid hormones in bone.** *J Cell Biochem* 2011, **112:**401-408.

23. Kasperk CH, Wergedal JE, Farley JR, Linkhart TA, Turner RT, Baylink DJ: **Androgens directly stimulate proliferation of bone cells in vitro.** *Endocrinology* 1989, **124:**1576-1578.

24. Takeuchi M, Kakushi H, Tohkin M: **Androgens directly stimulate mineralization and increase androgen receptors in human osteoblast-like osteosarcoma cells.** *Biochem Biophys Res Commun* 1994, **204:**905-911.

25. Chiang C, Chiu M, Moore AJ, Anderson PH, Ghasem-Zadeh A, McManus JF, Ma C, Seeman E, Clemens TL, Morris HA, et al: **Mineralization and bone resorption are regulated by the androgen receptor in male mice.** *J Bone Miner Res* 2009, **24:**621-631.

26. Krum SA, Miranda-Carboni GA, Hauschka PV, Carroll JS, Lane TF, Freedman LP, Brown M: **Estrogen protects bone by inducing Fas ligand in osteoblasts to regulate osteoclast survival.** *EMBO J* 2008, **27:**535-545.

27. Bernhardt A, Thieme S, Domaschke H, Springer A, Rosen-Wolff A, Gelinsky M: **Crosstalk of osteoblast and osteoclast precursors on mineralized collagen-- towards an in vitro model for bone remodeling.** *J Biomed Mater Res A* 2010, **95:**848-856.

28. **National Osteoporosis Foundation**

29. Stubelius A, Andreasson E, Karlsson A, Ohlsson C, Tivesten A, Islander U, Carlsten H: **Role of 2-methoxyestradiol as inhibitor of arthritis and osteoporosis in a model of postmenopausal rheumatoid arthritis.** *Clin Immunol* 2011.

30. Kawai M, Modder UI, Khosla S, Rosen CJ: **Emerging therapeutic opportunities for skeletal restoration.** *Nat Rev Drug Discov* 2011, **10:**141-156.

31. McCarthy MM, Schwarz JM, Wright CL, Dean SL: **Mechanisms mediating oestradiol modulation of the developing brain.** *J Neuroendocrinol* 2008, **20:**777-783.

32. Pozzi S, Benedusi V, Maggi A, Vegeto E: **Estrogen action in neuroprotection and brain inflammation.** *Ann N Y Acad Sci* 2006, **1089:**302-323.

33. Marin R, Ramirez C, Morales A, Gonzalez M, Alonso R, Diaz M: **Modulation of Abeta-induced neurotoxicity by estrogen receptor alpha and other associated proteins in lipid rafts.** *Steroids* 2008, **73:**992-996.

34. Sun B, Karin M: **NF-kappaB signaling, liver disease and hepatoprotective agents.** *Oncogene* 2008, **27:**6228-6244.

35. Liu WH, Yeh SH, Lu CC, Yu SL, Chen HY, Lin CY, Chen DS, Chen PJ: **MicroRNA-18a Prevents Estrogen Receptor-alpha Expression, Promoting Proliferation of Hepatocellular Carcinoma Cells.** *Gastroenterology* 2008.

36. Xing D, Nozell S, Chen YF, Hage F, Oparil S: **Estrogen and mechanisms of vascular protection.** *Arterioscler Thromb Vasc Biol* 2009, **29:**289-295.

37. Dai Z, Li Y, Quarles LD, Song T, Pan W, Zhou H, Xiao Z: **Resveratrol enhances proliferation and osteoblastic differentiation in human mesenchymal stem cells via ER-dependent ERK1/2 activation.** *Phytomedicine* 2007, **14:**806-814.

38. Gu G, Hentunen TA, Nars M, Harkonen PL, Vaananen HK: **Estrogen protects primary osteocytes against glucocorticoid-induced apoptosis.** *Apoptosis* 2005, **10:**583-595.

39. Cheskis BJ, Greger JG, Nagpal S, Freedman LP: **Signaling by estrogens.** *J Cell Physiol* 2007, **213:**610-617.

40. Lipsett MB: **Hormones, nutrition, and cancer.** *Cancer Res* 1975, **35:**3359-3361.

41. Coelingh Bennink HJ: **Are all estrogens the same?** *Maturitas* 2004, **47:**269-275.

42. Revankar CM, Cimino DF, Sklar LA, Arterburn JB, Prossnitz ER: **A transmembrane intracellular estrogen receptor mediates rapid cell signaling.** *Science* 2005, **307:**1625-1630.

43. Thomas P, Pang Y, Filardo EJ, Dong J: **Identity of an estrogen membrane receptor coupled to a G protein in human breast cancer cells.** *Endocrinology* 2005, **146:**624-632.

44. Windahl SH, Andersson N, Chagin AS, Martensson UE, Carlsten H, Olde B, Swanson C, Moverare-Skrtic S, Savendahl L, Lagerquist MK, et al: **The role of the G protein-coupled receptor GPR30 in the effects of estrogen in ovariectomized mice.** *Am J Physiol Endocrinol Metab* 2009, **296:**E490-496.

45. Haas E, Bhattacharya I, Brailoiu E, Damjanovic M, Brailoiu GC, Gao X, Mueller-Guerre L, Marjon NA, Gut A, Minotti R, et al: **Regulatory role of G protein-coupled estrogen receptor for vascular function and obesity.** *Circ Res* 2009, **104:**288-291.

46. Pedram A, Razandi M, Levin ER: **Nature of functional estrogen receptors at the plasma membrane.** *Mol Endocrinol* 2006, **20:**1996-2009.

47. Maggiolini M, Picard D: **The unfolding stories of GPR30, a new membrane-bound estrogen receptor.** *J Endocrinol* 2010, **204:**105-114.

48.   Heldring N, Pike A, Andersson S, Matthews J, Cheng G, Hartman J, Tujague M, Strom A, Treuter E, Warner M, Gustafsson JA: **Estrogen receptors: how do they signal and what are their targets.** *Physiol Rev* 2007, **87:**905-931.

49.   Lubahn DB, Moyer JS, Golding TS, Couse JF, Korach KS, Smithies O: **Alteration of reproductive function but not prenatal sexual development after insertional disruption of the mouse estrogen receptor gene.** *Proc Natl Acad Sci U S A* 1993, **90:**11162-11166.

50.   Dupont S, Krust A, Gansmuller A, Dierich A, Chambon P, Mark M: **Effect of single and compound knockouts of estrogen receptors alpha (ERalpha) and beta (ERbeta) on mouse reproductive phenotypes.** *Development* 2000, **127:**4277-4291.

51.   Laboratory J: **Mouse Genome Informatics.**

52.   Aguirre JI, Plotkin LI, Gortazar AR, Millan MM, O'Brien CA, Manolagas SC, Bellido T: **A novel ligand-independent function of the estrogen receptor is essential for osteocyte and osteoblast mechanotransduction.** *J Biol Chem* 2007, **282:**25501-25508.

53.   Armstrong VJ, Muzylak M, Sunters A, Zaman G, Saxon LK, Price JS, Lanyon LE: **Wnt/beta-catenin signaling is a component of osteoblastic bone cell early responses to load-bearing and requires estrogen receptor alpha.** *J Biol Chem* 2007, **282:**20715-20727.

54.   Jessop HL, Suswillo RF, Rawlinson SC, Zaman G, Lee K, Das-Gupta V, Pitsillides AA, Lanyon LE: **Osteoblast-like cells from estrogen receptor alpha knockout mice have deficient responses to mechanical strain.** *J Bone Miner Res* 2004, **19:**938-946.

55.   Ke HZ, Brown TA, Qi H, Crawford DT, Simmons HA, Petersen DN, Allen MR, McNeish JD, Thompson DD: **The role of estrogen receptor-beta, in the early age-related bone gain and later age-related bone loss in female mice.** *J Musculoskelet Neuronal Interact* 2002, **2:**479-488.

56.   Saxon LK, Robling AG, Castillo AB, Mohan S, Turner CH: **The skeletal responsiveness to mechanical loading is enhanced in mice with a null mutation in estrogen receptor-beta.** *Am J Physiol Endocrinol Metab* 2007, **293:**E484-491.

57.   McCauley LK, Tozum TF, Kozloff KM, Koh-Paige AJ, Chen C, Demashkieh M, Cronovich H, Richard V, Keller ET, Rosol TJ, Goldstein SA: **Transgenic models of metabolic bone disease: impact of estrogen receptor deficiency on skeletal metabolism.** *Connect Tissue Res* 2003, **44 Suppl 1:**250-263.

58.	Marino M, Ascenzi P, Acconcia F: **S-palmitoylation modulates estrogen receptor alpha localization and functions.** *Steroids* 2006, **71:**298-303.

59.	Marino M, Ascenzi P: **Membrane association of estrogen receptor alpha and beta influences 17beta-estradiol-mediated cancer cell proliferation.** *Steroids* 2008, **73:**853-858.

60.	Acconcia F, Ascenzi P, Bocedi A, Spisni E, Tomasi V, Trentalance A, Visca P, Marino M: **Palmitoylation-dependent estrogen receptor alpha membrane localization: regulation by 17beta-estradiol.** *Mol Biol Cell* 2005, **16:**231-237.

61.	Galluzzo P, Caiazza F, Moreno S, Marino M: **Role of ERbeta palmitoylation in the inhibition of human colon cancer cell proliferation.** *Endocr Relat Cancer* 2007, **14:**153-167.

62.	Lannigan DA: **Estrogen receptor phosphorylation.** *Steroids* 2003, **68:**1-9.

63.	Arnold SF, Melamed M, Vorojeikina DP, Notides AC, Sasson S: **Estradiol-binding mechanism and binding capacity of the human estrogen receptor is regulated by tyrosine phosphorylation.** *Mol Endocrinol* 1997, **11:**48-53.

64.	Migliaccio A, Di Domenico M, Castoria G, de Falco A, Bontempo P, Nola E, Auricchio F: **Tyrosine kinase/p21ras/MAP-kinase pathway activation by estradiol-receptor complex in MCF-7 cells.** *Embo J* 1996, **15:**1292-1300.

65.	Manolagas SC, Kousteni S, Jilka RL: **Sex steroids and bone.** *Recent Prog Horm Res* 2002, **57:**385-409.

66.	Cheskis BJ, Greger J, Cooch N, McNally C, McLarney S, Lam HS, Rutledge S, Mekonnen B, Hauze D, Nagpal S, Freedman LP: **MNAR plays an important role in ERa activation of Src/MAPK and PI3K/Akt signaling pathways.** *Steroids* 2008, **73:**901-905.

67.	Chambliss KL, Yuhanna IS, Mineo C, Liu P, German Z, Sherman TS, Mendelsohn ME, Anderson RG, Shaul PW: **Estrogen receptor alpha and endothelial nitric oxide synthase are organized into a functional signaling module in caveolae.** *Circ Res* 2000, **87:**E44-52.

68.	Mann V, Huber C, Kogianni G, Jones D, Noble B: **The influence of mechanical stimulation on osteocyte apoptosis and bone viability in human trabecular bone.** *J Musculoskelet Neuronal Interact* 2006, **6:**408-417.

69.	Plotkin LI, Mathov I, Aguirre JI, Parfitt AM, Manolagas SC, Bellido T: **Mechanical stimulation prevents osteocyte apoptosis: requirement of integrins, Src kinases, and ERKs.** *Am J Physiol Cell Physiol* 2005, **289:**C633-643.

70.   Cherney A, Edgell H, Krukoff TL: **NO mediates effects of estrogen on central regulation of blood pressure in restrained, ovariectomized rats.** *Am J Physiol Regul Integr Comp Physiol* 2003, **285:**R842-849.

71.   Gingerich S, Krukoff TL: **Estrogen modulates endothelial and neuronal nitric oxide synthase expression via an estrogen receptor beta-dependent mechanism in hypothalamic slice cultures.** *Endocrinology* 2005, **146:**2933-2941.

72.   O'Shaughnessy MC, Polak JM, Afzal F, Hukkanen MV, Huang P, MacIntyre I, Buttery LD: **Nitric oxide mediates 17beta-estradiol-stimulated human and rodent osteoblast proliferation and differentiation.** *Biochem Biophys Res Commun* 2000, **277:**604-610.

73.   Kemp-Harper B, Schmidt HH: **cGMP in the vasculature.** *Handb Exp Pharmacol* 2009**:**447-467.

74.   Kang HY, Cho CL, Huang KL, Wang JC, Hu YC, Lin HK, Chang C, Huang KE: **Nongenomic androgen activation of phosphatidylinositol 3-kinase/Akt signaling pathway in MC3T3-E1 osteoblasts.** *J Bone Miner Res* 2004, **19:**1181-1190.

75.   Wade CB, Robinson S, Shapiro RA, Dorsa DM: **Estrogen receptor (ER)alpha and ERbeta exhibit unique pharmacologic properties when coupled to activation of the mitogen-activated protein kinase pathway.** *Endocrinology* 2001, **142:**2336-2342.

76.   Marino M, Acconcia F, Bresciani F, Weisz A, Trentalance A: **Distinct nongenomic signal transduction pathways controlled by 17beta-estradiol regulate DNA synthesis and cyclin D(1) gene transcription in HepG2 cells.** *Mol Biol Cell* 2002, **13:**3720-3729.

77.   Singh M, Setalo G, Jr., Guan X, Warren M, Toran-Allerand CD: **Estrogen-induced activation of mitogen-activated protein kinase in cerebral cortical explants: convergence of estrogen and neurotrophin signaling pathways.** *J Neurosci* 1999, **19:**1179-1188.

78.   Bulayeva NN, Gametchu B, Watson CS: **Quantitative measurement of estrogen-induced ERK 1 and 2 activation via multiple membrane-initiated signaling pathways.** *Steroids* 2004, **69:**181-192.

79.   Zivadinovic D, Watson CS: **Membrane estrogen receptor-alpha levels predict estrogen-induced ERK1/2 activation in MCF-7 cells.** *Breast Cancer Res* 2005, **7:**R130-144.

80. Nuedling S, Kahlert S, Loebbert K, Meyer R, Vetter H, Grohe C: **Differential effects of 17beta-estradiol on mitogen-activated protein kinase pathways in rat cardiomyocytes.** *FEBS Lett* 1999, **454:**271-276.

81. Honda K, Shimohama S, Sawada H, Kihara T, Nakamizo T, Shibasaki H, Akaike A: **Nongenomic antiapoptotic signal transduction by estrogen in cultured cortical neurons.** *J Neurosci Res* 2001, **64:**466-475.

82. Huang A, Sun D, Wu Z, Yan C, Carroll MA, Jiang H, Falck JR, Kaley G: **Estrogen elicits cytochrome P450--mediated flow-induced dilation of arterioles in NO deficiency: role of PI3K-Akt phosphorylation in genomic regulation.** *Circ Res* 2004, **94:**245-252.

83. Koga M, Hirano K, Hirano M, Nishimura J, Nakano H, Kanaide H: **Akt plays a central role in the anti-apoptotic effect of estrogen in endothelial cells.** *Biochem Biophys Res Commun* 2004, **324:**321-325.

84. Jessop HL, Sjoberg M, Cheng MZ, Zaman G, Wheeler-Jones CP, Lanyon LE: **Mechanical strain and estrogen activate estrogen receptor alpha in bone cells.** *J Bone Miner Res* 2001, **16:**1045-1055.

85. Migliaccio S, Wetsel WC, Fox WM, Washburn TF, Korach KS: **Endogenous protein kinase-C activation in osteoblast-like cells modulates responsiveness to estrogen and estrogen receptor levels.** *Mol Endocrinol* 1993, **7:**1133-1143.

86. Ekstein J, Nasatzky E, Boyan BD, Ornoy A, Schwartz Z: **Growth-plate chondrocytes respond to 17beta-estradiol with sex-specific increases in IP3 and intracellular calcium ion signalling via a capacitative entry mechanism.** *Steroids* 2005, **70:**775-786.

87. Okabe K, Okamoto F, Kajiya H, Takada K, Soeda H: **Estrogen directly acts on osteoclasts via inhibition of inward rectifier K+ channels.** *Naunyn Schmiedebergs Arch Pharmacol* 2000, **361:**610-620.

88. Valverde MA, Rojas P, Amigo J, Cosmelli D, Orio P, Bahamonde MI, Mann GE, Vergara C, Latorre R: **Acute activation of Maxi-K channels (hSlo) by estradiol binding to the beta subunit.** *Science* 1999, **285:**1929-1931.

89. Moriarty K, Kim KH, Bender JR: **Minireview: estrogen receptor-mediated rapid signaling.** *Endocrinology* 2006, **147:**5557-5563.

90. Lodish H BA, Zipursky SL, et al.: *Molecular Cell Biology.* 4th edn. New York: W. H. Freeman; 2000.

91. Marc Pellegrini AS: *Caspases: Their Role in Cell Death and Cell Survival.* Austin, TX: Landes Bioscience and Springer Science+Business Media; 2003.

92.   Kelly PN, Strasser A: **The role of Bcl-2 and its pro-survival relatives in tumourigenesis and cancer therapy.** *Cell Death Differ* 2011.

93.   Tait SW, Green DR: **Caspase-independent cell death: leaving the set without the final cut.** *Oncogene* 2008, **27:**6452-6461.

94.   Pfeifer A, Aszodi A, Seidler U, Ruth P, Hofmann F, Fassler R: **Intestinal secretory defects and dwarfism in mice lacking cGMP-dependent protein kinase II.** *Science* 1996, **274:**2082-2086.

95.   Pfeifer A, Klatt P, Massberg S, Ny L, Sausbier M, Hirneiss C, Wang GX, Korth M, Aszodi A, Andersson KE, et al: **Defective smooth muscle regulation in cGMP kinase I-deficient mice.** *EMBO J* 1998, **17:**3045-3051.

Chapter 2:

The NO/cGMP Pathway Mediates the Osteocyte-protective

Effects of Estrogen via Differential Actions of cGMP-

dependent Protein Kinases I and II

ABSTRACT

Estrogens promote bone health in part by increasing osteocyte survival, an effect that requires activation of the protein kinases Akt and ERK1/2, but the molecular mechanisms involved are only partly understood. Since estrogens also increase nitric oxide (NO) synthesis and NO can have anti-apoptotic effects, we examined the role of NO/cGMP signaling in estrogen regulation of osteocyte survival. In MLO-Y4 osteocyte-like cells, etoposide-induced cell death, assessed by trypan blue staining, caspase-3 cleavage, and TUNEL assays, was completely prevented when cells were pre-treated with estradiol. This protective effect was mimicked when cells were pre-treated with a membrane-permeable cGMP analog, and blocked in the presence of pharmacological inhibitors of NO synthase, soluble guanylate cyclase, or cGMP-dependent protein kinases (PKGs), supporting a requirement for NO/cGMP/PKG signaling downstream of estrogen. siRNA-mediated knock-down and viral reconstitution of individual PKG isoforms demonstrated that the anti-apoptotic effects of estradiol and cGMP were mediated by PKG Iα and PKG II. Akt and ERK1/2 activation by estradiol required PKG II, and cGMP mimicked the effects of estradiol on Akt and ERK, including induction of ERK nuclear translocation. cGMP induced BAD phosphorylation on several sites, and experiments with phosphorylation-deficient BAD mutants demonstrated that the anti-apoptotic effects of cGMP and estradiol required BAD phosphorylation on Ser^{136} and Ser^{155}, which are targeted by Akt and PKGI, respectively, and regulate BAD interaction with Bcl-2. In conclusion, estradiol protects osteocytes against apoptosis by activating the NO/cGMP/PKG cascade; PKG II is required for estradiol-induced activation of ERK and Akt, and PKG Iα contributes to pro-survival signaling by directly phosphorylating BAD.

INTRODUCTION

Skeletal integrity and maintenance of bone mass require continuous bone remodeling through resorption by osteoclasts and new bone formation by osteoblasts. Normal aging and estrogen deficiency are associated with progressive bone loss and increased bone fragility; both conditions are characterized by decreasing osteoblast numbers and increased apoptosis of osteoblasts and mature osteocytes [1, 2]. Estrogens prevent bone loss by prolonging the life span of osteoblasts and osteocytes, while shortening the life span of osteoclasts [2]. Previous work has shown that estradiol protects osteoblasts and osteocytes from apoptosis by activating the protein kinases Akt and ERK via a plasma membrane-bound estrogen receptor; these effects do not require nuclear localization of the estrogen receptor, but nuclear translocation of ERK [3-6].

In different cell types, including osteoblasts, estrogens increase the synthesis of NO through transcriptional and post-transcriptional regulation of endothelial NO synthase (eNOS), which generates NO from L-arginine [7-10]. Among other effects, NO binds to and activates soluble guanylate cyclase (sGC), generating cGMP, which in turn regulates cGMP-dependent protein kinases (PKGs) and phosphodiesterases [11]. The PKG I gene encodes two splice variants differing in the N-terminal ~100 amino acids, PKG Iα and Iβ, which are largely cytosolic enzymes, and the PKG II gene encodes a membrane-bound enzyme [11]. PKG I and II differ in their tissue distribution, but both genes are expressed in osteoblasts and osteocytes [11, 12]. We recently showed that stimulation of osteoblasts and osteocytes by fluid shear stress increases NO and cGMP levels, leading to PKG activation, and found that PKGII mediates Src and ERK activation, induction of *fos* family genes, and increased osteoblast proliferation in

response to fluid shear stress [12, 13]. PKGII-null mice show defective Src and ERK signaling in osteoblasts, and decreased *c-fos* expression in bone [13]; these mice also exhibit dwarfism caused by defective chondroblast differentiation [14].

NO/cGMP signaling has been implicated in the regulation of apoptosis in different cell types [15]. Fluid shear stress and NO donors protect osteocytes and osteoblasts from tumor necrosis factor (TNF)-α-induced apoptosis but the downstream targets of NO are unclear [16, 17]. NO donors counteract estrogen deficiency-induced osteopenia in ovarectomized rats, and show promise in ameliorating osteoporosis in post-menopausal women [18-20]. Experiments in eNOS-deficient mice suggest that at least some of the bone-protective effects of estrogens are mediated by the NO pathway [21]. We, therefore, decided to determine the role of NO/cGMP signaling in estrogen-regulation of osteocyte survival. We found that the protective effect of estradiol against osteocyte apoptosis required NO/cGMP stimulation of both PKGIα and PKGII, and involved activation of Akt and ERK via PKG II, and BAD phosphorylation by Akt and PKG Iα.

MATERIALS AND METHODS

Reagents. 17β-estradiol and etoposide were purchased from Sigma. Antibodies specific for phospho-ERK1 (Tyr[204]), total ERK 1/2, α-tubulin and β-actin were from Santa Cruz Biotechnology. Antibodies specific for phospho-Akt (Ser[473]), total Akt, cleaved caspase-3, phospho-BAD (Ser[112], Ser[136], or Ser[155]) and total BAD were from Cell Signaling. The HA-epitope antibody was from Roche. The cGMP agonist 8-(4-chlorophenylthio)-cGMP (8-pCPT-cGMP) and antagonist 8-(4-chlorophenylthio)-β-phenyl-1,N^2-ethenoguanosine-3',5'-cyclic phosphothioate, Rp isomer [(Rp)-8-pCPT-PET-cGMPS] were from Biolog. The NOS inhibitor N-nitro-L-arginine methyl ester (L-NAME), and the sGC inhibitor 1H-[1,2,4]oxadiazolo[4,3-a]quinoxalin-1-one (ODQ), were from Cayman.

Cell Culture. The murine osteocyte-like cell line MLO-Y4 was a gift from Dr. Linda Bonewald (University of Missouri, Kansas City), and was maintained on collagen-coated plates in αMEM supplemented with 2.5% enriched calf serum and 2.5% heat-inactivated fetal bovine serum [22]. For most experiments, cells were incubated overnight in phenol red-free αMEM with 0.1% charcoal-stripped fetal calf serum prior to stimulation with estradiol.

DNA and siRNA Transfections and RT-PCR. MLO-Y4 cells were transiently transfected using Lipofectamine 2000 (Invitrogen). HA-tagged BAD constructs were a gift from Dr. Tom Chittenden (ImmunoGen Inc, MA). Experimental treatments occurred 48 h post-transfection for DNA-transfected cells and 24-48 hours post-transfection for siRNA-transfected cells. siRNA oligoribonucleotides were purchased from Qiagen. The target sequence for PKGIα/β was 5'-CCGGACAUUUAAAGACAGCAA-3' (PKGI) and

for PKGII was 5'-CTGCTTGGAAGTGGAATACTA-3' (PKGII[a]) and 5'-CCGGGTTTCTTGGGGTAGTCAA- 3' (PKGII[b]). mRNA knockdown and protein depletion were quantified by real-time RT-PCR and Western blotting, respectively, at 24 h after transfection as described [12].

PCR primer sequences for PKGI were (forward) 5'-GTCACTAGGGATTCTGATGTATGA-3' and (reverse) 5'-AGAATTTCCAAAGAAG-ATTGCAAA-3'. The mRNA levels of PKGII were measured using the primers (forward) 5'-GTGACACAGCGCGGTTGTT-3' and (reverse) 5'-TGGGAATGGAAAAG-GACAAC- 3'. PKG mRNA levels were normalized to *gapdh* mRNA levels as described [12].

Quantification of Cell Death. MLO-Y4 cells were treated with vehicle or 100μM R$_p$-8-pCPT-PET-cGMPS for 1 h prior to stimulation with 100nM estradiol or 100μM 8-pCPT-cGMP for 1 h. Subsequently, cells were treated with 50μM etoposide for 8 h. A minumum of 200 cells for each condition were examined by trypan blue uptake, and etoposide-induced cell death was calculated by subtracting the percentage of trypan-blue positive cells observed in vehicle-treated samples from the experimental sample. Apoptosis was quantified similarly by TUNEL staining after 6 h of etoposide treatment, using the DeadEnd™ Colorimetric TUNEL System according to the manufacturer's instructions (Promega). Apoptotic cells were also visualized by immunofluorescence staining with an antibody specific for cleaved caspase-3 (Cell Signaling). With both assays, a minimum of 100 cells from three randomly selected fields were assessed for each condition and percentage of apoptotic cells was calculated by subtracting the

percentage of TUNEL- or cleaved caspase-3 positive cells quantified in the control samples from the experimental sample.

I*n Vitro Phosphorylation of BAD*. 293T cells were transiently transfected with vectors encoding HA-tagged wildtype or mutant BAD constructs. Cells were lysed in 50 mM Tris-HCl, pH 7.5, 137 mM NaCl, 1% Triton X-100, 1 mM EDTA, 1 mM EGTA, 1 mM DTT, and protease inhibitors at 24 h after transfection. Cell lysates were subjected to immunoprecipitation using anti-HA-agarose beads (Sigma) and incubated in the presence of 5 μCi $[\gamma^{32}P]$ATP and purified catalytic domain of PKGI. Phosphorylation was analysed by SDS-polyacrylamide gel eletrophoresis (SDS-PAGE) and autoradiography.

Western Blot Analyses. Western blots were developed with horseradish peroxidase- conjugated secondary antibody and enhanced chemiluminescence as described [23]. Bar graphs were generated by densitometry scanning using ImageJ software.

Statistical Analyses. Data were analyzed by one-way analysis of variance (ANOVA) with Bonferroni post-test. A *p* value of <0.05 was considered statistically significant. Bar graphs are shown as the mean ± SEM of at least three independent experiments. All other results are shown as representative results of at least three independent experiments.

RESULTS

Estradiol and cGMP Protect Osteocytes from Apoptosis. Since estradiol can increase NO synthesis in various cell types, leading to increased intracellular cGMP concentrations [24-26], and since NO/cGMP have been implicated in the regulation of apoptosis [15], we questioned if cGMP could mimic the effects of estradiol on osteocyte apoptosis. When MLO-Y4 osteocyte-like cells were exposed to either serum starvation or the DNA-damaging agent etoposide, the number of trypan blue-positive, dead cells increased by 5.8% and 7.7%, respectively, over basal levels measured in control cells growing in full serum. We used TUNEL staining to identify early apoptotic cells containing fragmented DNA, and found that etoposide treatment increased the number of apoptotic cells by 12.6%. When cells were pre-treated with 100 nM estradiol or 100 μM 8-pCPT-cGMP prior to serum starvation or etoposide exposure, the number of trypan blue- or TUNEL-positive cells was reduced to near basal levels (Fig. 1A and B). Inhibition of cGMP-dependent protein kinases with the pharmacological inhibitor *R*p-8-pCPT-PET-cGMPS (abbreviated Rp-cGMPS) prevented the pro-survival effects of both estradiol and 8-pCPT-cGMP (Fig. 1B and C), as quantified by trypan blue uptake and TUNEL staining. These data suggest that the cGMP/PKG pathway is integral in protecting osteocytes from apoptosis.

PKGIα and PKGII are Independently Required for Estradiol- and cGMP-mediated Protection from Apoptosis. Since the global PKG inhibitor *R*p-8-pCPT-PET-cGMPS prevented the anti-apoptotic effects of estradiol and cGMP, we used an siRNA approach to determine which PKG isoform was involved. MLO-Y4 cells were transfected with

siRNAs targeting either the common C-terminal region of PKGIα and Iβ or PKGII, with an siRNA targeting green fluorescent protein (GFP) serving as a control. Quantitative RT-PCR showed that PKGI mRNA levels were reduced by 71% in cells transfected with PKGI siRNA while PKGII mRNA levels were unaffected. Cells transfected with siRNA targeting PKGII showed a 76% reduction in PKGII mRNA levels without change in PKGI mRNA (Fig. 2A). Expression of PKGI or PKGII protein was reduced correspondingly in PKGI or PKGII siRNA-transfected cells (Supplemental Fig. 1 and C).

In control siRNA-transfected MLO-Y4 cultures, etoposide increased the number of trypan blue-positive cells by 12%, and the number of apoptotic cells staining positive for cleaved caspase-3 by 20% (Fig. 2B and C). The effects of etoposide were abrogated with estradiol or 8-pCPT-cGMP pre-treatment, similar to results obtained for trypan blue staining and TUNEL assay in untransfected cells. However, in cells transfected with either PKGI- or PKGII-specific siRNA, etoposide increased cell death regardless of the presence or absence of estradiol or 8-pCPT-cGMP, indicating necessary and non-redundant roles for both PKG isoforms in estradiol- and cGMP-induced protection from cell death (Fig. 2B shows etoposide-induced increases in trypan blue-positive cells, and Fig. 2C and D show etoposide-induced apoptosis quantified by immunofluorescence staining for cleaved caspase-3).

To ensure that these results were not due to off-target effects of the siRNAs, we reconstituted expression of each PKG isoform in siRNA-transfected cells using adenoviral vectors encoding siRNA-resistant PKGIα, PKGIβ, or PKGII. While reconstituting PKGIα in PKGI-depleted cells, and PKGII in PKGII-depleted cells restored the ability of estradiol and 8-pCPT-cGMP to reverse etoposide-induced cell

death, reconstituting PKGIβ in PKGI-depleted cells had no effect (Fig. 2E and F show viral infection of PKGI- and PKGII-depleted cells, respectively, with adenovirus encoding LacZ serving as a negative control). Similar results were obtained when apoptotic cells were quantified by immunofluorescence staining for cleaved caspase-3 (data not shown). Infection of PKGI-depleted MLO-Y4 cells with adenoviral vectors encoding PKGIα or Iβ resulted in similar levels of PKGI protein measured by Western blotting with an antibody specific for the common C-terminus of both PKGI isoforms (Supplemental Fig. 1A), and cGMP treatment of these cells effected similar levels of PKGI activity, as shown by phosphorylation of vasodilator-stimulated protein on Ser^{259} (a site specifically phosphorylated by PKG, Supplemental Fig. 1B). The viral vectors produced levels of PKGI or PKGII above those of the endogenous enzymes (Supplemental Fig. 1A and C). We conclude that estradiol and cGMP require both PKGIα and PKGII to protect osteocytes from apoptosis.

Estradiol-induced Akt and ERK Activation in Osteocytes is Mediated by cGMP and PKGII. We have recently shown that fluid shear stress-induced ERK activation in osteoblasts and osteocytes is mediated by NO/cGMP activation of PKGII [12]. Since the anti-apoptotic effects of estradiol in osteocytes require Akt and ERK activation [27], we wanted to explore the role of NO/cGMP/PKG signaling in estradiol-induced Akt and ERK activation. We found that pharmacological inhibition of NO synthase, sGC, or PKG in MLO-Y4 cells largely prevented estradiol-induced Akt and ERK phosphorylation on activating sites (Fig. 3A). Using the above-described siRNAs, we determined that only PKGII, and but not PKGI, was required for activation of Akt and ERK by estrogen (Fig.

3B). Reconstitution of PKGII by adenoviral infection restored both Akt and ERK phosphorylation in PKGII-depleted cells (Fig. 3C). Previous work has shown that the anti-apoptotic effects of estradiol require transient nuclear localization of ERK; we found that cGMP mimicked this effect of estradiol and induced nuclear translocation of ERK in a PKGII-dependent manner (Fig. 3D and E). We conclude that NO/cGMP activation of PKGII is necessary for estradiol-induced Akt and ERK activation.

Osteocyte Protection from Apoptosis by Estradiol or cGMP Requires BAD Phosphorylation on Ser^{136} and Ser^{155}, but Not Ser^{112}. Osteoblast and osteocyte survival is regulated by the balance of pro- and anti-apoptotic Bcl-2 family proteins [28, 29]. The pro-apoptotic family member BAD sensitizes cells to apoptosis by binding and inactivating anti-apoptotic Bcl-2 family members, and BAD function is regulated by phosphorylation on serines 112, 136 and 155. BAD phosphorylation on Ser^{112} or Ser^{136} enables binding of 14-3-3 proteins and allows for the subsequent phosphorylation of Ser^{155} to fully disassociate BAD from the anti-apoptotic Bcl-2 family member [30]. To determine the role of BAD phosphorylation in the anti-apoptotic effects of estradiol and cGMP, we used mutant BAD constructs containing serine to alanine substitutions in each of the three phosphorylation sites. Etoposide-treated osteocytes expressing a BAD S112A mutant showed similar protection by estradiol and 8-pCPT-cGMP as cells expressing wild type BAD: etoposide induced 12.7% and 13.6% cell death in wild type and BAD S112A-expressing cells, respectively, which was reduced to basal levels by estradiol or 8-pCPT-cGMP (Fig. 4A). However, etoposide-treated MLO-Y4 cells expressing BAD S136A or BAD S155A continued to show high levels of apoptosis despite treatment with

estradiol or 8-pCPT-cGMP (Fig. 4A). Similar results were obtained when probing for cleaved caspase-3 in cells transfected with wild type or S155A-mutant BAD (Fig. 4B). Transfection efficiency of MLO-Y4 cells was approximately 60-70% (Suppl. Fig. 2), and all three BAD mutants were expressed at levels slightly lower than wild type BAD (Fig. 4A). The mutant BAD S136A and S155A constructs appear to act in a dominant-negative fashion likely by dimerizing with endogenous Bcl-2 or Bcl-X_L, and preventing estradiol- and cGMP-induced protection from cell death. These results suggest that BAD phosphorylation on Ser[136] and Ser[155] are crucial for the effects of estradiol and cGMP on osteocyte apoptosis.

PKG I Phosphorylates BAD on Ser[155]. Previous *in vitro* studies suggest that PKGIα is able to phosphorylate BAD on Ser[155] [31]. Using wild type and mutant BAD constructs isolated from 293T cells, we confirmed that PKGI directly phosphorylated BAD Ser[155], since alanine substitution for Ser[155] completely prevented *in vitro* phosphorylation of the immunoprecipitated BAD protein by the purified kinase (Fig. 4C). Mutation of Ser[112] or Ser[136] slightly reduced $^{32}PO_4$ incorporation, possibly because phosphorylation of these sites in wildtype BAD by other kinases in 293T cells may enhance the efficiency of Ser[155] phosphorylation by PKG, as has been shown for BAD Ser[155] phosphorylation by cAMP-dependent protein kinase [32]. To examine the kinetics of BAD Ser[155] phosphorylation in intact cells, we used a phospho-specific antibody. We confirmed specificity of the antibody for BAD phosphorylated on Ser[155] (data not shown), but detection of BAD phosphorylation required transfection of wild type BAD; cells were infected with the PKGIα adenovirus to enhance PKG activity corresponding to the

increase in substrate level. Using this system, we found that BAD Ser^{155} phosphorylation was increased within 10 min after adding 8-CPT-cGMP to MLO-Y4 cells, and remained elevated at 2 hours (Fig. 4D). Only adenoviral expression of PKGIα, but not PKGIβ, enhanced cGMP-induced BAD Ser^{155} phosphorylation in intact cells (Fig. 4E).

Treatment of MLO-Y4 cells with cGMP also increased BAD phosphorylation on Ser^{112} and Ser^{136} (Fig. 4F); this was most likely through cGMP/PKGII-mediated activation of ERK and Akt (Fig. 3B), since BAD Ser^{112} and Ser^{136} are targets of RSK (acting downstream of ERK) and Akt, respectively [33]. Consistent with this hypothesis, siRNA-mediated depletion of PKGII prevented Ser^{112} and Ser^{136} phosphorylation of BAD (Fig. 4E). Ser^{155} phosphorylation was also undetectable in PKGII siRNA-transfected cells, consistent with previous studies that indicate BAD must be phosphorylated on Ser^{136} and bound to 14-3-3 proteins, before final phosphorylation of Ser^{155} by cAMP-dependent protein kinase can occur [30].

Since BAD phosphorylation on both Ser^{136} and Ser^{155} were required for estradiol and cGMP-mediated protection from apoptosis, and both PKGIα and PKGII were necessary for the effects of estradiol and cGMP, we conclude that PKGI and PKGII signaling converges on BAD to regulate apoptosis, with PKGII necessary for BAD Ser^{136} phosphorylation by Akt, which precedes direct phosphorylation of Ser^{155} by PKGIα.

DISCUSSION

Increased numbers of apoptotic osteocytes are observed with aging, as well as in animal models of estrogen deficiency after gonadectomy, and in humans after pharmacological induction of a hypoestrogenic state through administration of gonadotropin releasing hormone. In transgenic mice with osteocyte-specific expression of the diphtheria toxin receptor, induction of osteocyte death through injection of the toxin leads to bone loss and fragility; thus, osteocyte viability is a key determinant of bone strength and bone mineral density [34]. Estrogens enhance bone formation by increasing osteoblast proliferation and protecting osteoblasts and osteocytes from apoptosis [35, 36]. A more complete understanding of the mechanisms whereby estrogens protect osteocytes from apoptosis is important for improving pharmacological treatment of osteoporosis.

Previous work in osteocytes, osteoblasts, and other cell types has established that estrogens protect cells against a number of apoptosis-inducing stimuli [36-38]. Estrogens activate signaling pathways involving Akt and ERK through extra-nuclear actions of a membrane-bound receptor [39]. The anti-apoptotic effects of estradiol in osteocyte-like cells are blocked by pharmacological or genetic inhibition of the ERK and Akt pathways, and require nuclear translocation of ERK as well as the regulation of Bcl-2 family proteins [4, 27]. We found that protection of MLO-Y4 cells from etoposide- or serum starvation-induced apoptosis by estradiol required NO and cGMP synthesis and activation of PKG. cGMP mimicked the anti-apoptotic effects of estradiol, and we found that PKGIα and PKGII performed independent anti-apoptotic functions converging on the regulation of BAD. While PKGIα directly phosphorylated BAD on Ser^{155}, PKGII indirectly increased BAD phosphorylation on Ser^{112} and Ser^{136} by activating ERK and

Akt. We previously showed that PKGII activates ERK in osteoblasts and osteocytes via activation of Src, and that membrane-bound PKGII is uniquely situated to stimulate Src through activation of a Shp-1/2 phosphatase complex [12, 13]. Estradiol-induced ERK and Akt activation are dependent on Src activation [39, 40], and we found that Akt activation by PKGII also requires Src (manuscript in preparation). Akt is upstream of several pro-survival pathways, but one of the most prominent pro-survival effects of Akt is phosphorylation of BAD on Ser[136], which is required for binding of 14-3-3 proteins and a pre-requisite for full BAD phosphorylation and dissociation from Bcl-2 [30].

The NO/cGMP/PKG pathway can regulate apoptosis in a positive or negative fashion, dependent on the cell type. For example, NO donors and cGMP analogs protect neuronal and myocardial cells from cell death induced by ischemia/reperfusion injury, growth factor withdrawal, or tumor necrosis factor-α exposure [41, 42]. In contrast, PKG activation promotes apoptosis in intestinal epithelial cells. MC3T3 osteoblast-like cells are protected from TNF-α-induced apoptosis by NO, but the authors of the study concluded that this effect was not cGMP/PKG-mediated, because of lack of reversal by a pharmacological inhibitor of PKG which has shown varied efficacy in other studies [17]. MLO-Y4 osteocytes are protected from TNF-α-induced apoptosis by exposure to fluid shear stress; this effect is NO-dependent, but downstream effects of NO were not examined [16]. While this manuscript was in preparation, Wong and Fiscus described a role for cGMP/PKGI in protecting OP9 bone marrow stromal osteoprogenitor cells from spontaneous apoptosis [43].

Using siRNA-mediated depletion of PKGI and reconstitution with adenoviral vectors encoding either PKG Iα or Iβ, we found that only PKG Iα, but not Iβ mediates

the anti-apoptotic effects of cGMP, despite similar expression levels of both kinases and comparable activities toward the shared substrate VASP. We are not aware of other examples of PKG Iα-specific functions for which PKG Iβ cannot substitute; in PKGI null mice, it appears that either PKGI isoform alone can rescue basic vascular and intestinal smooth muscle functions [44]. However, due to their unique N-terminal dimerization/leucine zipper domain, PKG Iα and Iβ bind to some isoform-specific G-kinase interaction proteins (GKIPs), which may target the kinases to unique subcellular localizations and substrates. For example, PKGIα specifically binds to the regulator of G-protein signaling and the myosin-targeting subunit of myosin phosphatase [45, 46], whereas PKGIβ specifically binds to the inositol 1,4,5-trisphosphate receptor-associated G-kinase substrate IRAG and the transcriptional regulator TFII-I [47, 48]. PKGIα may be targeted to a subcellular compartment that favors its ability to phosphorylate BAD Ser[155] in intact cells.

In conclusion, we identified PKG Iα and PKG II as important mediators of the anti-apoptotic effects of estradiol in osteocytes. These results help explain why ovarectomized eNOS-deficient mice exhibit a defective anabolic response to exogenous estrogens, L-NAME reduces estradiol-induced bone formation in intact mice, and NO donors alleviate ovarectomy-induced bone loss in rats [19, 49, 50]. Several epidemiological studies and clinical trials suggest that NO donors may be as effective as estrogens in preventing bone loss in post-menopausal women [20]. However, NO donors may have detrimental effects due to their ability to generate oxidative stress [51], and our results provide a rationale for the use of direct activators of sGC or PKG as bone-protective agents.
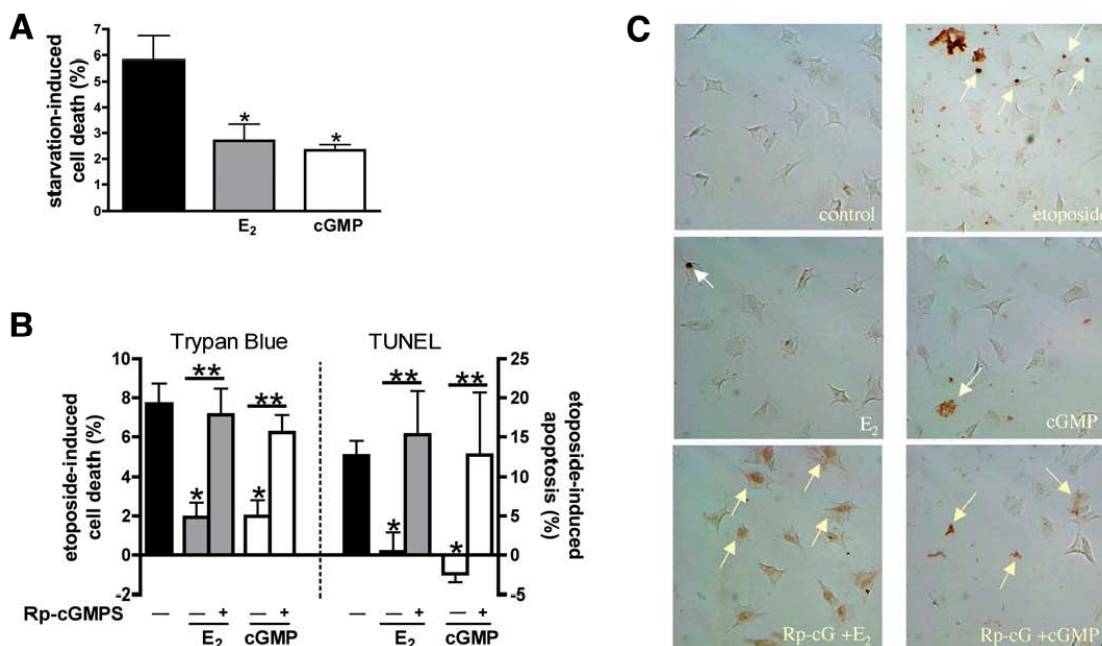
Figure 1: **Serum starvation- and etoposide-induced apoptosis is prevented by E₂ and cGMP and is mediated through PKG.** *A*. MLO-Y4 cells were treated with vehicle, 100 nM E₂, or 100 μM 8-pCPT-cGMP (cGMP) and serum starved for 18 h. Trypan blue uptake was measured as described in "Materials and Methods". *B*. MLO-Y4 cells were pretreated with 100 μM *R*p-8-CPT-PET-cGMPS (Rp-cGMPS) for 1 h where indicated followed by 100 nM E₂ or 100 μM cGMP for 1 h and then treated with etoposide for 8 h (trypan blue, left graph) or 6 h (TUNEL assay, right graph). *C*. Representative images of TUNEL staining in MLO-Y4 cells. Cells were treated as in *B*. *, p< 0.05 compared to apoptotic stimulus alone. **, p< 0.05 compared between presence and absence of Rp-cGMPS.
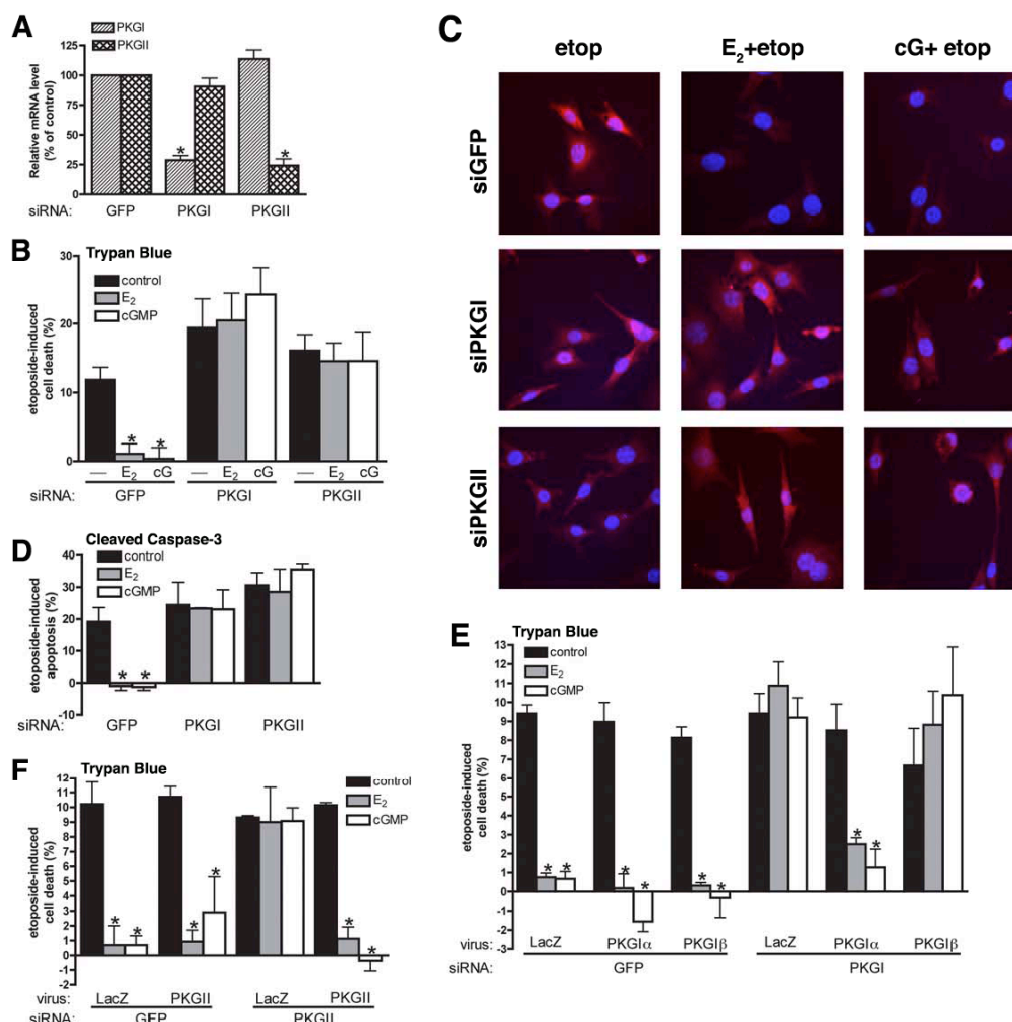
Figure 2: **PKGIα and PKGII are required for E₂- and cGMP-mediated protection from etoposide-induced apoptosis.** MLO-Y4 cells were transfected as described in "Materials and Methods" with siRNA targeting GFP, PKGI or PKGII as indicated. *A.* mRNA levels of PKGI and PKGII were measured 24 h after transfection. PKG mRNA levels measured in GFP (control) siRNA-transfected cells were considered 100% (internal normalization to *gapdh*). *B.* Twnety-four h after transfection, MLO-Y4 cells were treated with 100 nM E₂ or 100 μM cGMP for 1 h followed by an 8 h treatment with 50 μM etoposide. Trypan blue uptake was measured as described in "Materials and Methods". *C* and *D*. MLO-Y4 cells were treated as in *B* but cells were fixed, permeablized, and stained for cleaved caspase-3 and Hoechst to mark apoptotic cells. *C* shows representative pictures, *D* shows quantification of apoptotic cells. *E*. MLO-Y4 cells were infected with siRNA-resistant PKGIα or PKGIβ adenovirus 24 h post-transfection. Cells were treated with 100 nM E₂ or 100 μM cGMP for 1 h prior to treatment for 8 h with 50 μM etoposide. Trypan blue uptake was measured as in *B*. *F*. Cells were treated as in *E* except for transfection with PKGII siRNA and subsequent infection with a PKGII adenovirus. *****, p< 0.05 compared to control.
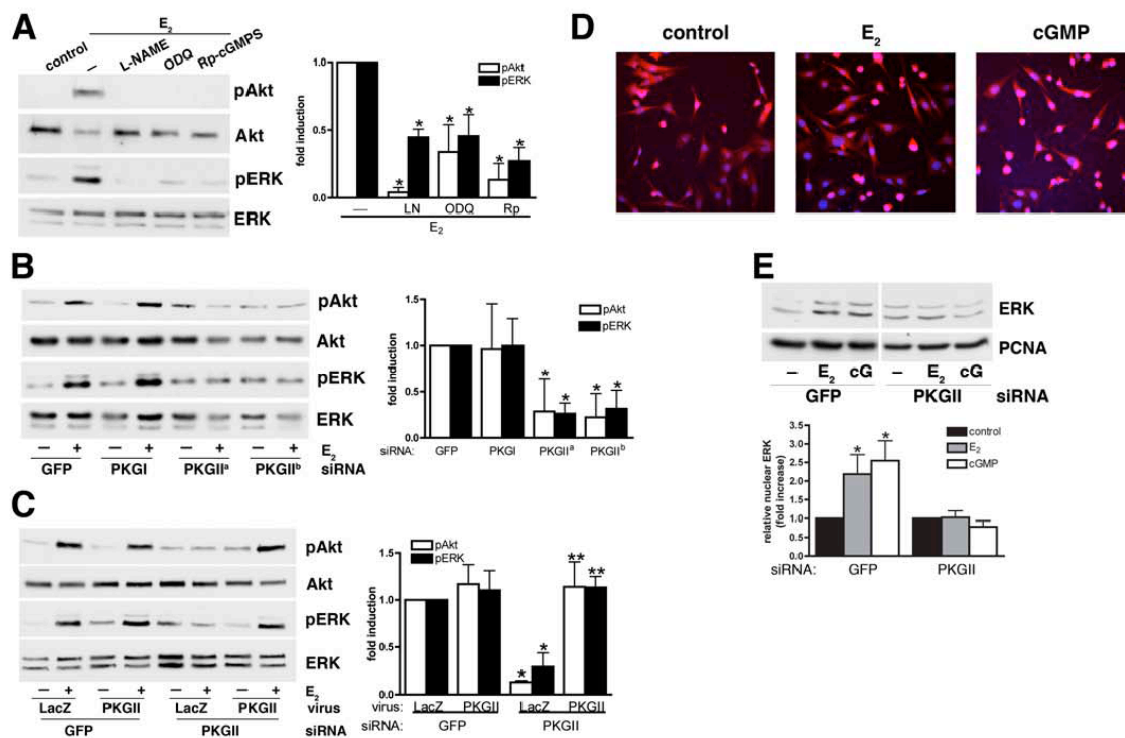
Figure 3:**E$_2$-induced Akt and ERK phosphorylation and ERK nuclear translocation is mediated by PKGII.** *A*. Serum-starved MLO-Y4 cells were pretreated with 4 mM L-NAME, 10 µM ODQ, or 100 µM *R*p-8-CPT-PET-cGMPS (Rp-cGMPS) for 1 h then stimulated with 100 nM E$_2$ for 5 min. *B*. MLO-Y4 cells were transfected with siRNA targeting GFP, PKGI, or PKGII (PKGII[a] and PKGII[b]). Twenty-four h post-transfection, cells were serum-starved for 12 h then stimulated with 100 nM E$_2$ for 5 min. *C*. Twenty-four h after GFP or PKGII siRNA transfection, MLO-Y4 cells were infected with adenoviruses encoding β-galactosidase (LacZ) or PKGII as indicated, for 10 h and then serum-starved for 18 h. Cells were then treated with 100 nM E$_2$ for 5 min. *D*. Cells were treated with 100 nM E$_2$ or 100 µM cGMP for 1 h and stained for ERK (red) and Hoechst (blue). *E*. MLO-Y4 cells were transfected with GFP or PKGII siRNA. Twenty-four h after transfection, cells were treated with 100 nM E$_2$ or 100 µM cGMP for 1 h. Cells were fractionated by differential centrifugation and the nuclear fraction was analyzed by Western blotting using antibodies specific for ERK and proliferating cell nuclear antigen (PCNA). *, $p < 0.05$ compared to control. **, $p < 0.05$ compared to cells transfected with PKGII siRNA and infected with the LacZ virus.
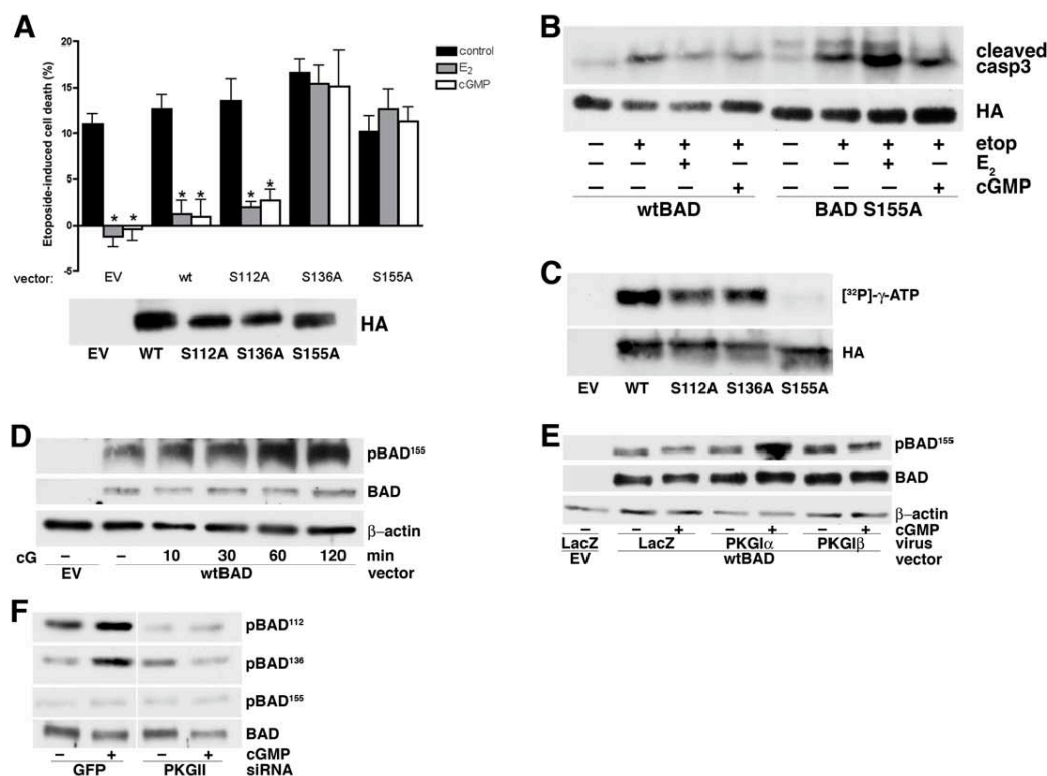
Figure 4: **BAD phosphorylation at Ser[155] is mediated by PKGIα and is necessary to prevent apoptosis.** *A*. MLO-Y4 cells were transfected with HA epitope-tagged wildtype or mutant BAD constructs as indicated. Forty-eight h post-transfection, cells were treated with 100 nM E_2 or 100 μM cGMP prior to treatment with 50 μM etoposide for 8 h. Trypan blue uptake was measured as described in "Materials and Methods". The lower panel shows expression of wildtype and mutant expression of BAD constructs in MLO-Y4 cells. *B*. MLO-Y4 cells were treated as in *A*. Cells were lysed and analyzed by Western blot using an antibody specific for cleaved caspase-3 and BAD expression was shown using an anti-HA antiboy. *C*. 293T cells were transfected with wildtype or mutant BAD constructs, immunoprecipitated with an anti-HA epitope antibody, and subjected to *in vitro* phosphorylation with purified PKGI in the presence of $[^{32}P]$-γ-ATP. *D*. MLO-Y4 cells were transfected with empty vector (EV) or wildtype BAD as indicated. Twenty-four h after transfection, cells were infected with PKGIα adenovirus. Twenty-four h post-infection, cells were treated with 100 μM cGMP for the indicated times. BAD phosphorylation was on Ser[155] was detected using a phospho-specific antibody. *E*. MLO-Y4 cells were transfected as in *D*. Twenty-four h later, cells were infected with either the LacZ, PKGIα, or PKGIβ adenoviruses. Twenty-four h post-infection, cells were treated with 100 μM cGMP for 1 h. Note that the endogenous PKGIα is no sufficient for phosphorylation of over-expressed BAD. *F*. MLO-Y4 cells were transfected with siRNA targeting GFP or PKGII. Twenty-four h later, cells were transfected with wildtype BAD. Twenty-four h post DNA-transfection, cells were infected with PKGIα virus for 24 h prior to 100 μM cGMP treatment for 1 h. *, $p < 0.05$ compared to control.
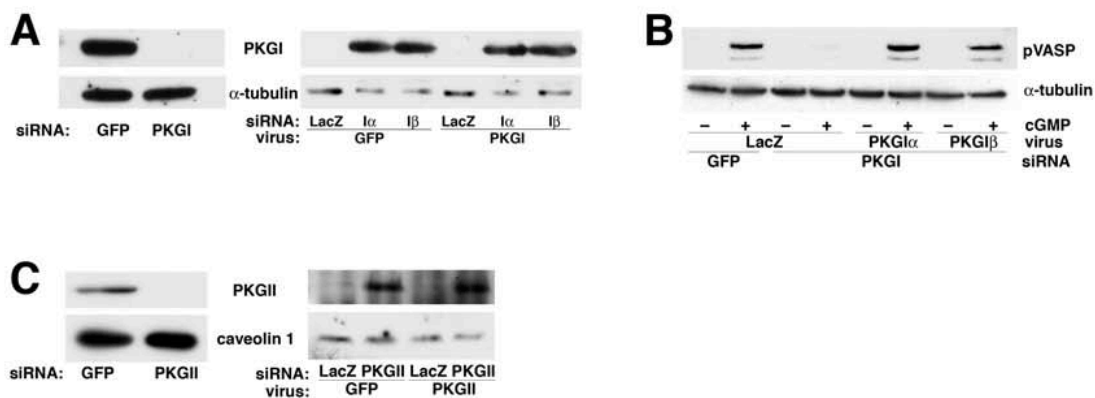
Supplemental Figure 1:**Knockdown and viral reconstitution of PKGI and II.** *A*. MLO-Y4 cells were transfected with GFP or PKGI siRNA as indicated. Twenty-four h later, cells were harvested (left panels) and fractionated. Cytosolic fractions are analyzed for endogenous PKGI expression. (right panels). Twenty-four h after siRNA transfection, cells were infected with adenoviruses encoding β-galactosidase (LacZ), PKGIα, or PKGIβ for another 24 h. Cells were harvested and fractionated by differential centrifugation; cytosolic fractions were analyzed for endogenous and viral PKGI. *B*. Serum-starved MLO-Y4 cells were treated with 100 μM cGMP for 30 min and blotted with an antibody specific for pVASP[259], a PKG specific phosphorylation site. *C*. MLO-Y4 cells were transfected with GFP or PKGII siRNA. Twenty-four h later, cells were harvested and fractionated; membrane fractions were examined for endogenous PKGII expression (left panels). Cells were infected with LacZ or PKGII adenovirus 24 h post-transfection. Cells were harvested 24 h later, fractionated, and membrane fractions were analyzed for endogenous and viral PKGII levels (right panels).
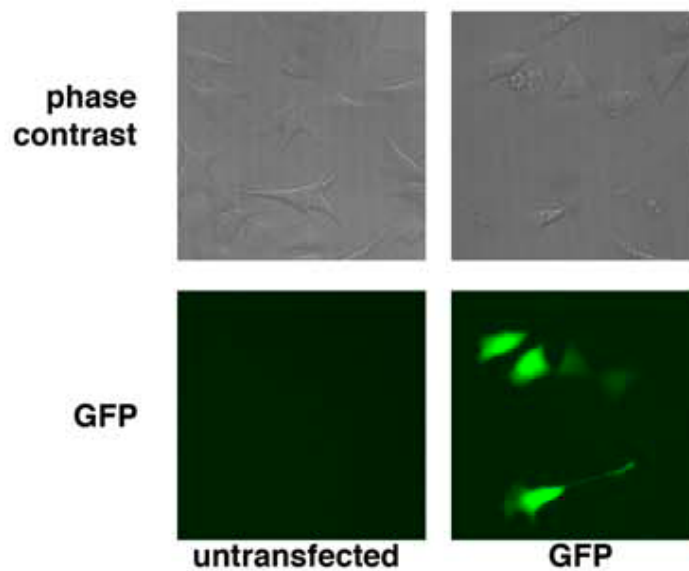
Supplemental Figure 2: **Transfection efficiency of MLO-Y4 cells.** MLO-Y4 cells were left untransfected or transfected with GFP. Forty-eight h post-transfection, cells were analyzed for GFP-positive cells.

REFERENCES

1.   Boskey AL, Coleman R: **Aging and bone.** *J Dent Res* 2010, **89:**1333-1348.

2.   Manolagas SC: **From estrogen-centric to aging and oxidative stress: a revised perspective of the pathogenesis of osteoporosis.** *Endocr Rev* 2010, **31:**266-300.

3.   Wessler S, Otto C, Wilck N, Stangl V, Fritzemeier KH: **Identification of estrogen receptor ligands leading to activation of non-genomic signaling pathways while exhibiting only weak transcriptional activity.** *J Steroid Biochem Mol Biol* 2006, **98:**25-35.

4.   Chen JR, Plotkin LI, Aguirre JI, Han L, Jilka RL, Kousteni S, Bellido T, Manolagas SC: **Transient versus sustained phosphorylation and nuclear accumulation of ERKs underlie anti-versus pro-apoptotic effects of estrogens.** *J Biol Chem* 2005, **280:**4632-4638.

5.   Kousteni S, Han L, Chen JR, Almeida M, Plotkin LI, Bellido T, Manolagas SC: **Kinase-mediated regulation of common transcription factors accounts for the bone-protective effects of sex steroids.** *J Clin Invest* 2003, **111:**1651-1664.

6.   Jessop HL, Sjoberg M, Cheng MZ, Zaman G, Wheeler-Jones CP, Lanyon LE: **Mechanical strain and estrogen activate estrogen receptor alpha in bone cells.** *J Bone Miner Res* 2001, **16:**1045-1055.

7.   Armour KE, Ralston SH: **Estrogen upregulates endothelial constitutive nitric oxide synthase expression in human osteoblast-like cells.** *Endocrinology* 1998, **139:**799-802.

8.   Huang A, Sun D, Koller A, Kaley G: **17beta-estradiol restores endothelial nitric oxide release to shear stress in arterioles of male hypertensive rats.** *Circulation* 2000, **101:**94-100.

9.   Sakamoto M, Uen T, Nakamura T, Hashimoto O, Sakata R, Kin M, Ogata R, Kawaguch T, Torimura T, Sata M: **Estrogen upregulates nitric oxide synthase expression in cultured rat hepatic sinusoidal endothelial cells.** *J Hepatol* 2001, **34:**858-864.

10.   van't Hof RJ, Ralston SH: **Nitric oxide and bone.** *Immunology* 2001, **103:**255-261.

11.   Francis SH, Busch JL, Corbin JD, Sibley D: **cGMP-dependent protein kinases and cGMP phosphodiesterases in nitric oxide and cGMP action.** *Pharmacol Rev* 2010, **62:**525-563.

12. Rangaswami H, Marathe N, Zhuang S, Chen Y, Yeh JC, Frangos JA, Boss GR, Pilz RB: **Type II cGMP-dependent protein kinase mediates osteoblast mechanotransduction.** *J Biol Chem* 2009, **284:**14796-14808.

13. Rangaswami H, Schwappacher R, Marathe N, Zhuang S, Casteel DE, Haas B, Chen Y, Pfeifer A, Kato H, Shattil S, et al: **Cyclic GMP and protein kinase G control a Src-containing mechanosome in osteoblasts.** *Sci Signal* 2010, **3:**ra91.

14. Pfeifer A, Aszodi A, Seidler U, Ruth P, Hofmann F, Fassler R: **Intestinal secretory defects and dwarfism in mice lacking cGMP-dependent protein kinase II.** *Science* 1996, **274:**2082-2086.

15. Blaise GA, Gauvin D, Gangal M, Authier S: **Nitric oxide, cell signaling and cell death.** *Toxicology* 2005, **208:**177-192.

16. Cheung WY, Liu C, Tonelli-Zasarsky RM, Simmons CA, You L: **Osteocyte apoptosis is mechanically regulated and induces angiogenesis in vitro.** *J Orthop Res* 2011, **29:**523-530.

17. Chae HJ, Chin HY, Lee GY, Park HR, Yang SK, Chung HT, Pae HO, Kim HM, Chae SW, Kim HR: **Carbon monoxide and nitric oxide protect against tumor necrosis factor-alpha-induced apoptosis in osteoblasts: HO-1 is necessary to mediate the protection.** *Clin Chim Acta* 2006, **365:**270-278.

18. Wang J, Shang F, Mei Q, Wang J, Zhang R, Wang S: **NO-donating genistein prodrug alleviates bone loss in ovariectomised rats.** *Swiss Med Wkly* 2008, **138:**602-607.

19. Wimalawansa SJ, De Marco G, Gangula P, Yallampalli C: **Nitric oxide donor alleviates ovariectomy-induced bone loss.** *Bone* 1996, **18:**301-304.

20. Jamal SA, Cummings SR, Hawker GA: **Isosorbide mononitrate increases bone formation and decreases bone resorption in postmenopausal women: a randomized trial.** *J Bone Miner Res* 2004, **19:**1512-1517.

21. Grassi F, Fan X, Rahnert J, Weitzmann MN, Pacifici R, Nanes MS, Rubin J: **Bone re/modeling is more dynamic in the endothelial nitric oxide synthase(-/-) mouse.** *Endocrinology* 2006, **147:**4392-4399.

22. Kato Y, Windle JJ, Koop BA, Mundy GR, Bonewald LF: **Establishment of an osteocyte-like cell line, MLO-Y4.** *J Bone Miner Res* 1997, **12:**2014-2023.

23. Gudi T, Lohmann SM, Pilz RB: **Regulation of gene expression by cyclic GMP-dependent protein kinase requires nuclear translocation of the kinase: identification of a nuclear localization signal.** *Mol Cell Biol* 1997, **17:**5244-5254.

24.   Cherney A, Edgell H, Krukoff TL: **NO mediates effects of estrogen on central regulation of blood pressure in restrained, ovariectomized rats.** *Am J Physiol Regul Integr Comp Physiol* 2003, **285:**R842-849.

25.   Gingerich S, Krukoff TL: **Estrogen modulates endothelial and neuronal nitric oxide synthase expression via an estrogen receptor beta-dependent mechanism in hypothalamic slice cultures.** *Endocrinology* 2005, **146:**2933-2941.

26.   O'Shaughnessy MC, Polak JM, Afzal F, Hukkanen MV, Huang P, MacIntyre I, Buttery LD: **Nitric oxide mediates 17beta-estradiol-stimulated human and rodent osteoblast proliferation and differentiation.** *Biochem Biophys Res Commun* 2000, **277:**604-610.

27.   Kousteni S, Bellido T, Plotkin LI, O'Brien CA, Bodenner DL, Han L, Han K, DiGregorio GB, Katzenellenbogen JA, Katzenellenbogen BS, et al: **Nongenotropic, sex-nonspecific signaling through the estrogen or androgen receptors: dissociation from transcriptional activity.** *Cell* 2001, **104:**719-730.

28.   Chipuk JE, Green DR: **How do BCL-2 proteins induce mitochondrial outer membrane permeabilization?** *Trends Cell Biol* 2008, **18:**157-164.

29.   Wong WW, Puthalakath H: **Bcl-2 family proteins: the sentinels of the mitochondrial apoptosis pathway.** *IUBMB Life* 2008, **60:**390-397.

30.   Datta SR, Katsov A, Hu L, Petros A, Fesik SW, Yaffe MB, Greenberg ME: **14-3-3 proteins and survival kinases cooperate to inactivate BAD by BH3 domain phosphorylation.** *Mol Cell* 2000, **6:**41-51.

31.   Johlfs MG, Fiscus RR: **Protein kinase G type-Ialpha phosphorylates the apoptosis-regulating protein Bad at serine 155 and protects against apoptosis in N1E-115 cells.** *Neurochem Int* 2010, **56:**546-553.

32.   Lizcano JM, Morrice N, Cohen P: **Regulation of BAD by cAMP-dependent protein kinase is mediated via phosphorylation of a novel site, Ser155.** *Biochem J* 2000, **349:**547-557.

33.   Danial NN: **BAD: undertaker by night, candyman by day.** *Oncogene* 2008, **27 Suppl 1:**S53-70.

34.   Tatsumi S, Ishii K, Amizuka N, Li M, Kobayashi T, Kohno K, Ito M, Takeshita S, Ikeda K: **Targeted ablation of osteocytes induces osteoporosis with defective mechanotransduction.** *Cell Metab* 2007, **5:**464-475.

35.   Dai Z, Li Y, Quarles LD, Song T, Pan W, Zhou H, Xiao Z: **Resveratrol enhances proliferation and osteoblastic differentiation in human**

mesenchymal stem cells via ER-dependent ERK1/2 activation. *Phytomedicine* 2007, **14:**806-814.

36.   Gu G, Hentunen TA, Nars M, Harkonen PL, Vaananen HK: **Estrogen protects primary osteocytes against glucocorticoid-induced apoptosis.** *Apoptosis* 2005, **10:**583-595.

37.   Sun B, Karin M: **NF-kappaB signaling, liver disease and hepatoprotective agents.** *Oncogene* 2008, **27:**6228-6244.

38.   Xing D, Nozell S, Chen YF, Hage F, Oparil S: **Estrogen and mechanisms of vascular protection.** *Arterioscler Thromb Vasc Biol* 2009, **29:**289-295.

39.   Cheskis BJ, Greger JG, Nagpal S, Freedman LP: **Signaling by estrogens.** *J Cell Physiol* 2007, **213:**610-617.

40.   Moriarty K, Kim KH, Bender JR: **Minireview: estrogen receptor-mediated rapid signaling.** *Endocrinology* 2006, **147:**5557-5563.

41.   Gorbe A, Giricz Z, Szunyog A, Csont T, Burley DS, Baxter GF, Ferdinandy P: **Role of cGMP-PKG signaling in the protection of neonatal rat cardiac myocytes subjected to simulated ischemia/reoxygenation.** *Basic Res Cardiol* 2010, **105:**643-650.

42.   Kim YM, Chung HT, Kim SS, Han JA, Yoo YM, Kim KM, Lee GH, Yun HY, Green A, Li J, et al: **Nitric oxide protects PC12 cells from serum deprivation-induced apoptosis by cGMP-dependent inhibition of caspase signaling.** *J Neurosci* 1999, **19:**6740-6747.

43.   Wong JC, Fiscus RR: **Essential roles of the nitric oxide (no)/cGMP/protein kinase G type-Ialpha (PKG-Ialpha) signaling pathway and the atrial natriuretic peptide (ANP)/cGMP/PKG-Ialpha autocrine loop in promoting proliferation and cell survival of OP9 bone marrow stromal cells.** *J Cell Biochem* 2011, **112:**829-839.

44.   Weber S, Bernhard D, Lukowski R, Weinmeister P, Worner R, Wegener JW, Valtcheva N, Feil S, Schlossmann J, Hofmann F, Feil R: **Rescue of cGMP kinase I knockout mice by smooth muscle specific expression of either isozyme.** *Circ Res* 2007, **101:**1096-1103.

45.   Tang KM, Wang GR, Lu P, Karas RH, Aronovitz M, Heximer SP, Kaltenbronn KM, Blumer KJ, Siderovski DP, Zhu Y, Mendelsohn ME: **Regulator of G-protein signaling-2 mediates vascular smooth muscle relaxation and blood pressure.** *Nat Med* 2003, **9:**1506-1512.

46. Surks HK, Mochizuki N, Kasai Y, Georgescu SP, Tang KM, Ito M, Lincoln TM, Mendelsohn ME: **Regulation of myosin phosphatase by a specific interaction with cGMP- dependent protein kinase Ialpha.** *Science* 1999, **286:**1583-1587.

47. Casteel DE, Zhuang S, Gudi T, Tang J, Vuica M, Desiderio S, Pilz RB: **cGMP-dependent protein kinase I beta physically and functionally interacts with the transcriptional regulator TFII-I.** *J Biol Chem* 2002, **277:**32003-32014.

48. Schlossmann J, Ammendola A, Ashman K, Zong X, Huber A, Neubauer G, Wang GX, Allescher HD, Korth M, Wilm M, et al: **Regulation of intracellular calcium by a signalling complex of IRAG, IP3 receptor and cGMP kinase Ibeta.** *Nature* 2000, **404:**197-201.

49. Armour KE, Armour KJ, Gallagher ME, Godecke A, Helfrich MH, Reid DM, Ralston SH: **Defective bone formation and anabolic response to exogenous estrogen in mice with targeted disruption of endothelial nitric oxide synthase.** *Endocrinology* 2001, **142:**760-766.

50. Samuels A, Perry MJ, Gibson RL, Colley S, Tobias JH: **Role of endothelial nitric oxide synthase in estrogen-induced osteogenesis.** *Bone* 2001, **29:**24-29.

51. Wimalawansa SJ: **Rationale for using nitric oxide donor therapy for prevention of bone loss and treatment of osteoporosis in humans.** *Ann N Y Acad Sci* 2007, **1117:**283-297.

Chapter 3:

Apoptosis in Bone

ABSTRACT

Estradiols are known to decrease apoptosis in osteocytes. In chapter 2, we showed that this effect was mediated through the NO/cGMP pathway. In this chapter, we examine another hormone, triiodothyronine (T3), which also rapidly increases NO production and protects cells from undergoing apoptosis. We found that T3 prevented etoposide-induced apoptosis in osteocytes in a NO/cGMP/PKG- dependent manner. Furthermore, treatment with 8-pCPT-cGMP, a membrane-permeable cGMP analog, prevented etoposide-induced upregulation of *bim, bad*, and *bax* mRNA transcription. Lastly, UMR106 cells were also rescued from apoptosis with 8-pCPT-cGMP when challenged with the glucocorticoid, dexamethasone, suggesting that the effects of the NO/cGMP/PKG pathway can be generalized as an anti-apoptotic mechanism in bone cells.

INTRODUCTION

We show in Chapter 2 that estradiol signaling, mediated through cGMP and PKGs, is able to prevent apoptosis in osteocytes. However, this phenomenon is not limited to estradiol-mediated signal transduction in osteocytes or to apoptosis induced by etoposide.

Triiodothyronine (T3) is a thyroid hormone that is also known to elevate nitric oxide (NO) production [1]. T3 binding to the thyroid hormone receptor (TR-α or TR-β) allows for the receptor association with the p85 subunit of phosphoinositide-3-kinase (PI3K) and subsequent phosphorylation and activation of endothelial nitric oxide synthase (eNOS) [1]. Extragenomic signaling through the TR is also shown to prevent apoptosis in neuronal cells, hepatocytes and pancreatic islets *ex vivo* cultures [2-4]. Genetic knockout mice of each of the TRs show significant, albeit differing, skeletal defects. TR-α null mice show a transient growth delay, and as adults have osteosclerosis with increased trabecular bone volume due to impaired osteoclast resorption [5]. TR-β knockout mice have short stature but are osteoporotic because of increased bone resorption [5]. The double knockout mice have brittle bones and a reduced bone formation rate [5]. These data indicate that effects of T3 are important in bone development and skeletal maintenance.

Estradiol and T3 may also protect osteocytes from apoptosis through transcriptional regulation of anti-apoptotic genes. Both the estrogen receptor and the TR can translocate to the nucleus and control gene expression by either binding directly to the DNA or by forming a complex with other co-activators or co-repressors.

Additionally, the rapid signaling cascades induced by the hormones may also lead to transcriptional regulation of apoptotic genes.

Dexamethasone is a synthetic corticosteroid used in the treatment of inflammatory and autoimmune diseases [6]. However, a major side effect of long term dexamethasone (or any glucocorticoid) is glucocorticoid-induced osteoporosis [7]. It has been shown that dexamethasone induces osteoblast and osteocyte apoptosis, prevents osteoblast proliferation and differentiation and may increase osteoclastogenesis [8]. Glucocorticoids exert their effects by diffusing into the cell and binding to the cytosolic glucocorticoid receptors (GRs). These receptors then translocate to the nucleus and control transcription of target genes. A number of pro-inflammatory genes are down-regulated in response to dexamethasone and other glucocorticoids, including interleukins (IL)-3 and IL-5, chemokines, cytokines, granulocyte-macrophage colony stimulating factor (GM-CSF), and tumor necrosis factor alpha (TNFα) genes [9]. Additionally, glucocorticoids negatively regulate transcription of osteocalcin and stimulate expression of RANKL, a hormone secreted by osteoblasts to enhance resorption by osteoclasts [10].

In this chapter, we show that, similar to estradiol, the T3-induced NO production activated the NO/cGMP/PKG pathway, resulting in an anti-apoptotic effect. In addition to the rapid signaling effects, treatment with cGMP prevented the etoposide-induced increases in pro-apoptotic gene transcription. Furthermore, we demonstrate that the anti-apoptotic effects are not limited to protection against etoposide but can be generalized to other apoptosis-stimulating agents.

MATERIALS AND METHODS

Materials- 17β-estradiol, etoposide, and dexamethasone were purchased from Sigma. The cGMP agonist 8-(4-chlorophenylthio)-GMP (8-pCPT-cGMP) and cGMP antagonist 8-(4-chlorophenylthio)- β-phenyl-1,N^2-ethenoguanosine-3',5'-cyclic monophosphorothioate, *R*p isomer (*R*p-8-pCPT-PET-cGMPS) were from Biolog. The NOS inhibitor *N*-nitro-L-arginine methyl ester (L-NAME), the sGC inhibitor 1*H*-[1,2,4]oxadiazolo[4,3-*a*]quinoxalin-1-one (ODQ), were from Cayman.

Cell Culture- The murine osteocytic cell line MLO-Y4 was maintained in αMEM supplemented with 2.5% enriched calf serum and 2.5% heat-inactivated fetal bovine serum. The UMR106 rat osteosarcoma cell lime was maintained in Dulbecco's modified Eagle's medium with 10% fetal bovine serum.

Quantification of Apoptotic Cells- MLO-Y4 or UMR106 cells were treated with vehicle or inhibitors for 1 hour prior to a 1 hour stimulation with 1 nM T3 or 100 μM 8-pCPT-cGMP. Subsequently, cells were treated with 50 μM etoposide or 10 μM dexamethasone for 8 hours. A minumum of 200 cells for each condition were examined by trypan blue uptake for cell death. Induced cell death was calculated by subtracting the percentage of trypan-blue positive cells observed in vehicle-treated samples from the experimental sample.

RT-PCR- RNA was extracted using TriReagent (Molecular Research Center, Inc.) and 1μg was reversed transcribed using Superscript reverse transcriptase (Invitrogen). *gapdh* was used as an internal control. qRT-PCR values were analyzed using the $2^{-\Delta\Delta Ct}$ method. Primer sequences are given in Table 1.

Statistical Analyses- Data were analyzed by one- way analysis of variance (ANOVA) with Bonferroni post-test. A *p* value of <0.05 was considered statistically significant. Bar graphs are shown as the mean± SEM of at least two independent experiments.

RESULTS

T3 Mediates Osteocyte Apoptosis Through the NO/cGMP Pathway- T3 is known to increase NO production through the activation of eNOS and prevent apoptosis in a number of cell types [1-4]. We therefore examined if this protective effect extended to bone cells and was mediated through the NO/cGMP pathway. MLO-Y4 osteocytes were pretreated with vehicle, 4 mM L-NAME (NOS inhibitor), 10 μM ODQ (sGC inhibitor), 100 μM *R*p-8-pCPT-PET-cGMPS (PKG inhibitor), 10 μM PP2 (Src family inhibitor), or 10 μM PP3 (inactive analog of PP2) for 1 hour. Cells were then stimulated for 1 hour with 1 nM T3 prior to an 8 hour etoposide treatment. Cell death was measured by trypan blue uptake. Etoposide induced cell death in about 5% of the cell population. Etoposide-induced cell death was abolished with T3 treatment but remained high in the presence of the inhibitors listed above. PP3 did not affect the T3-mediated prevention of apoptosis (Fig. 1). These data suggest that the NO/cGMP/PKG pathway and a Src family kinase are integral in T3-mediated apoptosis protection in osteocytes.

Etoposide and cGMP Regulate Pro-apoptotic Gene Transcription- Since cGMP, through Akt and ERK (as described in Chapter 2), can ultimately influence a number of downstream transcription factors and co-regulators, we sought to determine if cGMP regulated mRNA expression of Bcl-2 family genes. We examined three pro-apoptotic genes: Bim, BAD, and Bax. Bim and BAD are BH3-domain only proteins which function sequestering the anti-apoptotic Bcl-2 family members [11]. Bax is a multi-domain pro-apoptotic protein which is an integral part of the mitochondrial outer membrane permeabilization pore [12]. Etoposide increased the mRNA expression level of each of

these genes by as much as 3-fold while pretreatment with cGMP prevented this increase in pro-apoptotic gene expression (Fig. 2). *gapdh* was used as an internal control and its expression was not affected by either treatment. These results indicate that the pro-survival effects cGMP occur, in part, through repression of pro-apoptotic genes.

Dexamethasone Induces Cell Death which is Prevented Through the Activation of NO/cGMP/PKG- We further tested whether activation of the NO/cGMP/PKG pathway could protect UMR106 rat osteoblastic cells from death induced by another apoptotic stimulus. The UMR106 cells needed to be sensitized to apoptosis by pretreatment with a sub-lethal concentration of PP2. One μM dexamethasone treatment alone for 8 hours did not affect cell death but, in conjunction with 1 μM PP2, it induced cell death in over 15% of the cell population (Fig. 3). 8-pCPT-cGMP decreased cell death to basal levels. PP3 did not sensitize the UMR106 cells to dexamethasone treatment.

To further examine the role of the NO/cGMP pathway, UMR106 cells were additionally pretreated with either ODQ or *R*p-8-pCPT-PET-cGMPS and stimulated with either 3 μM DETA-NONOate (an NO donor) or 100 μM 8-pCPT-cGMP prior to dexamethasone treatment. Both DETA-NONOate and 8-pCPT-cGMP were able to reduce apoptosis. However, ODQ prevented the protective effect of NO, while *R*p-8-pCPT-PET-cGMPS prevented the cGMP-mediated pro-survival effect (Fig. 4). Therefore, we conclude that NO and cGMP, acting through PKG, can prevent dexamethasone-induced apoptosis.

DISCUSSION

We found that T3 had a similar mechanism for promoting cell survival as estradiol. We also observed that the NO/cGMP pathway regulated dexamethasone-induced cell death in osteosarcoma cells. This supports the concept of the NO/cGMP pathway as a general pro-survival pathway in bone-forming since similar results were obtained using two different NO-elevating agents, two apoptosis-inducing agents, and two cell lines.

The anti-apoptotic effect may be mediated, in part, by lowering the etoposide-induced mRNA transcription of *bim, bad,* and *bax*. Expression of *bim, bad,* and *bax* mRNA, as well as protein, has been previously been shown to increase following etoposide treatment in C2C12 skeletal myoblast cells [13]. The effect of cGMP on mRNA expression may be the result of downstream signaling from PKGII-activated Akt and ERK since both kinases exhibit such strong pro-survival effects. Experiments in neuronal cells indicate that stimulating PKG activity attenuated a serum-deprivation induced increase in BAX protein expression [14]. Hsu *et al* also describe an increase in Bcl-2 protein which we did not observe in the etoposide-induced osteocytes [14]. Furthermore, transcription of *bim* mRNA has been shown to be controlled by the forkhead transcription factor, FOXO3a, in a number of cell types [15-17]. The FOXO family of transcription factors modulates cell fate by controlling genes involved in apoptosis, cell cycle, and DNA repair [18]. FOXO3a is inactivated by Akt phosphorylation [18, 19]. Thus, *bim* mRNA expression could be regulated by a mechanism whereby PKGII-activation of Akt leads to inactivation of FOXO3a, resulting in no increase in *bim* mRNA expression. Additionally, both *bad* and *bax* gene expression

has been shown to be controlled by the tumor suppressor, p53, in lung cancer cells [20]. Since p53 is also regulated downstream of Akt [21], it is possible that Akt activation by PKGII and cGMP leads to downstream repression of *bim, bad* and *bax* gene expression. To test this hypothesis, pharmacological inhibition of PI3K or Akt, or siRNA targeting Akt should result in an etoposide-induced increase in *bim, bad*, and *bax* mRNA expression, regardless of the presence or absence of cGMP pretreatment. cGMP stimulation of MLO-Y4 cells should also reveal FOXO3a phosphorylation and p53 degradation, which would be prevented by siRNA targeting Akt or PKGII. Taken together, these data could uncover a role of PKGII activation of Akt in regulating apoptotic genes.

Acknowledgements:

The work presented in this chapter was performed by the dissertation author.

Table 1: **qRT-PCR primers**

Gene		Primer (5'-3')
gapdh	sense	AGGTCGGTGTGAACGGATTTG
	antisense	TGTAGACCATGTAGTTGAGGTCA
bim	sense	CGACAGTCTCAGGAGGAACC
	antisense	CCTTCTCCATACCAGACGGA
bad	sense	AAGTCCGATCCCGGAATCC
	antisense	GCTCACTCGGCTCAAACTCT
bax	sense	TGAAGACAGGGGCCTTTTTG
	antisense	AATTCGCCGGAGACACTCG
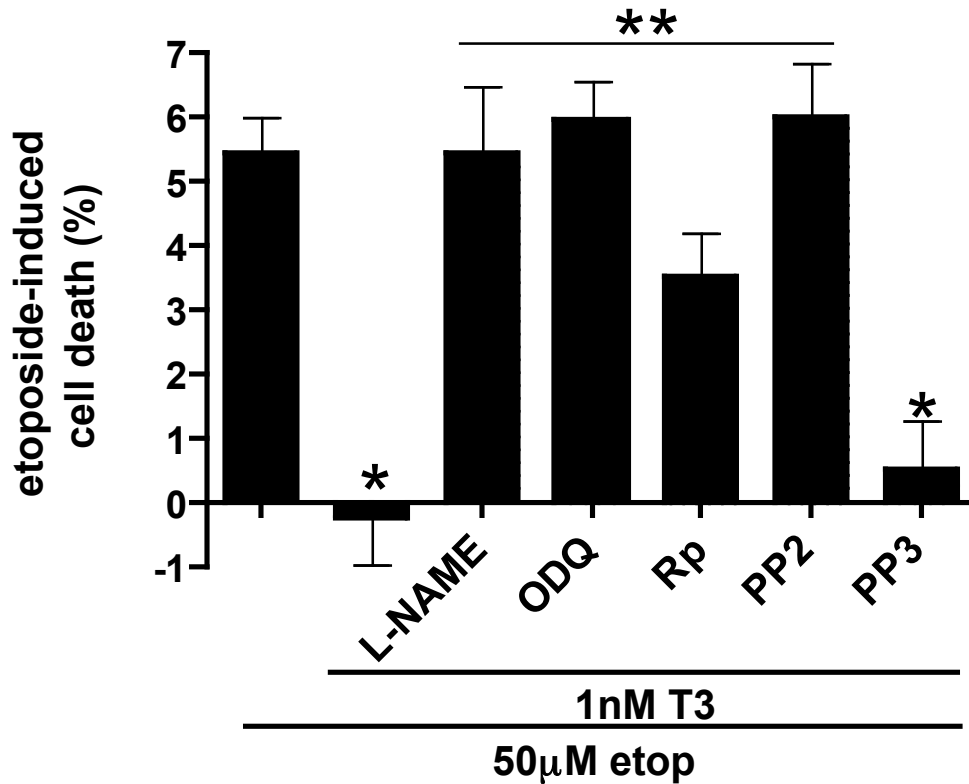
Figure 1: **T3 mediates cell survival through the NO/cGMP pathway and Src.** MLO-Y4 osteocytes were pretreated with 4 mM L-NAME, 10 μM ODQ, 100 μM *R*p-8-pCPT-cGMPS (Rp), 10 μM PP2, or 10 μM PP3 for 1 h prior to 1 nM T3 stimulation for 1 h and 50 μM etoposide (etop) for 8 h. Cell death was quantified by trypan blue uptake. *, $p < 0.05$ compared with etoposide. **, $p < 0.05$ compared with T3. ($n \geq 3$ experiments)
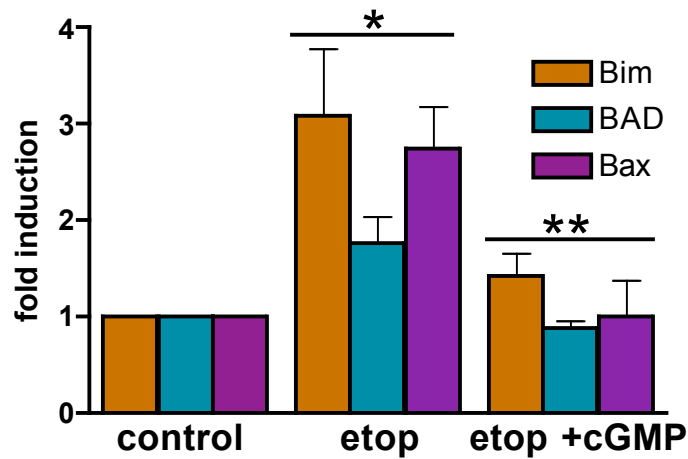
Figure 2: **cGMP regulates mRNA expression of *bim*, *bad*, and *bax*.** Where indicated, MLO-Y4 cells were pretreated with 100 μM 8-pCPT-cGMP for 1 h prior to treatment with 50 μM etoposide (etop) for 5 h. RNA was harvested and subjected to qRT-PCR as described in "Materials and Methods". Gene expression was standardized to *gapdh*. Sham-treated cells were considered as control and normalized as 1. *, $p < 0.05$ compared to control. **, $p < 0.05$ compared to etop. (n=3 experiments)
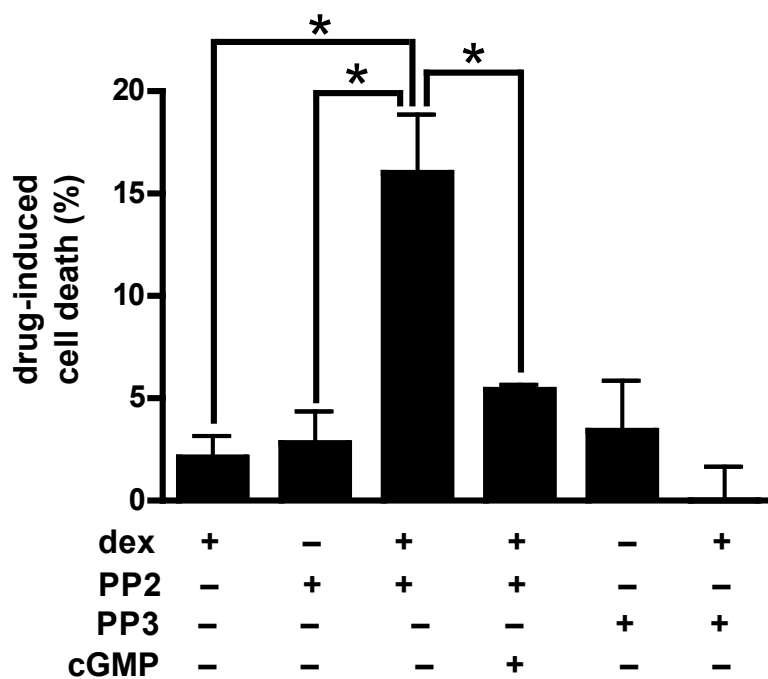
Figure 3: **Dexamethasone-induced cell death.** UMR106 cells were subjected to 100 μM 8-pCPT-cGMP (cGMP) pretreatment for 1 h, sensitization with 1 μM PP2 or PP3 for 30 min, and treatment with 1 μM dexamethasone (dex) for 8 h. Cell death was measured by trypan blue uptake. *, $p < 0.05$. (n≥2 experiments)
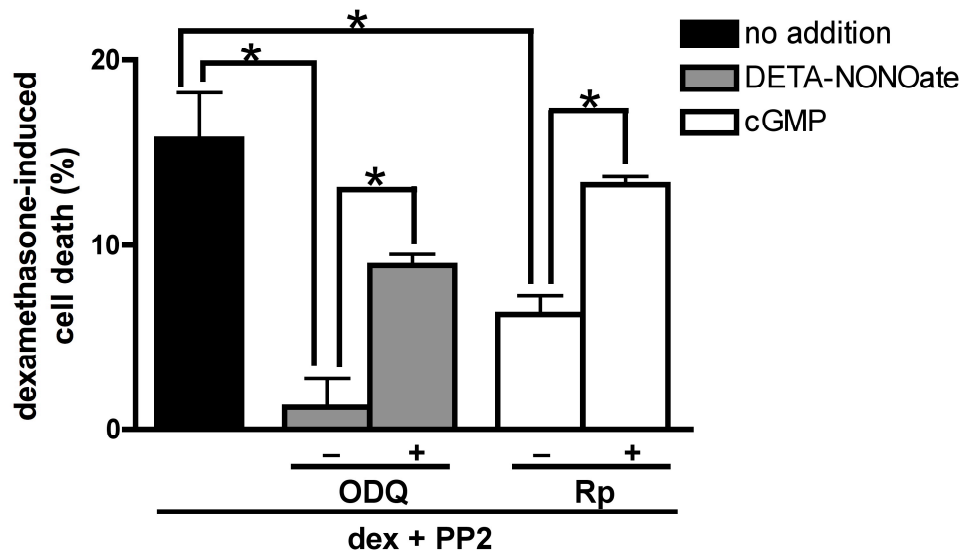
Figure 4: **The NO/cGMP pathway prevents dexamethasone-induced cell death.** As indicated, some UMR106 cells were pretreated with 10 μM ODQ or 100 μM R_p-8-pCPT-cGMPS (Rp) prior to stimulation with 3 μM DETA-NONOate or 100 μM 8-pCPT-cGMP and treatment with 1 μM PP2 and 1 μM dexamethasone (dex). Cell death was measured by trypan blue uptake. *, $p < 0.05$. (n≥ 2 experiments)

REFERENCES

1.   Hiroi Y, Kim HH, Ying H, Furuya F, Huang Z, Simoncini T, Noma K, Ueki K, Nguyen NH, Scanlan TS, et al: **Rapid nongenomic actions of thyroid hormone.** *Proc Natl Acad Sci U S A* 2006, **103:**14104-14109.

2.   Cao X, Kambe F, Yamauchi M, Seo H: **Thyroid-hormone-dependent activation of the phosphoinositide 3-kinase/Akt cascade requires Src and enhances neuronal survival.** *Biochem J* 2009, **424:**201-209.

3.   Verga Falzacappa C, Mangialardo C, Raffa S, Mancuso A, Piergrossi P, Moriggi G, Piro S, Stigliano A, Torrisi MR, Brunetti E, et al: **The thyroid hormone T3 improves function and survival of rat pancreatic islets during in vitro culture.** *Islets* 2010, **2:**96-103.

4.   Sukocheva OA, Carpenter DO: **Anti-apoptotic effects of 3,5,3'-tri-iodothyronine in mouse hepatocytes.** *J Endocrinol* 2006, **191:**447-458.

5.   Gogakos AI, Duncan Bassett JH, Williams GR: **Thyroid and bone.** *Arch Biochem Biophys* 2010, **503:**129-136.

6.   **D e x a m e t h a s o n e   O r a l** [http://www.ncbi.nlm.nih.gov/pubmedhealth/PMH0000773/]

7.   Limbourg FP, Liao JK: **Nontranscriptional actions of the glucocorticoid receptor.** *J Mol Med* 2003, **81:**168-174.

8.   Caplan L, Saag KG: **Glucocorticoids and the risk of osteoporosis.** *Expert Opin Drug Saf* 2009, **8:**33-47.

9.   Newton R: **Molecular mechanisms of glucocorticoid action: what is important?** *Thorax* 2000, **55:**603-613.

10. Ferron M, Wei J, Yoshizawa T, Del Fattore A, DePinho RA, Teti A, Ducy P, Karsenty G: **Insulin signaling in osteoblasts integrates bone remodeling and energy metabolism.** *Cell* 2010, **142:**296-308.

11. Lomonosova E, Chinnadurai G: **BH3-only proteins in apoptosis and beyond: an overview.** *Oncogene* 2008, **27 Suppl 1:**S2-19.

12. Danial NN: **BAD: undertaker by night, candyman by day.** *Oncogene* 2008, **27 Suppl 1:**S53-70.

13. Biswas G, Guha M, Avadhani NG: **Mitochondria-to-nucleus stress signaling in mammalian cells: nature of nuclear gene targets, transcription regulation, and induced resistance to apoptosis.** *Gene* 2005, **354:**132-139.

14. Hsu YY, Liu CM, Tsai HH, Jong YJ, Chen IJ, Lo YC: **KMUP-1 attenuates serum deprivation-induced neurotoxicity in SH-SY5Y cells: roles of PKG, PI3K/Akt and Bcl-2/Bax pathways.** *Toxicology* 2010, **268:**46-54.

15. Meng J, Fang B, Liao Y, Chresta CM, Smith PD, Roth JA: **Apoptosis induction by MEK inhibition in human lung cancer cells is mediated by Bim.** *PLoS One* 2010, **5:**e13026.

16. Gilley J, Coffer PJ, Ham J: **FOXO transcription factors directly activate bim gene expression and promote apoptosis in sympathetic neurons.** *J Cell Biol* 2003, **162:**613-622.

17. Sunters A, Fernandez de Mattos S, Stahl M, Brosens JJ, Zoumpoulidou G, Saunders CA, Coffer PJ, Medema RH, Coombes RC, Lam EW: **FoxO3a transcriptional regulation of Bim controls apoptosis in paclitaxel-treated breast cancer cell lines.** *J Biol Chem* 2003, **278:**49795-49805.

18. Huang H, Tindall DJ: **Dynamic FoxO transcription factors.** *J Cell Sci* 2007, **120:**2479-2487.

19. Huang H, Tindall DJ: **FOXO factors: a matter of life and death.** *Future Oncol* 2006, **2:**83-89.

20. Jiang P, Du W, Heese K, Wu M: **The Bad guy cooperates with good cop p53: Bad is transcriptionally up-regulated by p53 and forms a Bad/p53 complex at the mitochondria to induce apoptosis.** *Mol Cell Biol* 2006, **26:**9071-9082.

21. Ogawara Y, Kishishita S, Obata T, Isazawa Y, Suzuki T, Tanaka K, Masuyama N, Gotoh Y: **Akt enhances Mdm2-mediated ubiquitination and degradation of p53.** *J Biol Chem* 2002, **277:**21843-21850.

Chapter 4:

Type II cGMP-dependent Protein Kinase Mediates Osteoblast

Mechanotransduction

ABSTRACT

Mechanical stimulation of bone is crucial for bone growth and differentiation. Interstitial fluid flow ultimately promotes osteoblastic and osteocytic proliferation through a number of second messengers including nitric oxide (NO) but the mechanisms by which fluid shear stress regulates these anabolic responses is incompletely understood. We found that primary human osteoblasts and MC3T3-E1 murine osteoblast-like cells responded to fluid shear stress by inducing expression of genes encoding transcription factors essential for skeletal integrity, namely *c-fos, fra-1, fra-2*, and *fosB*/Δ*fosB*, in a NO/ cGMP/PKG-dependent mechanism. Increased NO production resulting from fluid shear stress elevated intracellular cGMP concentrations and activated PKG, leading to activation of the MEK/ERK pathway and downstream *fos* family gene regulation. Inhibition of this pathway by pharmacological inhibitors or siRNA targeting PKGII prevented fluid shear stress-induced ERK1/2 phosphorylation and stimulation of all four *fos* genes. Loss of PKGI did not affect either ERK1/2 phosphorylation or *fos* family mRNA expression. A membrane permeable analog of cGMP was able to partially mimic the effects of fluid shear stress; cGMP combined with a calcium ionophore was more completely able to reproduce the *fos* family gene induction observed in fluid shear stressed cells. Fluid shear stress- and cGMP-dependent osteoblast proliferation was also discovered to occur in a Src-dependent manner. PKGII was found to indirectly activate Src through a mechanism whereby PKGII directly phosphorylates and activates SHP-1. SHP-1, in turn, dephosphorylates the inhibitory phosphorylation site on Src. This process also required the interaction of Src with β_3 integrins and SHP-2; fluid shear stress triggered the recruitment of PKGII, Src, SHP-1, and SHP-2 to β_3 integrins and the

formation of a mechanosome to convert extracellular fluid shear stress into intracellular signaling promoting cell growth.

Type II cGMP-dependent Protein Kinase Mediates Osteoblast Mechanotransduction[*][S]

Hema Rangaswami[‡], Nisha Marathe[‡], Shunhui Zhuang[‡], Yongchang Chen[‡], Jiunn-Chern Yeh[§], John A. Frangos[§], Gerry R. Boss[‡], and Renate B. Pilz[‡1]

From the [‡]Department of Medicine and Cancer Center, University of California, San Diego, La Jolla, California 92093 and the [§]La Jolla Bioengineering Institute, La Jolla, California 92037

ASBMB

The Journal of Biological Chemistry

Continuous bone remodeling in response to mechanical loading is critical for skeletal integrity, and interstitial fluid flow is an important stimulus for osteoblast/osteocyte growth and differentiation. However, the biochemical signals mediating osteoblast anabolic responses to mechanical stimulation are incompletely understood. In primary human osteoblasts and murine MC3T3-E1 cells, we found that fluid shear stress induced rapid expression of c-fos, fra-1, fra-2, and fosB/ΔfosB mRNAs; these genes encode transcriptional regulators that maintain skeletal integrity. Fluid shear stress increased osteoblast nitric oxide (NO) synthesis, leading to activation of cGMP-dependent protein kinase (PKG). Pharmacological inhibition of the NO/cGMP/PKG signaling pathway blocked shear-induced expression of all four fos family genes. Induction of these genes required signaling through MEK/Erk, and Erk activation was NO/cGMP/PKG-dependent. Treating cells with a membrane-permeable cGMP analog partly mimicked the effects of fluid shear stress on Erk activity and fos family gene expression. In cells transfected with small interfering RNAs (siRNA) specific for membrane-bound PKG II, shear- and cGMP-induced Erk activation and fos family gene expression was nearly abolished and could be restored by transducing cells with a virus encoding an siRNA-resistant form of PKG II; in contrast, siRNA-mediated repression of the more abundant cytosolic PKG I isoform was without effect. Thus, we report a novel function for PKG II in osteoblast mechanotransduction, and we propose a model whereby NO/cGMP/PKG II-mediated Erk activation and induction of c-fos, fra-1, fra-2, and fosB/ΔfosB play a key role in the osteoblast anabolic response to mechanical stimulation.

jbc

Mechanical stress is a primary determinant of bone growth and remodeling; the strength of bone increases with weight bearing and muscular activity and decreases with unloading and disuse (1, 2). Weight bearing and locomotion stimulate interstitial fluid flow through the bone canalicular system, and the resultant shear stress is thought to be a major mechanism whereby mechanical forces stimulate bone growth (1–4). Fluid shear stress activates various signal transduction pathways and initiates an anabolic response in osteocytes and osteoblasts, leading to changes in gene expression and increased cell proliferation and differentiation (1, 5). As part of this response, a rapid and transient increase in intracellular calcium, nitric oxide (NO),[2] and prostaglandin E_2 occurs, and transcription of genes such as c-fos, cox-2, and igf-1/2 is induced (1, 2, 5).

The transcription factor complex AP1, composed of Fos and Jun proteins, plays an essential role in bone development and post-natal skeletal homeostasis (6). De-regulated c-fos expression in mice interferes with normal bone development and induces osteosarcomas, whereas c-Fos-deficient mice develop osteopetrosis because of an early arrest in osteoclast differentiation (7, 8). Mice overexpressing Fra-1, Fra-2, or ΔFosB (a splice variant of FosB) exhibit a progressive increase in bone mass because of enhanced osteoblast differentiation and bone formation in the presence of normal osteoclast activity (6, 9, 10). In contrast, conditional loss of Fra-1, Fra-2, or JunB leads to defective osteoblast differentiation and severe osteopenia (6, 11, 12). Mechanical loading of long bones or vertebral bodies in rodents rapidly induces c-fos mRNA in osteoblasts/osteocytes (13–16). The same response occurs in cultured osteoblasts exposed to diverse mechanical stimuli such as fluid shear stress, stretch, pulsed ultrasound, or gravitational force (17–24). The mechanism(s) regulating mechanically induced c-fos expression are poorly understood, and inhibition of calcium influx and NO or prostaglandin synthesis appears to affect c-fos induction differentially, depending on the type of mechanical stimulation (14, 15, 17, 19, 21).

NO synthesis inhibitors prevent new bone formation induced by mechanical stimulation (14, 25), and endothelial NO synthase (eNOS, type III NOS) appears to be the predominant NOS isoform expressed in bone (26). eNOS-deficient mice demonstrate reduced post-natal bone mass because of

2 The abbreviations used are: NO, nitric oxide; 8-pCPT-cGMP, 8-(4-chlorophenylthio)-cGMP; CREB, cAMP-response element-binding protein; eNOS, endothelial nitric-oxide synthase; Erk, extracellular signal-regulated kinase; gapd, glyceraldehyde-3-phosphate dehydrogenase; hPOB, human primary osteoblasts; IBMX, isobutylmethylxanthine; L-NAME, N-nitro-L-arginine methyl ester; ODQ, 1H-[1,2,4]oxadiazolo[4,3-a]quinoxalin-1-one; MAPK, mitogen-activated protein kinase; MEK, mitogen-activated protein kinase/extracellular signal-regulated kinase kinase; PAPA-NONOate, 3-(2-hydroxy-2-nitroso-1-propylhydrazino)-1-propanamine; PKG, cGMP-dependent protein kinase; (R_p)-8-pCPT-PET-cGMPS, 8-(4-chlorophenylthio)-β-phenyl-1,N^2-ethenoguanosine-3',5'-cyclic monophosphorothioate (R_p isomer); sGC, soluble guanylate cyclase; siRNA, small interfering RNA; RT, reverse transcription; GFP, green fluorescent protein.

defects in osteoblast number and maturation and impaired bone formation in response to mechanical stimulation and estrogens (27–29). Osteoblasts exhibit a biphasic response to NO donors, with low doses promoting proliferation and differentiation, and high doses inducing apoptosis (30–32). Low doses of NO donors alleviate ovariectomy-induced bone loss in rats, and a randomized, placebo-controlled trial in healthy post-menopausal women demonstrated increased bone formation in subjects receiving the NO donor isosorbide mononitrate (33, 34). These data indicate an important role of NO in osteoblast biology, but little is known about signaling downstream of NO in osteoblasts (35).

One of the major intracellular targets of NO is soluble guanylate cyclase (sGC), which is activated on NO binding to the heme prosthetic group of the enzyme. The resultant increase in cGMP affects multiple target proteins, including cGMP-dependent protein kinases (PKGs), phosphodiesterases, and cyclic nucleotide-gated ion channels (36, 37). Type I PKG is cytosolic and widely expressed, with high levels in smooth muscle cells and platelets, whereas type II PKG is membrane-anchored, with high levels in brain and intestinal mucosa (37). Studies in PKG I- and PKG II-deficient mice have demonstrated a multitude of functions for PKG I, but there are few established functions for PKG II (37). PKG II-deficient mice are dwarfs because of a severe defect in endochondral ossification at the growth plates, secondary to impaired chondrocyte proliferation and differentiation (38, 39). Both PKG I and II are expressed in osteoblasts, but their physiological significance in these cells is largely unknown (38, 40, 41).

We previously showed that NO and cGMP regulate c-*fos* transcription in different cell types (40, 42–47). In this study, we found that fluid shear -stress induces c-*fos*, *fra-1*, *fra-2*, and *fosB/ΔfosB* mRNA expression in osteoblasts via NO/cGMP, and we define a new function for PKG II as a regulator of gene expression and activator of the extracellular signal-regulated kinases (Erk)-1/2 in mechanically stimulated osteoblasts.

EXPERIMENTAL PROCEDURES

Materials—Antibodies against eNOS, Erk1/2, and α-tubulin and phospho-specific antibodies for eNOS (Ser(P)[1177]) and Erk1 (Tyr(P)[204], clone E-4) were from Santa Cruz Biotechnology; an antibody specific for dually phosphorylated Erk1 (Thr(P)[202]/Tyr(P)[204]) was from Promega. Antibodies specific for vasodilator-stimulated phosphoprotein (VASP) phosphorylated on Ser[239] (clone 16C2) and against the C terminus of PKG I were from Calbiochem/EMD; a PKG II-specific antibody was from Abgent. The calcium ionophore A23187, the intracellular calcium chelator 1,2-bis(2-aminophenoxy) ethane-*N,N,N′,N′*-tetraacetic acid, the MAPK/Erk kinase (MEK) inhibitor U0126, and the p38 inhibitor SB203580 were from Calbiochem/EMD. The cGMP agonist 8-(4-chlorophenylthio)-GMP (8-pCPT-cGMP) and cGMP antagonist 8-(4-chlorophenylthio)-β-phenyl-1,N^2-ethenoguanosine-3′,5′-cyclic monophosphorothioate, R_p isomer (R_p)-8-pCPT-PET-cGMPS) were from Biolog. The NOS inhibitor *N*-nitro-L-arginine methyl ester (L-NAME), the sGC inhibitor 1*H*-[1,2,4]oxadiazolo[4,3-*a*]quinoxalin-1-one (ODQ), the NO donor 3-(2-hydroxy-2-nitroso-1-propylhydrazino)-1-propanamine (PAPA-NONOate),

and an antibody against the β1 subunit of sGC were from Cayman.

Cell Culture and Characterization of Human Primary Osteoblasts—Murine MC3T3-E1 osteoblastic cells with high differentiation potential (clone 4, hereafter referred to as MC3T3 cells) and UMR106 rat osteosarcoma cells were from the American Tissue Culture Collection. MC3T3 cells were grown in minimal essential medium without ascorbic acid and UMR106 cells in Dulbecco's modified Eagle's medium; both cell lines were maintained in the presence of 10% fetal bovine serum (FBS) and used at <12 passages. Human umbilical vein endothelial cells were isolated and cultured as described previously (48). Human primary osteoblasts (hPOBs) were established from trabecular bone obtained from surgical specimens of patients undergoing joint replacement for degenerative joint disease, according to an institutionally approved human subjects protocol as described previously (41). Primary cultures were maintained for a maximum of five passages in Dulbecco's modified Eagle's medium with 10% FBS and exhibited histochemical staining for alkaline phosphatase activity in >85% of cells; in addition, cells demonstrated a >16-fold induction of osteocalcin mRNA in response to 1,25-dihydroxyvitamin D$_3$ (10 nM) (41, 49).

Exposure of Cells to Fluid Shear Stress—Cells were plated on 38 × 75-mm NaOH-etched glass slides at 0.5–1 × 10^6 cells/slide in minimal essential medium or Dulbecco's modified Eagle's medium containing 10% FBS. After 18 h, they were serum-deprived for 24 h, and the slides were transferred to a parallel plate flow chamber (Cytodyne Inc., San Diego). Minimal essential medium with 1 mg/ml fatty acid-free bovine serum albumin (Sigma) was injected into the chamber using a syringe pump at a flow rate that generated 12 dynes/cm^2 of shear for up to 20 min (50). The flow chamber, media, and accompanying apparatus were maintained at 37 °C throughout the experiment. Sham-treated cells served as "static controls"; they were grown under identical conditions and mounted into the flow chamber but were not subjected to shear stress. After shear stress, cells were left in the chamber without flow for the indicated time before harvesting.

Reverse Transcription (RT)-PCR—RNA was extracted using TriReagent™ (Molecular Research Center, Inc.); 1 μg of total RNA was subjected to reverse transcription using Superscript™ reverse transcriptase (Invitrogen) and PCR was performed on 5 or 10% of the RT product as described (51). The PCR primers for amplification of murine and human glyceraldehyde-3-phosphate dehydrogenase (*gapd*), c-*fos*, *fra-1*, *fra-2*, *fosB/ΔfosB*, *pkg I* and *pkg II* mRNA are described in supplemental Table 1. Semi-quantitative PCR conditions for c-*fos* and *gapd* were 30 s of denaturation at 95 °C, 30 s annealing at 65 °C, and 30 s extension at 72 °C for 23 cycles; for *fra-1/2* and *fosB* annealing and extension were 45 s at 60 °C for 25 cycles. Control experiments with variable amounts of input cDNA demonstrated a linear increase in a single PCR product over a >20-fold range. Quantitative RT-PCR was performed using an MX3000 real time PCR detection system (Stratagene) and IQ™ SYBR Green Supermix (Bio-Rad). Melting curves after 40 cycles confirmed a single PCR product for each primer pair. Standard curves were generated by plotting C_t values *versus* the amount

PKG and Shear Stress-induced Gene Expression

of input RNA, and demonstrated similar amplification efficiencies for all primers. Relative changes in mRNA expression were analyzed using the $2^{-\Delta\Delta Ct}$ method, with *gapd* serving as an internal reference to correct for differences in RNA extraction or reverse transcription efficiencies (52).

Quantitation of NO_x and cGMP—Nitric oxide production was monitored based on nitrite and nitrate accumulation in the medium using a two-step colorimetric assay kit according to the manufacturer's protocol (Active Motif), but the assay was scaled down 10-fold, and samples were read using a Nano-Drop™ spectrophotometer (NanoDrop Technologies, Inc.). Experiments were performed in phenol red-free medium, with 5×10^5 cells/slide in the parallel plate flow chamber described above. cGMP production was measured in cell lysates using a competitive enzyme immunoassay from Cayman according to the manufacturer's protocol.

DNA and siRNA Transfections—MC3T3 cells (1.5×10^6) were transfected with 2 µg of expression vector encoding human VASP in 100 µl of solution V using the Amaxa Nucleoporator program D-24. After overnight recovery in full growth medium, cell from several transfections were pooled, and equal numbers of cells were plated on glass slides for shear experiments.

The sequence targeted by siRNA in the C terminus of PKG Iα/β was 5'-CCGGACAUUUAAAGACAGCAA-3' (siRNA PKG-1). The sequences targeted in PKG II were 5'-CTGCTT-GGAAGTGGAATACTA-3' (siRNA PKG-2a) and 5'-CCG-GGTTTCTTGGGTAGTCAA-3' (siRNA PKG-2b). siRNA oligoribonucleotides, including a control siRNA targeting green fluorescent protein (GFP), were produced by Qiagen. MC3T3 cells were plated at 1.3×10^5 cells per well of a 6-well dish or at 5×10^5 cells per glass slide and were transfected 18 h later (at ~40% confluency) with 100 pmol of siRNA and 3 µl of Lipofectamine 2000™ (Invitrogen) in 1 ml of 10% FBS-containing media. The medium was replaced 5 h later, and 18 h later, cells were transferred to medium containing 0.1% FBS.

Adenovirus Infection—Adenoviral vectors encoding either β-galactosidase (LacZ) or rat PKG II (53) were produced using the pAd/CMV/V5-DEST™ Gateway® system (Invitrogen). Cells were infected in full growth medium at an multiplicity of infection of ~30.

Western Blot Analyses, Cell Fractionation, and PKG Activity Assay—Western blots were generated using horseradish peroxidase-coupled secondary antibodies and enhanced chemiluminescence as described (45). To determine PKG II activity, MC3T3 cells were extracted by Dounce homogenization, and nuclei and cell debris were removed by centrifugation at $300 \times g$ for 10 min, and the supernatant was subjected to centrifugation at $50,000 \times g$ for 30 min to generate "cytosolic" (supernatant) and "membrane" (pellet) fractions. PKG II activity in the membrane fraction was determined in the presence of 1% Triton-X-100 and 500 mM NaCl, as described previously (40). For Western blotting, membranes were solubilized in 1% Triton X-100, 60 mM β-octyl glucoside. Films were scanned using ImageJ software (nih.gov).

Statistical Analyses—Pairwise comparison of data groups was done by two-tailed Student's *t* test and comparison of multiple groups by analysis of variance, with a Dunnett's post test
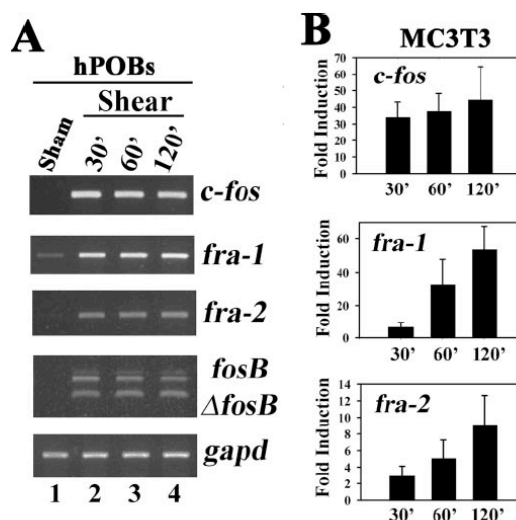

FIGURE 1. **Effect of fluid shear stress on osteoblast *c-fos*, *fra-1*, *fra-2*, and *fosB*/Δ*fosB* mRNA expression.** *A*, serum-deprived hPOBs were incubated in a parallel plate flow chamber for the indicated times; cells were exposed to laminar flow for the first 20 min (*lanes 2–4*) or kept under static conditions (*lane 1, Sham*). At the indicated times, which include the initial 20 min of laminar flow, total cytoplasmic mRNA was isolated, and *c-fos*, *fra-1*, *fra-2*, *fosB*/Δ*fosB*, or *gapd* mRNA levels were determined by semi-quantitative RT-PCR as described under "Experimental Procedures." PCR products were separated by nondenaturing agarose gel electrophoresis and visualized by ethidium bromide staining. Sham-treated cells were harvested at 30 min, but similar results were obtained with sham-treated cells harvested at 120 min. *B*, MC3T3 cells were treated as described for hPOBs in *A*, but *c-fos*, *fra-1*, and *fra-2* mRNA levels were quantified by real time RT-PCR and normalized relative to *gapd* mRNA levels as described under "Experimental Procedures"; the relative mRNA levels found in static controls were assigned a value of 1. *p* < 0.05 for the comparison between shear-stressed and sham-treated cells for all time points.

analysis to the control group; a *p* value of < 0.05 was considered statistically significant. Results shown in bar graphs represent the mean ± S.D. of at least three independent experiments, unless stated otherwise. All other results are representative experiments that were reproduced at least three times.

RESULTS

Fluid Shear Stress Induces c-fos, fra-1, fra-2, and fosB/ΔfosB mRNA Expression in Osteoblasts—Osteoblast *c-fos* and *fosB*/Δ*fosB* mRNA and protein are induced rapidly by mechanical loading in rat vertebrae and mouse limb bones *in vivo* and by fluid shear stress in osteoblast cell lines or primary rodent osteoblasts (13–18, 54). Genetic experiments have implicated *fra-1* and *fra-2* in regulating osteoblast differentiation and bone mass (6). We found that *c-fos*, *fra-1*, *fra-2*, and *fosB*/Δ*fosB* mRNAs were strongly induced 30 min after the onset of flow in both MC3T3 cells and hPOBs and remained elevated for at least 2 h (Fig. 1*A* shows hPOBs, results for MC3T3 cells are shown in supplemental Fig. 1*A*). The housekeeping gene glyceraldehyde-3-phosphate dehydrogenase (*gapd*) was not affected by fluid shear in either cell type. Real time RT-PCR analysis in MC3T3 cells showed that *c-fos* mRNA increased 30–40-fold at all time points, and that *fra-1* and *fra-2* mRNA levels increased progres-
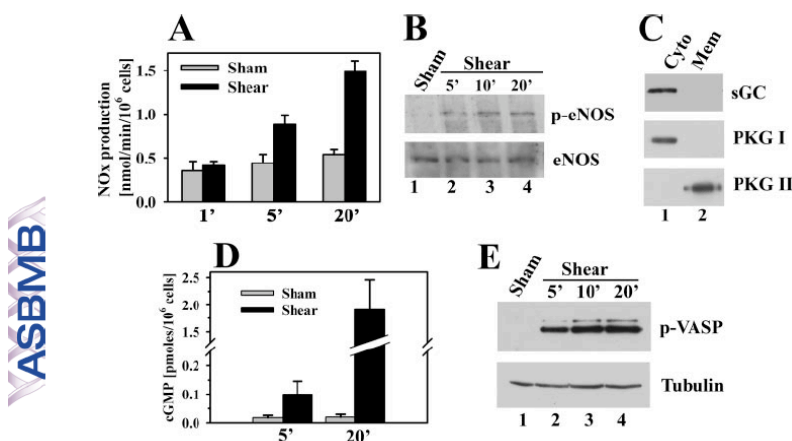
A

B

C

D

E

FIGURE 2. **Effect of fluid shear stress on osteoblast NO and cGMP production, eNOS and VASP phosphorylation.** *A*, MC3T3 cells were placed in the flow chamber as described in Fig. 1; they were kept either under static conditions (*gray bars*) or were exposed to laminar flow (*black bars*) for the indicted times. At the end of flow (or static incubation), cells were kept in the chamber for 3 additional min, and nitrate plus nitrite (NO$_x$) concentrations were measured in the media collected from the chamber. Thus, NO$_x$ production was measured over a 3-min interval after the cessation of flow. $p < 0.05$ was the comparison between shear-stressed and sham-treated cells for the 5- and 20-min time points. *B*, cells were kept under static conditions for 20 min or were exposed to fluid shear stress for the indicated times, and cell lysates were analyzed by SDS-PAGE/Western blotting using antibodies specific for eNOS phosphorylated on Ser[1177] (*upper panel*) or recognizing eNOS irrespective of its phosphorylation state (*lower panel*). *C*, cells were extracted by Dounce homogenization and fractionated by differential centrifugation; cytosolic (*Cyto, lane 1*) and membrane (*Mem, lane 2*) fractions were analyzed by SDS-PAGE/Western blotting using antibodies specific for soluble guanylate cyclase β1 subunit (sGC, *upper panel*), PKG I (*middle panel*), or PKG II (*lower panel*). *D*, cells were placed into the flow chamber and incubated for 15 min in the presence of 0.5 mM IBMX; cells were then either kept under static conditions (*gray bars*) or were exposed to fluid shear stress (*black bars*), both in the presence of IBMX. Cells were harvested at the indicated times, and the intracellular cGMP concentration was determined as described under "Experimental Procedures." *E*, MC3T3 cells expressing human VASP were treated as described in *B*, but Western blots were probed with antibodies specific for VASP phosphorylated on Ser[239] (*upper panel*) or α-tubulin (*lower panel*).

sively up to 50- and 10-fold, respectively, at 2 h compared with sham-treated control cells (Fig. 1*B*). Basal mRNA levels of all four *fos* genes were somewhat variable in sham-treated cells, explaining the relatively large standard deviations in Fig. 1*B*; this may be due to the sensitivity of the cells to even small changes in fluid flow that can occur during mounting of the slides. Similar results were obtained in UMR106 rat osteosarcoma cells (data not shown).

Fluid Shear Stress Induces NO and cGMP Production, eNOS, and VASP Phosphorylation—Mechanical stimulation of osteoblasts or osteocytes induces NO synthesis and increased shear rates correlate with increased NO production (55–58). To determine the amount of NO produced in our system, we measured the concentration of stable NO oxidation products (nitrites and nitrates, referred to as NO$_x$) in media collected 3 min after the end of flow, allowing calculation of the rate of NO$_x$ production during this 3-min period (Fig. 2*A*). In MC3T3 cells exposed to 5 min of fluid shear, NO$_x$ production nearly doubled compared with sham-treated cells, and it reached 1.5 ± 0.1 nmol/min/10^6 cells after 20 min. In contrast, 20 min of fluid shear stress increased NO$_x$ production to 3.4 ± 0.4 nmol/min/10^6 cells in human umbilical vein endothelial cells (supplemental Fig. 1*B*). The rate of NO$_x$ production in MC3T3 cells is comparable with that of primary mouse osteoblasts exposed to pulsating fluid flow (58). The NO$_x$ concentration in the medium of shear-stressed MC3T3 cells continued to rise up to

40 min after the cessation of flow, suggesting a sustained activation of NOS (supplemental Fig. 1*C*).

To determine whether fluid shear stress increased eNOS activity in MC3T3 cells, we used an antibody specific for eNOS phosphorylated on Ser[1177]; phosphorylation of this site by multiple kinases increases enzyme activity (59). Little Ser[1177] phosphorylation was detectable in sham-treated cells, but as early as 5 min after the onset of flow, phosphorylation increased and remained elevated at 20 min (Fig. 2*B*, *upper panel*; the *lower panel* shows total eNOS expression that was not changed by fluid shear).

To document presence of the full NO/cGMP/PKG signal transduction pathway in osteoblasts, we examined MC3T3 cells for sGC and PKG. We found that sGC protein was easily detectable in cytosolic extracts of MC3T3 cells, and that PKG I and II were present in cytosolic and membrane fractions of MC3T3 cells, respectively (Fig. 2*C*). Fig. 2*D* shows that the increased NO in shear-stressed MC3T3 cells dramatically increased the intracellular cGMP concentration; cGMP was measured in cells treated with the phosphodiesterase inhibitor isobutylmethylxanthine (IBMX) to block cGMP catalysis. To determine whether the shear-induced increase in cGMP activated PKG in intact osteoblasts in the absence of phosphodiesterase inhibitors, we used a phospho-specific antibody to examine VASP phosphorylation on Ser[259], a preferred PKG phosphorylation site (61). VASP Ser[259] phosphorylation was undetectable in sham-treated cells but increased within 5 min of initiating fluid shear stress and reached a maximum level at 10–20 min (Fig. 2*E* shows MC3T3 cells transfected with a vector expressing human VASP, but similar results were obtained in hPOBs, which express endogenous VASP, as shown in supplemental Fig. 1*D*).

Inhibition of NO/cGMP Signaling Blocks Shear-induced c-fos, fra-1, fra-2, and fosB/ΔfosB mRNA Expression—The experiments in Figs. 1 and 2 show that fluid shear stress leads to rapid NO$_x$ and cGMP accumulation, PKG activation, and induction of *fos* family members but do not establish a causal relationship between NO/cGMP/PKG signaling and increased gene expression. To address this question, we treated MC3T3 cells and hPOBs for 1 h with L-NAME (to inhibit NOS), ODQ (to inhibit sGC), or (R_p)-8-pCPT-PET-cGMPS (to inhibit PKG) prior to fluid shear stress. We found that all three agents severely reduced shear induction of *c-fos, fra-1, fra-2,* and *fosB/ΔfosB* mRNA, without affecting *gapd* mRNA (Fig. 3*A* shows semiquantitative RT-PCR results for hPOBs, and Fig. 3*B* summa-
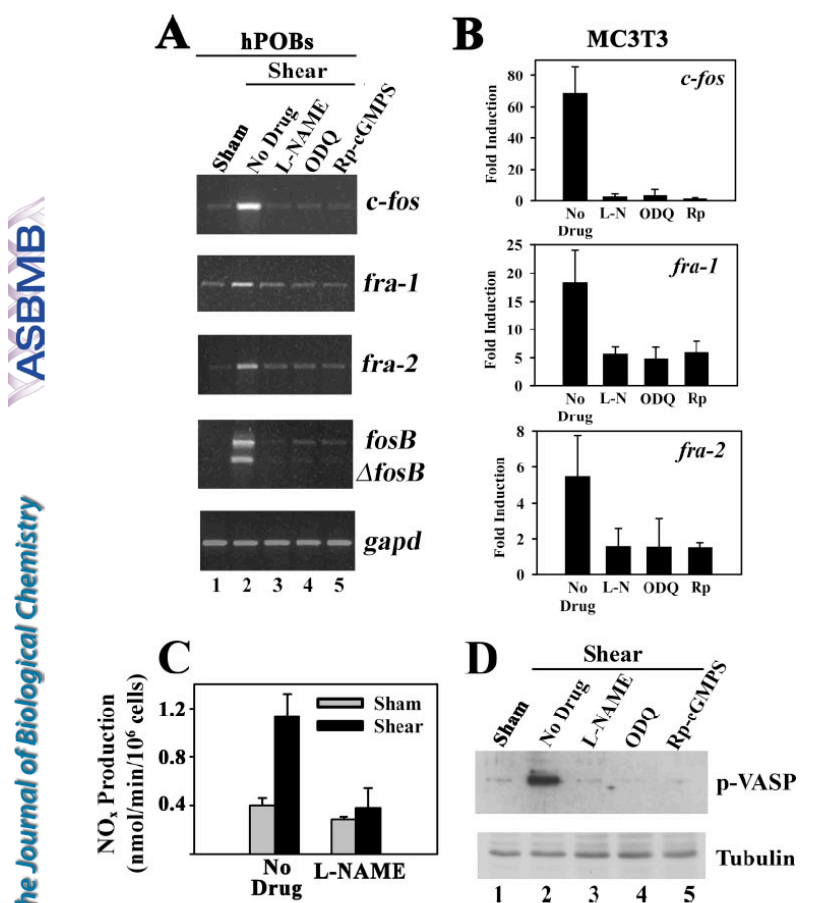
PKG and Shear Stress-induced Gene Expression

FIGURE 3. **Inhibition of NO/cGMP signaling prevents shear-induced *c-fos, fra-1, fra-2,* and *fosB/ΔfosB* mRNA expression.** *A,* serum-deprived hPOBs were placed in a flow chamber and were incubated for 1 h with either culture medium alone (*lanes 1* and *2*) or with medium containing 4 mM L-NAME (*lane 3*), 10 μM ODQ (*lane 4*), or 100 μM (R_p)-8-pCPT-PET-cGMPS ((*Rp*)-*cGMPS, lane 5*). Cells were then either kept under static conditions (*lane 1*) or were exposed to laminar flow for 20 min (*lanes 2–5*). Ten minutes after the cessation of flow, total RNA was extracted, and *c-fos, fra-1, fra-2, fosB/ΔfosB,* or *gapd* mRNA levels were determined by semi-quantitative RT-PCR as described in Fig. 1*A*. *B,* MC3T3 cells were treated as described for hPOBs in *A,* but *c-fos, fra-1,* and *fra-2* mRNA levels were quantified after 60 min by real time RT-PCR as described in Fig. 1*B*. $p < 0.05$ for the comparison between control cells receiving no drug and cells treated with L-NAME (*L-N*), ODQ, or (R_p)-cGMPS (*Rp*). *C,* MC3T3 cells were kept under static conditions (*gray bars*) or were exposed to laminar flow for 20 min (*black bars*); 5 min after the cessation of flow, media were collected from the chamber, and nitrate plus nitrite (NO$_x$) concentrations were measured. *D,* MC3T3 cells expressing human VASP were incubated for 1 h with medium alone (*lanes 1* and *2*) or with medium containing 4 mM L-NAME (*lane 3*), 10 μM ODQ (*lane 4*), or 100 μM (R_p)-8-pCPT-PET-cGMPS (*Rp*-cGMPS, lane 5*). Cells were kept under static conditions (*lane 1*) or were exposed to 20 min of fluid shear stress (*lanes 2–5*), and 10 min after the cessation of flow, cell lysates were analyzed by SDS-PAGE/Western blotting using antibodies specific for VASP phosphorylated on Ser[239] (*upper panel*) or α-tubulin (*lower panel*).

rizes real time PCR results for *c-fos, fra-1* and *fra-2* in MC3T3 cells). The three inhibitors almost completely prevented shear induction of *c-fos* and *fra-2* mRNAs; however, there was some residual shear induction of *fra-1* mRNA, suggesting that some NO/cGMP/PKG-independent mechanism may contribute to the mechanical stimulation of *fra-1*. Control experiments demonstrated that the drugs inhibited NO/cGMP/PKG signaling effectively; L-NAME reduced the rate of NO$_x$ production in

fluid shear-stressed cells to the level found in sham-treated control cells (Fig. 3*C*); all three agents blocked shear-induced VASP Ser[259] phosphorylation (Fig. 3*D*); and ODQ and (R_p)-8-pCPT-PET-cGMPS blocked VASP phosphorylation in cells treated with the NO donor PAPA-NONOate (data not shown). These results suggest that fluid shear stress induction of *fos* family genes requires PKG activation by NO/cGMP.

cGMP Partly Mimics the Effects of Fluid Shear Stress on c-fos, fra-1, fra-2, and fosB/ΔfosB mRNA Expression, and cGMP Cooperates with Calcium—To determine whether direct PKG activation can reproduce the effects of fluid shear stress on *fos* family gene expression, we treated cells with a membrane-permeable cGMP agonist. Exposure of serum-starved MC3T3 cells or hPOBs to 8-pCPT-cGMP for 30 min, 1 h, or 2 h increased *c-fos, fra-1, fra-2,* and *fosB/ΔfosB* mRNA expression, but when cells were pretreated with the PKG inhibitor (R_p)-8-pCPT-PET-cGMPS, the effects of 8-pCPT-cGMP on all four *fos* family genes were abolished (Fig. 4*A* shows hPOBs, and Fig. 4*B* summarizes real time RT-PCR results for *c-fos, fra-1,* and *fra-2* in MC3T3 cells, with *black* and *gray bars* representing cells treated with 8-pCPT-cGMP in the absence and presence of the PKG inhibitor, respectively). (R_p)-8-pCPT-PET-cGMPS prevented VASP Ser[259] phosphorylation in cells treated with 8-pCPT-cGMP, demonstrating effective inhibition of PKG activity by the cGMP antagonist (Fig. 4*C*).

When MC3T3 cells were treated with the NO donor sodium nitroprusside to activate PKG through sGC stimulation, *c-fos, fra-1* and *fra-2* mRNAs were induced to a similar extent as seen with 8-pCPT-cGMP (compare Fig. 4*D* to Fig. 4*B*). However, we noticed that sodium nitroprusside and 8-pCPT-cGMP induced the *fos* genes to a lesser extent than observed in fluid shear-stressed MC3T3 cells (compare the *y* axis in Fig. 4, *B* and *D*, with that in Fig. 1*B*), suggesting that the NO/cGMP/PKG signaling pathway cooperates with other pathways to induce *fos* family genes in mechanically stimulated osteoblasts.
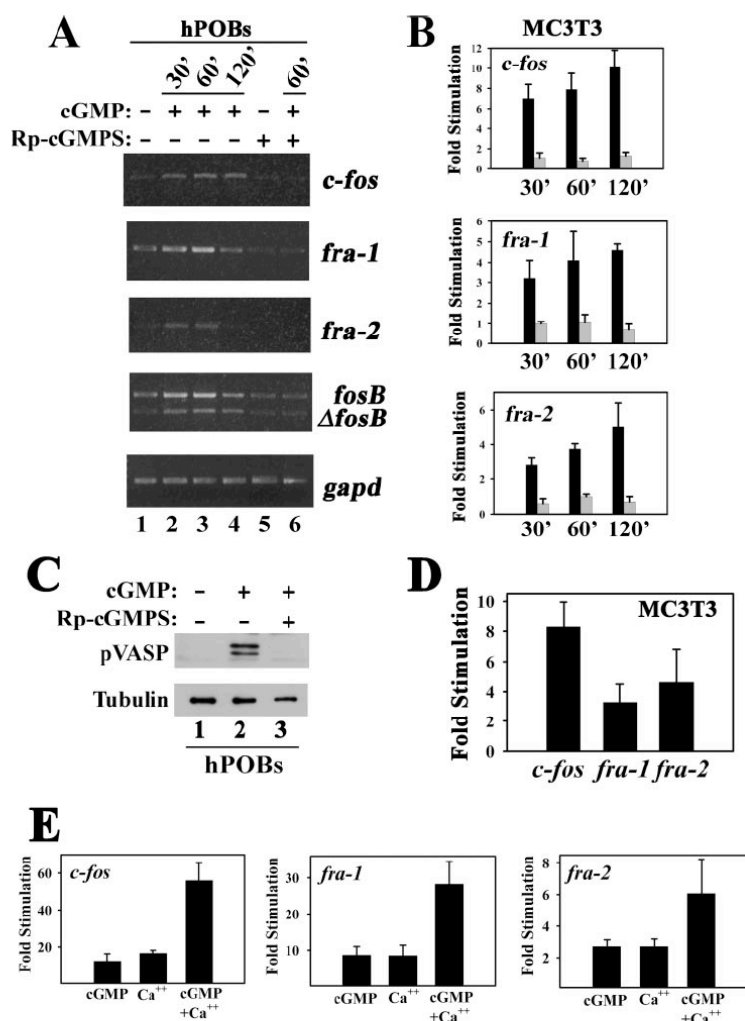
FIGURE 4. **cGMP partly mimics the effects of fluid shear stress on osteoblast *c-fos*, *fra-1*, *fra-2*, and *fosB/ΔfosB* mRNA expression.** *A*, serum-deprived hPOBs were incubated for 1 h in the absence (*lanes 1–4*) or presence of 100 μM (R_p)-8-pCPT-PET-cGMPS (Rp-cGMPS, *lanes 5* and *6*) before adding 50 μM 8-pCPT-cGMP (cGMP) to all cells for the indicated times. *c-fos*, *fra-1*, *fra-2*, *fosB/ΔfosB* or *gapd* mRNA levels were determined by semi-quantitative RT-PCR as described in Fig. 1*A*. *B*, MC3T3 cells were incubated in the absence (*black bars*) or presence (*gray bars*) of (R_p)-8-pCPT-PET-cGMPS and then stimulated with 8-pCPT-cGMP as described in *A* for hPOBs, but *c-fos*, *fra-1*, and *fra-2* mRNA levels were quantified by real time RT-PCR. Relative mRNA levels (normalized to *gapd*) measured in mock-treated cells were assigned a value of 1. $p < 0.05$ for the comparison between cells treated with (R_p)-cGMPS plus cGMP *versus* cGMP alone for all time points. *C*, hPOBs were preincubated in the absence (*lanes 1* and *2*) or presence (*lane 3*) of 100 μM (R_p)-8-pCPT-PET-cGMPS for 1 h and treated with 50 μM 8-pCPT-cGMP (*lanes 2* and *3*) for 30 min. VASP phosphorylation on Ser[259] was assessed using a phosphorylation site-specific antibody; a duplicate Western blot was probed with an anti-α-tubulin antibody. *D*, MC3T3 cells were treated for 1 h with 10 μM sodium nitroprusside, and *c-fos*, *fra-1*, and *fra-2* mRNA levels were quantified by real time RT-PCR. *E*, MC3T3 cells were treated for 1 h with either cGMP (100 μM 8-pCPT-cGMP), calcium ionophore (0.3 μM A23187), or both agents, and *fos* family gene expression was measured as in *B*.

cium influx via mechano-sensitive and/or L-type voltage-gated calcium channels; calcium chelation prevents fluid shear stress-induced *c-fos* and *fosB/ΔfosB* expression (17, 19, 54, 62–65). We confirmed these latter results, and we found that treating MC3T3 cells with 1,2-bis(2-aminophenoxy) ethane-*N*, *N,N',N'*-tetraacetic acid or EGTA to chelate intra- or extracellular calcium, respectively, also reduced fluid shear stress induction of *fra-1* and *-2* mRNA (supplemental Fig. 2*A*). We previously showed that calcium and cGMP cooperate to increase c-*fos* mRNA expression (40, 47). Therefore, we examined the effect of the calcium ionophore A23187 alone and in combination with 8-pCPT-cGMP on the expression of all four *fos* family genes in MC3T3 cells and hPOBs. Increasing the intracellular calcium concentration with A23187 stimulated expression of *c-fos, fra-1, fra-2*, and *fosB/ΔfosB* mRNA to a similar extent as treatment with 8-pCPT-cGMP; together the effect was at least additive (Fig. 4*E* and supplemental Fig. 2*B* show results for MC3T3 cells, but similar results were obtained in hPOBs). Combined treatment with calcium ionophore plus cGMP induced c-*fos* and *fra-1/2* mRNAs to levels comparable with those found in shear-stressed osteoblasts (compare Fig. 4*E* and Fig. 1*B*). These results suggest that induction of *fos* family genes in shear-stressed osteoblasts is due to a combined effect of increased intracellular calcium and cGMP, although calcium and cGMP signaling may be partly interdependent, as discussed below.

Shear- and cGMP-induced c-fos, fra-1, fra-2, and fosB/ΔfosB mRNA Expression Is Mediated by PKG II and Not PKG I—Having established that fluid shear stress induces *fos* family gene expression in osteoblasts via NO/cGMP/PKG signaling, we examined whether gene induction occurred via PKG I, PKG II, or both. Because there are no specific inhibitors for PKG I *versus* II, we used an siRNA approach. In MC3T3 cells transfected with an siRNA targeting a C-terminal PKG I sequence

Fluid shear stress rapidly increases the intracellular calcium concentration in MC3T3 cells and primary osteoblasts/osteocytes through calcium release from intracellular stores and cal-

PKG and Shear Stress-induced Gene Expression
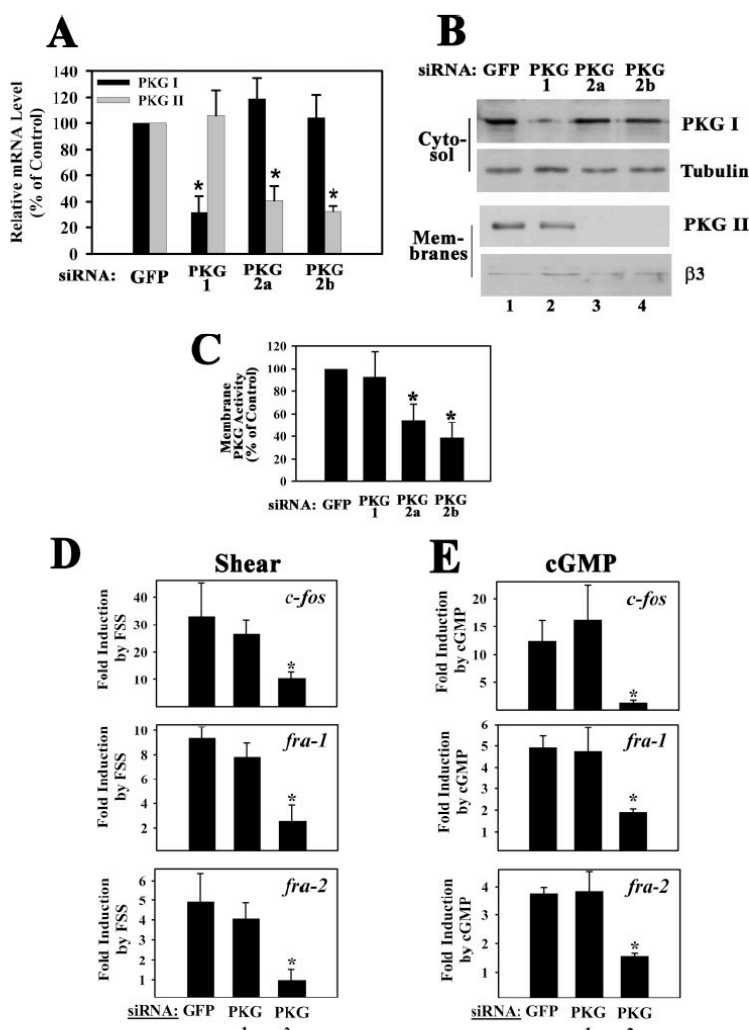
A

B

C

D Shear

E cGMP

FIGURE 5. **Effect of siRNA-mediated PKG I or PKG II knockdown on shear- and cGMP-induced c-fos, fra-1, fra-2, and fosB/ΔfosB mRNA expression.** MC3T3 cells were transfected with siRNAs specific for GFP (control), or received siRNAs targeting sequences in PKG I (siRNA PKG-1) or PKG II (siRNAs PKG-2a and -2b) as described under "Experimental Procedures." *A*, at 48 h after transfection, mRNA levels of PKG I (*black bars*) and PKG II (*gray bars*) were quantified by real time PCR; levels were normalized to *gapd* mRNA, which was not affected by any of the siRNAs. Relative PKG mRNA levels measured in GFP (control) siRNA-transfected cells were assigned a value of 100%. *, *p* < 0.05 for the comparison between control siRNA and PKG siRNA-treated cells. *B*, in parallel experiments, cells were extracted by Dounce homogenization and fractionated by differential centrifugation; cytosolic fractions (*upper two panels*) and membrane fractions (*lower two panels*) were analyzed by SDS-PAGE/Western blotting using an antibody specific for the C terminus of PKG I common to PKG Iα and Iβ (*upper panel*), an anti-α-tubulin antibody (*2nd panel*), an antibody specific for PKG II (*3rd panel*), and an anti-β3 integrin antibody (*lowest panel*). *C*, siRNA-transfected cells were fractionated as described in *B*, and PKG activity was determined in the membrane fractions as described under "Experimental Procedures." *, *p* < 0.05 for the comparison between control siRNA and PKG siRNA-treated cells. *D*, cells transfected with the siRNAs targeting GFP, PKG I, or PKG II (PKG-2a siRNA) were kept either under static conditions or were subjected to fluid shear stress for 20 min. Cells were harvested 60 min after the onset of flow, and *c-fos*, *fra-1*, and *fra-2* mRNA levels were determined by quantitative RT-PCR; relative mRNA levels (normalized to *gapd*) measured in GFP siRNA-transfected static control cells were assigned a value of 1. *E*, cells transfected with the indicated siRNAs were either mock-treated or were treated with 50 μM 8-pCPT-cGMP for 1 h, and *c-fos*, *fra-1*, or *fra-2* mRNA levels were determined by quantitative RT-PCR. Relative mRNA levels (normalized to *gapd*) measured in GFP siRNA-transfected mock-treated cells were assigned a value of 1. *, *p* < 0.05 for the comparison between GFP and PKG II siRNA-treated cells (*D* and *E*).

(siRNA PKG-1, targeting both PKG Iα and PKG Iβ splice variants), PKG I mRNA levels were reduced by 68%, compared with the levels found in control siRNA-transfected cells, whereas PKG II mRNA levels were unaffected (Fig. 5*A*; PKG I and II mRNA levels are shown in *black* and *gray bars*, respectively). Using an antibody specific for the common C terminus of PKG Iα and Iβ, we found that PKG I protein in cytosolic extracts was reduced in proportion to the mRNA knockdown (Fig. 5*B*, *top panel*; the *2nd panel* shows a duplicate Western blot probed with a tubulin antibody to demonstrate equal loading). In MC3T3 cells transfected with siRNA sequences targeting PKG II (siRNAs PKG-2a and -2b), PKG II mRNA levels were reduced by 60 and 68%, respectively, compared with control siRNA-transfected cells, but PKG I mRNA levels were not altered (Fig. 5*A*). PKG II protein levels in the membranes of cells transfected with control or PKG I-specific siRNAs were similar, but levels were below detection in cells transfected with PKG II-specific siRNAs (Fig. 5*B*, *3rd panel*; loading was shown by re-probing the blot with an antibody specific for β3 integrin, as shown in the *bottom panel*). We measured similar PKG activities in membrane preparations of control siRNA- and PKG I siRNA-transfected MC3T3 cells and significantly reduced activity in PKG II siRNA-transfected cells (Fig. 5*C*). The residual membrane-bound PKG activity in PKG II siRNA-transfected cells is likely explained by the higher sensitivity of the activity assay compared with Western blotting. Because siRNA knockdown of PKG I did not affect membrane-associated PKG activity, and Western blots failed to detect PKG I in membrane preparations, we conclude that membrane-associated PKG activity in MC3T3 cells represents predominantly PKG II, which is consistent with results in other cell types (40, 53, 66, 67).

When we examined the effects of siRNA-mediated down-regulation of PKG I and PKG II on shear-in-

duced *fos* family gene expression in MC3T3 cells, we were surprised to find that knockdown of PKG I had no significant effect on gene expression, whereas knockdown of PKG II significantly diminished fluid shear stress-induced c-*fos*, *fra-1*, and *fra-2* mRNA expression (Fig. 5*D*; results for PKG-2a siRNA are shown, but similar results were obtained with PKG-2b siRNA). We also examined 8-pCPT-cGMP-induced *fos* family gene expression in siRNA-transfected MC3T3 cells. Neither basal nor cGMP-induced c-*fos*, *fra-1* or *fra-2* mRNA levels were altered in PKG I siRNA-transfected cells, whereas cGMP-induced mRNA levels were severely reduced in cells transfected with the PKG II-specific siRNA (Fig. 5*E*). Similar results were obtained for *fosB*/Δ*fosB* (supplemental Fig. 3). Thus, fluid shear stress- and cGMP-induced c-*fos*, *fra-1*, *fra-2* and *fosB*/Δ*fosB* mRNA expression in osteoblasts requires PKG II but not PKG I.

To confirm these results, we used a second PKG II-specific siRNA (PKG-2b) and an adenoviral vector encoding rat PKG II, which is resistant to the effects of this siRNA. In MC3T3 cells transfected with the mouse PKG II-specific siRNA, infection with rat PKG II virus, but not with a control LacZ virus, restored cGMP-induced *fos* family gene expression to the levels found in control GFP siRNA-transfected cells (Fig. 6*A*). Viral transduction of PKG II in control siRNA-transfected cells did not further enhance cGMP-induced c-*fos* or *fra-2* mRNA expression, suggesting that endogenous PKG II levels, although low, were not rate-limiting. However, cGMP stimulation of *fra-1* mRNA was enhanced in cells with elevated PKG II levels (Fig. 6*A*, $p <$ 0.05 for the comparison of GFP siRNA-treated cells infected with LacZ *versus* PKG II virus). Viral PKG II expression was demonstrated by Western blotting of membranes prepared from PKG II virus-infected MC3T3 cells (Fig. 6*B*; again, endogenous PKG II levels in PKG II siRNA-transfected cells were below detection).

Induction of c-fos, fra-1, fra-2, and fosB/ΔfosB mRNA Expression by Fluid Shear Stress Is MEK/Erk-dependent—Mechanical stimulation enhances osteoblast proliferation via activation of the MEK/Erk pathway (20, 54, 62, 68). Whether MEK inhibition prevents c-*fos* mRNA expression appears to depend on the type of mechanical stimulus and/or the source of osteoblasts, with variable results also reported for the effect of p38 MAPK inhibitors on mechanically induced c-*fos* expression (20–22, 24, 54). We therefore investigated the effects of MEK and p38 inhibitors in fluid shear-stressed osteoblasts.

We found that fluid shear stress rapidly increased Erk1/2 phosphorylation on a site that correlates with Erk1/2 activation (Fig. 7*A* shows results in MC3T3 cells, but similar results were obtained in hPOBs and UMR106 cells). Maximal induction of Erk phosphorylation after 10 min of shear stress was 11.4-fold compared with sham-treated cells. Pretreating cells with the MEK inhibitor U0126 blocked Erk phosphorylation and almost completely prevented shear induction of c-*fos*, *fra-1*, *fra-2*, and *fosB*/Δ*fosB* mRNAs (Fig. 7, *B* and *C*; U0126 inhibition of *fosB*/Δ*fosB* mRNA induction was measured by semi-quantitative RT-PCR; data not shown). The p38 inhibitor SB203580, however, did not affect Erk or *fos* family genes (Fig. 7, *B* and *C*; SB203580 inhibited UV stress-induced p38 activation in control experiments; data not shown). A similar effect of U0126 on
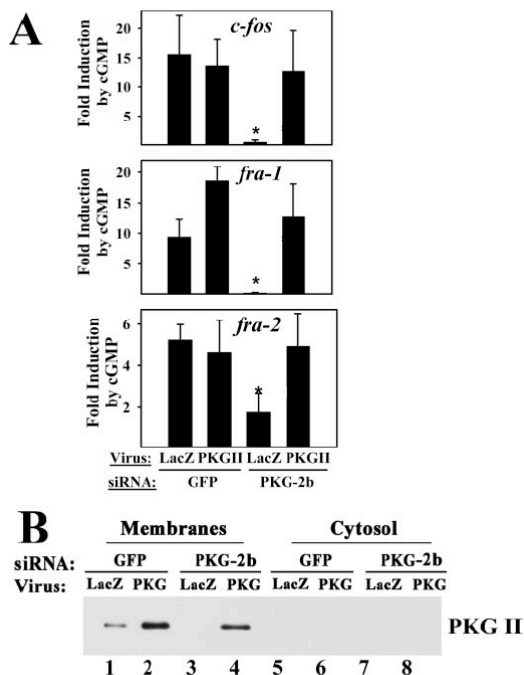
FIGURE 6. Rescue of PKG II siRNA-transfected cells with a virus encoding siRNA-resistant PKG II. *A*, MC3T3 cells were transfected with either GFP siRNA or the mouse PKG II-specific siRNA (PKG-2b), and 24 h later, cells were infected with either control virus encoding β-galactosidase (LacZ) or virus encoding siRNA-resistant rat PKG II as indicated. Forty eight hours later, cells were either mock-treated or were treated with 8-pCPT-cGMP for 1 h, and *fos* family gene expression was determined as described in Fig. 5*E*. *, $p <$ 0.05 for the comparison between GFP *versus* PKG II siRNA-treated cells infected with LacZ virus and the comparison between PKG II siRNA-treated cells infected with LacZ *versus* PKG II virus. *B*, cells were transfected with GFP siRNA (*lanes 1, 2, 5,* and *6*) or PKG-2b siRNA (*lanes 3, 4, 7,* and *8*) and were infected with LacZ virus (*odd lanes*) or PKG II virus (*even lanes*) as described in *A*. Levels of endogenous murine PKG II and virally expressed rat PKG II were examined by Western blotting of membrane and cytosolic proteins.

fluid shear stress-induced *fosB* mRNA expression was reported in primary rat osteoblasts (54).

Fluid Shear Stress-induced Erk Activation Requires NO/cGMP/PKG II Signaling—Because fluid shear stress induction of the four *fos* family genes required signaling through NO/cGMP/PKG II and the MEK/Erk pathway, we asked whether Erk activation occurred through NO/cGMP/PKG II. Pretreating osteoblasts with L-NAME, ODQ, or (R_p)-8-pCPT-PET-cGMPS prevented shear-induced Erk1/2 phosphorylation in MC3T3 cells (Fig. 8*A*); similar results were obtained in hPOBs (supplemental Fig. 4*A*; L-NAME not shown in hPOBs). Fluid shear stress-induced Erk phosphorylation was abolished in MC3T3 cells transfected with a PKG II-specific siRNA, but transfection of a PKG I-specific siRNA was without effect (Fig. 8*B*; results similar to those shown for PKG-2a siRNA were obtained with PKG-2b siRNA). Thus, Erk activation by shear stress, like shear-induced *fos* family gene expression, required NO/cGMP activation of PKG II.
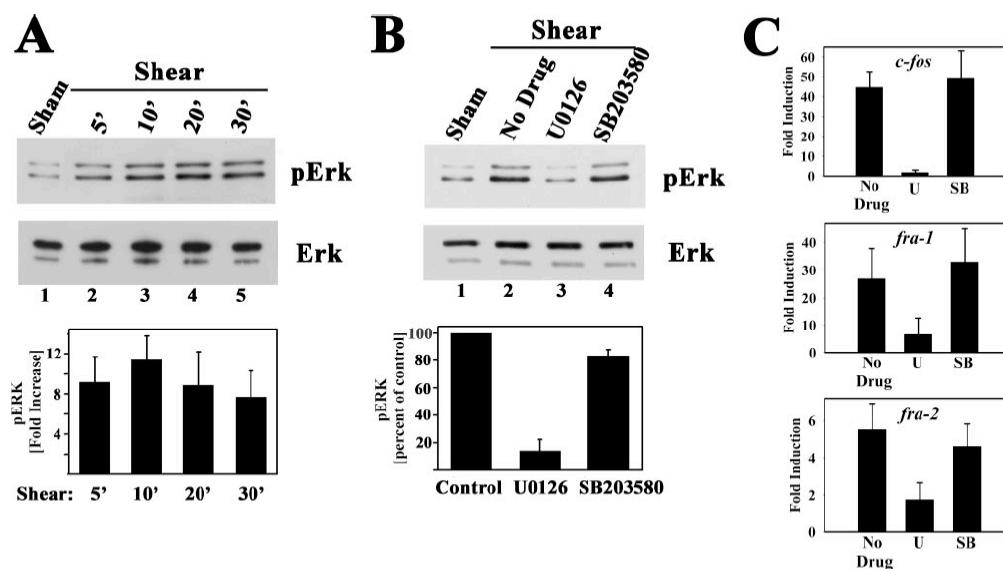
PKG and Shear Stress-induced Gene Expression

A

Sham | Shear 5' 10' 20' 30'

pErk

Erk

1 2 3 4 5

B

Shear

Sham | No Drug | U0126 | SB203580

pErk

Erk

1 2 3 4

C

c-fos

fra-1

fra-2

FIGURE 7. **Induction of c-fos, fra-1, and fra-2 mRNA expression by fluid shear stress is MEK/Erk-dependent.** A, serum-deprived MC3T3 cells were kept under static conditions for 30 min (sham-treated, lane 1) or were subjected to laminar flow for 5 min (lane 2), 10 min (lane 3), or 20 min (lanes 4 and 5); cells in lane 5 were kept in the flow chamber for an additional 10 min after the 20- min exposure to flow. Cell lysates were analyzed by Western blotting using a phospho-Erk1/2-specific antibody (clone E-4, upper panel); duplicate blots were probed with an antibody recognizing Erk1/2 irrespective of their phosphorylation state (lower panel). The bar graph below summarizes results of three independent experiments; phospho-Erk1 bands were scanned, and the intensity of the band found in sham-treated cells was assigned a value of 1. B, serum-deprived MC3T3 cells were preincubated for 1 h in the flow chamber under static conditions with either culture medium alone or with medium containing 10 μM U0126 or 10 μM SB203580, and cells were exposed to laminar flow for 10 min; Erk phosphorylation was assessed as described in A, with phospho-Erk levels in shear-stressed cells incubated with media alone assigned a value of 100%. C, cells were treated as described in B; they were exposed to laminar flow for 20 min and were harvested 10 min later for determination of c-fos, fra-1, fra-2, and gapd mRNA levels by quantitative RT-PCR, as described in Fig. 1B. *, $p < 0.05$ for the comparison between cells treated with U0126 (U) versus control cells receiving no drug (in B and C). S, SB203580.

A

Shear

Sham | No Drug | L-NAME | ODQ | Rp-cGMPS

pErk

Erk

1 2 3 4 5

B

siRNA: GFP | PKG 1 | PKG 2a
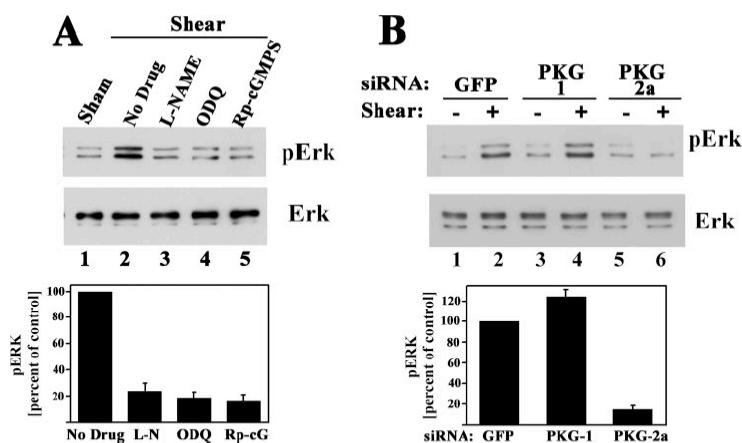Shear: - + - + - +

pErk

Erk

1 2 3 4 5 6

FIGURE 8. **Fluid shear stress-induced Erk activation requires NO/cGMP/PKG II signaling.** MC3T3 cells were serum-deprived for 24 h prior to the indicated treatments, and Erk phosphorylation was assessed as described in Fig. 7. A, cells were treated for 1 h with 4 mM L-NAME, 10 μM ODQ, or 100 μM (R_p)-8-pCPT-PET-cGMPS (Rp-cGMPS) as indicated, prior to a 10-min exposure to laminar flow (lanes 2–5); cells in lane 1 were kept under static conditions (sham-treated). In the bar graph below, three independent experiments are summarized. $p < 0.05$ for the comparison between control cells receiving no drug and cells treated with L-NAME, ODQ, or (R_p)-cGMPS. B, cells were transfected with control siRNAs specific for GFP or received siRNAs targeting PKG I (siRNA PKG-1) or PKG II (siRNA PKG-2a) as described in Fig. 5. Cells were either kept under static conditions (−) or were exposed to laminar flow (+) for 10 min. The bar graph summarizes two independent experiments. $p < 0.05$ for the comparison between cells transfected with PKG-2a siRNA versus GFP siRNA.

NO/cGMP Activation of PKG II Is Sufficient to Activate Erk1/2—We next examined whether direct PKG activation by 8-pCPT-cGMP affected Erk phosphorylation in osteoblasts. In serum-starved MC3T3 cells, 50 μM 8-pCPT-cGMP increased Erk1/2 phosphorylation 7.6-fold at 10 min, with phospho-Erk levels returning to base line at 30 min (Fig. 9A; comparable results were obtained in hPOBs, shown in supplemental Fig. 4B). In cells treated with A23187 to increase intracellular calcium, Erk phosphorylation increased to a similar extent as observed with 8-pCPT-cGMP, and the effect of both agents appeared additive (supplemental Fig. 2C). These results are consistent with the combined effects of calcium and cGMP on c-fos, fra-1, fra-2, and fosB/ΔfosB mRNA expression (Fig. 4E and supplemental Fig. 2, A and B).

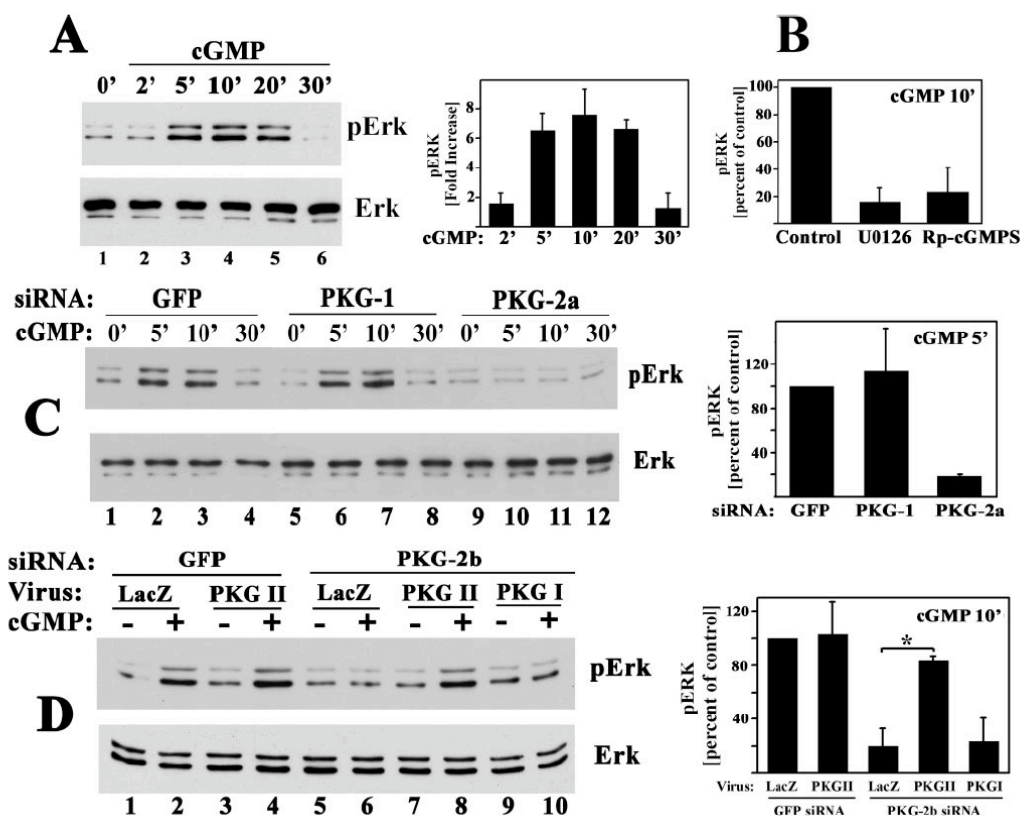Inhibition of MEK by U0126 or inhibition of PKG by (R_p)-8-

FIGURE 9. **NO/cGMP activation of PKG II is sufficient to activate Erk1/2.** Erk phosphorylation was assessed in serum-deprived MC3T3 cells as described in Fig. 7A. *A,* cells were treated with 50 μM 8-pCPT-cGMP for the indicated times. The *bar graph* summarizes three independent experiments. *B,* cells were preincubated for 1 h in medium alone or in medium containing 10 μM U0126 or 10 μM SB203580 as indicated, prior to receiving 50 μM 8-pCPT-cGMP (*cGMP*) for 10 min; phospho-Erk levels in cells treated with cGMP alone were assigned a value of 100%. *C,* cells were transfected with a control siRNA specific for GFP (*lanes 1–4*), or an siRNA targeting PKG I (siRNA PKG-1, *lanes 5–8*), or PKG II (siRNA PKG-2a, *lanes 9–12*) as described in Fig. 5 and were treated with 50 μM 8-pCPT-cGMP for the indicated times. The *bar graph* on the *right* summarizes phospho-Erk1 levels measured in cells treated with cGMP for 5 min; $p < 0.05$ was used for the comparison between cells transfected with PKG-2a siRNA *versus* GFP siRNA. *D,* cells were transfected with either GFP siRNA (*lanes 1–4*) or the mouse PKG II-specific siRNA PKG-2b (*lanes 5–10*); 8 h later, cells were infected with control virus (LacZ, *lanes 1, 2, 5,* and *6*), virus encoding siRNA-resistant rat PKG II (*lanes 3, 4, 7,* and *8*), or virus encoding PKG I (*lanes 9* and *10*). Forty eight hours later, cells were treated with 8-pCPT-cGMP for 10 min. The *bar graph* on the *right* summarizes cGMP-induced phospho-Erk1 levels; *, $p < 0.05$ for the comparison between LacZ and PKG II virus-infected cells transfected with PKG-2a siRNA.

pCPT-PET-cGMPS blocked cGMP-induced Erk phosphorylation in MC3T3 cells (Fig. 9B). ODQ inhibited Erk phosphorylation induced by the NO donor PAPA-NONOate, and (R_p)-8-pCPT-PET-cGMPS inhibited cGMP-induced Erk phosphorylation in hPOBs (supplemental Fig. 4B).

Consistent with PKG II mediating cGMP effects on *fos* family gene expression (Figs. 5 and 6), siRNA-mediated suppression of PKG II prevented cGMP-induced Erk activation, whereas suppression of PKG I was without effect (Fig. 9C). To confirm the role of PKG II in regulating Erk1/2, we transfected cells with the mouse-specific siRNA PKG-2b and restored PKG II expression by infecting cells with adenovirus encoding rat PKG II. Viral expression of PKG II restored cGMP-induced Erk phosphorylation in PKG-2b siRNA-transfected cells (Fig. 9D; viral expression of rat PKG II is shown in Fig. 6B). In contrast, infecting cells

with a LacZ- or PKG I-expressing adenovirus was without effect (viral expression of PKG I was confirmed by Western blotting and activity assay; data not shown). We conclude that cGMP activation of PKG II is necessary and sufficient to mediate Erk activation in osteoblasts and that PKG I cannot replace PKG II in this function.

DISCUSSION

We found that fluid shear stress induced a rapid and sustained increase in c-*fos, fra-1, fra-2,* and *fosB/ΔfosB* mRNA in human primary osteoblasts, MC3T3, and UMR106 cells. These *fos* family genes encode members of the AP-1 transcription factor family that regulate osteoblast proliferation and differentiation (6, 8, 10, 11). We determined that mechanical stimulation
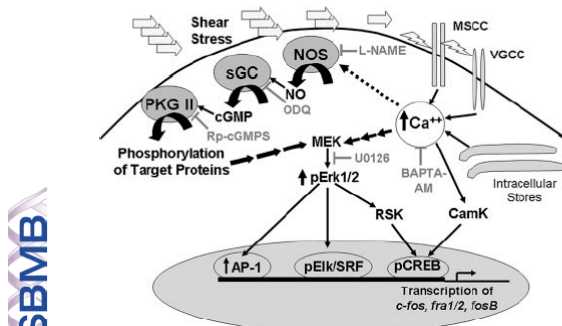
PKG and Shear Stress-induced Gene Expression

FIGURE 10. **NO/cGMP and calcium signaling in osteoblast mechanotransduction.** Osteoblast exposure to fluid shear stress leads to a rapid increase in intracellular calcium through activation of mechanosensitive and voltage-gated calcium channels (*MSCC* and *VGCC,* respectively), and possibly through calcium release from intracellular stores (17, 54, 62, 63, 69). An initial burst of NO synthesis may require calcium activation of NO synthase (*NOS*), but sustained NO synthesis is calcium-independent and may involve activation of NO synthase by phosphorylation (57, 59). NO activates sGC and the resulting cGMP activates membrane-bound PKG II, which phosphorylates substrates leading to activation of the MEK/Erk pathway. The MEK/Erk pathway increases transcription of *c-fos, fra-1, fra-2,* and *fosB/ΔfosB* through the following: (i) RSK-mediated phosphorylation and activation of the CREB; (ii) direct phosphorylation of Elk that forms a complex with and activates serum-response factor (*SRF*); and (iii) recruitment of AP-1 (Fos/Jun) complexes to the promoters (79). Calcium activates the MEK/Erk pathway through Ras/Raf activation of MEK, and can directly activate CREB through calmodulin-dependent protein kinase (*CamK*) (89). Inhibitors used in this study are indicated in *gray.* BAPTA-AM, 1,2-bis(2-aminophenoxy)ethane-*N,N,N′,N′*-tetraacetic acid.

of all four *fos* family genes was mediated by the NO/cGMP/PKG II signaling pathway and required PKG II-dependent Erk activation (Fig. 10).

One of the earliest effects of fluid shear stress on osteoblasts is an increase in the intracellular calcium concentration. In both MC3T3 cells and human osteoblasts, the increase is detectable within seconds of flow onset, and is sustained for at least several minutes (17, 63, 69). Increased intracellular calcium leads to activation of constitutively expressed NO synthases, and increased NO production in osteoblasts occurs within 5 min of flow onset (55, 56, 70) (Fig. 2*A*). However, only the initial burst of NO synthesis is calcium-dependent, whereas the later sustained phase of NO production is calcium-independent (57). Our results suggest that the sustained stimulation of NO synthase activity may occur through eNOS phosphorylation by multiple kinases, as observed in fluid shear-stressed endothelial cells (59, 71).

We found that fluid shear stress stimulates osteoblasts to produce sufficient NO to increase the intracellular cGMP concentration and activate PKG, based on increased VASP phosphorylation on Ser[259], a site targeted by both PKG I and II. Using an siRNA approach, we showed that PKG II, but not PKG I, is required for shear-induced *c-fos, fra-1, fra-2* and *fosB/ΔfosB* mRNA expression. This was surprising, because osteoblasts contain ~5-fold more cytosolic PKG activity (PKG I) than membrane-bound PKG activity (PKG II),[3] and PKG I and II share many substrates *in vitro* (72). However, PKG II may be uniquely situated for activation by shear-induced NO. In neu-

ronal cells, PKG II, NO synthase, and sGC localize to specialized synaptic membrane domains that contain glutamate receptors (66, 73). A similar co-localization of eNOS, sGC, and PKG II may occur in osteoblast membranes, near mechanoreceptors that transduce biophysical stimuli into biochemical signals. Possible mechanoreceptors include mechanosensitive calcium channels, G-proteins activated by membrane deformation, and integrin adhesions and cytoskeletal structures (3, 5, 74). We previously showed in osteoblasts that PKG II phosphorylates and inactivates glycogen synthase kinase-3, leading to increased DNA binding activity of CAAT enhancer-binding protein *β* (C/EBP-*β*); the latter cooperates with CREB in mediating cGMP regulation of c-*fos* (40, 75). In contrast, cGMP stimulation of interleukin-6 transcription in osteoblasts requires PKG I (41). Thus, PKG I and II have different roles in osteoblasts, consistent with our finding that PKG II, but not PKG I, mediates mechanotransduction.

Mice with a targeted deletion of PKG II and rats with a spontaneous deletion in the PKG II gene develop dwarfism because of impaired chondroblast differentiation (38, 76). In chondroblasts, PKG II regulates the switch from proliferation to hypertrophic differentiation by inhibiting the transcription factor Sox9 and by phosphorylating and inactivating glycogen synthase kinase-3; the latter suppresses *β*-catenin degradation, leading to increased differentiation (39, 77). Our results suggest that defective PKG II regulation of *c-fos, fra-1, fra-2,* and *fosB/ΔfosB* in osteoblasts and/or chondroblasts may contribute to the developmental bone defects observed in PKG II-deficient rodents. No obvious skeletal abnormalities have been observed in PKG I-deficient mice, but their life span is too short to determine whether PKG I contributes to post-natal skeletal homeostasis (78).

We found that fluid shear stress induction of *c-fos, fra-1, fra-2,* and *fosB/ΔfosB* mRNAs required signaling through the MEK/Erk but not the p38 MAPK pathway. These findings are consistent with previous work showing that the MEK inhibitor U0126 largely prevents c-*fos* induction in MC3T3 cells exposed to gravitational force and *fosB/ΔfosB* induction in mechanically stimulated primary rat osteoblasts, whereas the p38 inhibitor SB203580 has no effect (20, 24, 54). The MEK/Erk signal transduction pathway regulates transcription of all four *fos* family genes by targeting common *cis*-acting promoter elements, *i.e.* the serum-response element, cAMP-response element, and phorbol ester-response element(s) (AP-1-binding sites) (Fig. 10) (79). Erk phosphorylates the ternary complex factor Elk-1, causing it to associate with and activate serum-response factor at the serum-response element, and Erk activation recruits c-Jun/Fra-2-containing AP-1 complexes to the *fra-1* and *fra-2* promoters (80–85). The Erk-activated kinases of the RSK family phosphorylate and activate CREB, which plays a major role in fluid shear stress-induced transcription of *fosB/ΔfosB* (54, 84, 86). Erk regulation of c-*fos, fra-1, fra-2,* and *fosB/ΔfosB* expression may explain why Erk is essential for osteoblast growth and differentiation (20, 68, 87).

The mechanism of Erk1/2 activation in mechanically stimulated osteoblasts is only partly understood. In fluid shear-stressed MC3T3 cells, Erk activation is calcium-dependent and inhibited by chelation of intra- or extracellular calcium;

---

[3] S. Zhuang and R. Pilz, unpublished results.

whether it requires calcium entry through mechano-sensitive cation channels and/or L-type voltage-gated calcium channels is unclear (Fig. 10) (54, 62, 63). We found that fluid shear stress-induced Erk1/2 phosphorylation was blocked by pharmacological inhibition of either NO/cGMP synthesis or PKG activity, and siRNA experiments demonstrated that both shear- and cGMP-induced Erk activation was mediated by PKG II. Possible targets of PKG II leading to Erk activation include MEK, focal adhesion kinase, and Src family kinases. Consistent with our results, Kapur *et al.* (88) found that L-NAME blocked fluid shear stress-induced Erk phosphorylation in hPOBs, leading to decreased shear-induced DNA synthesis, but signaling downstream of NO was not examined. Chelation of both extra- or intracellular calcium prevents fluid shear stress-induced NO synthesis at early time points (57) and blocks Erk activation (54, 62, 63) and c-*fos, fra-1, fra-2,* and *fosB/ΔfosB* mRNA expression (supplemental Fig. 2A) (17, 54). These data suggest a linear pathway from calcium through NO/cGMP/PKG II to Erk activation and expression of *fos* family genes (Fig. 10). However, we found that calcium and cGMP cooperate to increase expression of the four *fos* genes. Calcium is known to regulate the c-*fos* promoter through multiple mechanisms, including Ras/Raf/MEK/Erk/RSK- and calcium/calmodulin-dependent protein kinase phosphorylation of CREB (89) (Fig. 10).

Fra-1, Fra-2, and ΔFosB are important for osteoblast proliferation and differentiation, as demonstrated *in vitro*, and by the dramatic osteosclerotic or osteoporotic phenotypes of mice that either overexpress or lack these proteins, respectively (6, 8, 10, 11). c-Fos is required for osteoblast cell cycle control, and all four *fos* genes are coordinately regulated during osteoblast differentiation (90–92). Fos proteins cooperate with the osteoblast-specific transcription factor Runx/Cbfa1 to regulate genes involved in osteoblast differentiation and extracellular matrix synthesis (93, 94). In addition, c-Fos, together with CREB and C/EBP-β, mediate fluid shear stress induction of cyclooxygenase-2, a gene implicated in the adaptive response of bone to mechanical stimulation (95). Induction of c-*fos* and *fosB/ΔfosB* mRNA by mechanical loading of bones in intact animals correlates with increased bone formation, and c-*fos* mRNA induction and bone formation *in vivo* are at least partly prevented by NO synthase inhibitors, consistent with the positive effects of NO donors on osteoblast growth and differentiation *in vitro* and bone formation *in vivo* (14, 16, 25, 30, 31, 33, 34, 54). We conclude that NO/cGMP/PKG II-mediated induction of c-*fos, fra-1, fra-2,* and *fosB/ΔfosB* likely plays an essential role in the anabolic response of bone to mechanical stimulation.

REFERENCES

1. Hughes-Fulford, M. (2004) *Sci. STKE 2004,* RE12
2. Ehrlich, P. J., and Lanyon, L. E. (2002) *Osteoporos. Int.* **13,** 688–700
3. Orr, A. W., Helmke, B. P., Blackman, B. R., and Schwartz, M. A. (2006) *Dev. Cell* **10,** 11–20
4. Hillsley, M. V., and Frangos, J. A. (1994) *Biotechnol. Bioeng.* **43,** 573–581
5. Rubin, J., Rubin, C., and Jacobs, C. R. (2006) *Gene (Amst.)* **367,** 1–16
6. Wagner, E. F., and Eferl, R. (2005) *Immunol. Rev.* **208,** 126–140
7. Ruther, U., Garber, C., Komitowski, D., Muller, R., and Wagner, E. F. (1987) *Nature* **325,** 412–416
8. Grigoriadis, A. E., Schellander, K., Wang, Z. Q., and Wagner, E. F. (1993) *J. Cell Biol.* **122,** 685–701
9. Jochum, W., David, J. P., Elliott, C., Wutz, A., Plenk, H., Jr., Matsuo, K., and Wagner, E. F. (2000) *Nat. Med.* **6,** 980–984
10. Sabatakos, G., Sims, N. A., Chen, J., Aoki, K., Kelz, M. B., Amling, M., Bouali, Y., Mukhopadhyay, K., Ford, K., Nestler, E. J., and Baron, R. (2000) *Nat. Med.* **6,** 985–990
11. Eferl, R., Hoebertz, A., Schilling, A. F., Rath, M., Karreth, F., Kenner, L., Amling, M., and Wagner, E. F. (2004) *EMBO J.* **23,** 2789–2799
12. Kenner, L., Hoebertz, A., Beil, T., Keon, N., Karreth, F., Eferl, R., Scheuch, H., Szremska, A., Amling, M., Schorpp-Kistner, M., Angel, P., and Wagner, E. F. (2004) *J. Cell Biol.* **164,** 613–623
13. Moalli, M. R., Caldwell, N. J., Patil, P. V., and Goldstein, S. A. (2000) *J. Bone Miner. Res.* **15,** 1346–1353
14. Chow, J. W., Fox, S. W., Lean, J. M., and Chambers, T. J. (1998) *J. Bone Miner. Res.* **13,** 1039–1044
15. Lean, J. M., Mackay, A. G., Chow, J. W., and Chambers, T. J. (1996) *Am. J. Physiol.* **270,** E937–E945
16. Raab-Cullen, D. M., Thiede, M. A., Petersen, D. N., Kimmel, D. B., and Recker, R. R. (1994) *Calcif. Tissue Int.* **55,** 473–478
17. Chen, N. X., Ryder, K. D., Pavalko, F. M., Turner, C. H., Burr, D. B., Qiu, J., and Duncan, R. L. (2000) *Am. J. Physiol.* **278,** C989–C997
18. Pavalko, F. M., Chen, N. X., Turner, C. H., Burr, D. B., Atkinson, S., Hsieh, Y. F., Qiu, J., and Duncan, R. L. (1998) *Am. J. Physiol.* **275,** C1591–C1601
19. Peake, M. A., Cooling, L. M., Magnay, J. L., Thomas, P. B., and El Haj, A. J. (2000) *J. Appl. Physiol.* **89,** 2498–2507
20. Hatton, J. P., Pooran, M., Li, C. F., Luzzio, C., and Hughes-Fulford, M. (2003) *J. Bone Miner. Res.* **18,** 58–66
21. Granet, C., Vico, A. G., Alexandre, C., and Lafage-Proust, M. H. (2002) *Cell. Signal.* **14,** 679–688
22. Kletsas, D., Basdra, E. K., and Papavassiliou, A. G. (2002) *J. Cell Physiol.* **190,** 313–321
23. Fitzgerald, J., and Hughes-Fulford, M. (1999) *FASEB J.* **13,** 553–557
24. Naruse, K., Miyauchi, A., Itoman, M., and Mikuni-Takagaki, Y. (2003) *J. Bone Miner. Res.* **18,** 360–369
25. Fox, S. W., Chambers, T. J., and Chow, J. W. (1996) *Am. J. Physiol.* **270,** E955–E960
26. MacPherson, H., Noble, B. S., and Ralston, S. H. (1999) *Bone (NY)* **24,** 179–185
27. Aguirre, J., Buttery, L., O'Shaughnessy, M., Afzal, F., de Marticorena, I. F., Hukkanen, M., Huang, P., MacIntyre, I., and Polak, J. (2001) *Am. J. Pathol.* **158,** 247–257
28. Bergula, A. P., Haidekker, M. A., Huang, W., Stevens, H. Y., and Frangos, J. A. (2004) *Bone (NY)* **34,** 562–569
29. Armour, K. E., Armour, K. J., Gallagher, M. E., Godecke, A., Helfrich, M. H., Reid, D. M., and Ralston, S. H. (2001) *Endocrinology* **142,** 760–766
30. Mancini, L., Moradi-Bidhendi, N., Becherini, L., Martineti, V., and MacIntyre, I. (2000) *Biochem. Biophys. Res. Commun.* **274,** 477–481
31. Iikiji, I., Shin, W. S., Oida, S., Takato, T., Koizumi, T., and Toyo-oka, T. (1997) *FEBS Lett.* **410,** 238–242
32. Chae, H. J., Park, R. K., Chung, H. T., Kang, J. S., Kim, M. S., Choi, D. Y., Bang, B. G., and Kim, H. R. (1997) *J. Pharm. Pharmacol.* **49,** 897–902
33. Wimalawansa, S. J., De, M. G., Gangula, P., and Yallampalli, C. (1996) *Bone (NY)* **18,** 301–304
34. Jamal, S. A., Cummings, S. R., and Hawker, G. A. (2004) *J. Bone Miner. Res.* **19,** 1512–1517
35. van't Hof, R. J., and Ralston, S. H. (2001) *Immunology* **103,** 255–261
36. Munzel, T., Feil, R., Mulsch, A., Lohmann, S. M., Hofmann, F., and Walter, U. (2003) *Circulation* **108,** 2172–2183
37. Schlossmann, J., Feil, R., and Hofmann, F. (2005) *Front. Biosci.* **10,** 1279–1289
38. Pfeifer, A., Aszòdi, A., Seidler, U., Ruth, P., Hofmann, F., and Fässler, R. (1996) *Science* **274,** 2082–2086
39. Chikuda, H., Kugimiya, F., Hoshi, K., Ikeda, T., Ogasawara, T., Shimoaka,

PKG and Shear Stress-induced Gene Expression

T., Kawano, H., Kamekura, S., Tsuchida, A., Yokoi, N., Nakamura, K., Komeda, K., Chung, U. I., and Kawaguchi, H. (2004) *Genes Dev.* **18**, 2418–2429

40. Chen, Y., Zhuang, S., Cassenaer, S., Casteel, D. E., Gudi, T., Boss, G. R., and Pilz, R. B. (2003) *Mol. Cell. Biol.* **23**, 4066–4082
41. Broderick, K. E., Zhang, T., Rangaswami, H., Zeng, Y., Zhao, X., Boss, G. R., and Pilz, R. B. (2007) *Mol. Endocrinol.* **21**, 1148–1162
42. Pilz, R. B., Suhasini, M., Idriss, S., Meinkoth, J. L., and Boss, G. R. (1995) *FASEB J.* **9**, 552–558
43. Gudi, T., Huvar, I., Meinecke, M., Lohmann, S. M., Boss, G. R., and Pilz, R. B. (1996) *J. Biol. Chem.* **271**, 4597–4600
44. Idriss, S. D., Gudi, T., Casteel, D. E., Kharitonov, V. G., Pilz, R. B., and Boss, G. R. (1999) *J. Biol. Chem.* **274**, 9489–9493
45. Gudi, T., Lohmann, S. M., and Pilz, R. B. (1997) *Mol. Cell. Biol.* **17**, 5244–5254
46. Gudi, T., Casteel, D. E., Vinson, C., Boss, G. R., and Pilz, R. B. (2000) *Oncogene* **19**, 6324–6333
47. Gudi, T., Hong, G. K. P., Vaandrager, A. B., Lohmann, S. M., and Pilz, R. B. (1999) *FASEB J.* **13**, 2143–2152
48. Kuchan, M. J., Jo, H., and Frangos, J. A. (1994) *Am. J. Physiol.* **267**, C753–C758
49. Gallagher, J. A. (2003) *Methods Mol. Med.* **80**, 3–18
50. Stevens, H. Y., and Frangos, J. A. (2003) *Methods Mol. Med.* **80**, 381–398
51. Casteel, D. E., Zhuang, S., Gudi, T., Tang, J., Vuica, M., Desiderio, S., and Pilz, R. B. (2002) *J. Biol. Chem.* **277**, 32003–32014
52. Zeng, Y., Zhuang, S., Gloddek, J., Tseng, C. C., Boss, G. R., and Pilz, R. B. (2006) *J. Biol. Chem.* **281**, 16951–16961
53. Jarchau, T., Haeusler, C., Markert, T., Poehler, D., Vandekerckhove, J., De Jonge, H. R., Lohmann, S. M., and Walter, U. (1994) *Proc. Natl. Acad. Sci. U. S. A.* **91**, 9426–9430
54. Inoue, D., Kido, S., and Matsumoto, T. (2004) *J. Biol. Chem.* **279**, 49795–49803
55. Bacabac, R. G., Smit, T. H., Mullender, M. G., Dijcks, S. J., Van Loon, J. J., and Klein-Nulend, J. (2004) *Biochem. Biophys. Res. Commun.* **315**, 823–829
56. Johnson, D. L., McAllister, T. N., and Frangos, J. A. (1996) *Am. J. Physiol.* **271**, E205–E208
57. McAllister, T. N., and Frangos, J. A. (1999) *J. Bone Miner. Res.* **14**, 930–936
58. Bakker, A. D., Soejima, K., Klein-Nulend, J., and Burger, E. H. (2001) *J. Biomech.* **34**, 671–677
59. Fleming, I., and Busse, R. (2003) *Am. J. Physiol.* **284**, R1–R12
60. Deleted in proof
61. Smolenski, A., Bachmann, C., Reinhard, K., Hoenig-Liedl, P., Jarchau, T., Hoschuetzky, H., and Walter, U. (1998) *J. Biol. Chem.* **273**, 20029–20035
62. Liu, D., Genetos, D. C., Shao, Y., Geist, D. J., Li, J., Ke, H. Z., Turner, C. H., and Duncan, R. L. (2008) *Bone (NY)* **42**, 644–652
63. You, J., Reilly, G. C., Zhen, X., Yellowley, C. E., Chen, Q., Donahue, H. J., and Jacobs, C. R. (2001) *J. Biol. Chem.* **276**, 13365–13371
64. Donahue, S. W., Donahue, H. J., and Jacobs, C. R. (2003) *J. Biomech.* **36**, 35–43
65. Ajubi, N. E., Klein-Nulend, J., Alblas, M. J., Burger, E. H., and Nijweide, P. J. (1999) *Am. J. Physiol.* **276**, E171–E178
66. Serulle, Y., Zhang, S., Ninan, I., Puzzo, D., McCarthy, M., Khatri, L., Arancio, O., and Ziff, E. B. (2007) *Neuron* **56**, 670–688
67. Vaandrager, A. B., Edixhoven, M., Bot, A. G. M., Kroos, M. A., Jarchau, T., Lohmann, S., Genieser, H.-G., and De Jonge, H. R. (1997) *J. Biol. Chem.* **272**, 11816–11823
68. Jiang, G. L., White, C. R., Stevens, H. Y., and Frangos, J. A. (2002) *Am. J. Physiol.* **283**, E383–E389
69. Jacobs, C. R., Yellowley, C. E., Davis, B. R., Zhou, Z., Cimbala, J. M., and Donahue, H. J. (1998) *J. Biomech.* **31**, 969–976
70. Klein-Nulend, J., Helfrich, M. H., Sterck, J. G., MacPherson, H., Joldersma, M., Ralston, S. H., Semeins, C. M., and Burger, E. H. (1998) *Biochem. Biophys. Res. Commun.* **250**, 108–114
71. Boo, Y. C., and Jo, H. (2003) *Am. J. Physiol.* **285**, C499–C508
72. Gamm, D. M., Francis, S. H., Angelotti, T. P., Corbin, J. D., and Uhler, M. D. (1995) *J. Biol. Chem.* **270**, 27380–27388
73. Wang, H. G., Lu, F. M., Jin, I., Udo, H., Kandel, E. R., de Vente, J., Walter, U., Lohmann, S. M., Hawkins, R. D., and Antonova, I. (2005) *Neuron* **45**, 389–403
74. Gudi, S., Nolan, J. P., and Frangos, J. A. (1998) *Proc. Natl. Acad. Sci. U. S. A.* **95**, 2515–2519
75. Zhao, X., Zhuang, S., Chen, Y., Boss, G. R., and Pilz, R. B. (2005) *J. Biol. Chem.* **280**, 32683–32692
76. Chikuda, H., Kugimiya, F., Hoshi, K., Ikeda, T., Ogasawara, T., Kamekura, S., Ogata, N., Nakamura, K., Chung, U. I., and Kawaguchi, H. (2005) *J. Bone Miner. Metab.* **23**, 200–204
77. Kawasaki, Y., Kugimiya, F., Chikuda, H., Kamekura, S., Ikeda, T., Kawamura, N., Saito, T., Shinoda, Y., Higashikawa, A., Yano, F., Ogasawara, T., Ogata, N., Hoshi, K., Hofmann, F., Woodgett, J. R., Nakamura, K., Chung, U. I., and Kawaguchi, H. (2008) *J. Clin. Investig.* **118**, 2506–2515
78. Pfeifer, A., Klatt, P., Massberg, S., Ny, L., Sausbier, M., Hirneib, C., Wang, G.-X., Korth, M., Aszòdi, A., Andersson, K.-E., Krombach, F., Mayerhofer, A., Ruth, P., Fassler, R., and Hofmann, F. (1998) *EMBO J.* **17**, 3045–3051
79. Hazzalin, C. A., and Mahadevan, L. C. (2002) *Nat. Rev. Mol. Cell Biol.* **3**, 30–40
80. Gille, H., Kortenjann, M., Strahl, T., and Shaw, P. E. (1996) *Mol. Cell. Biol.* **16**, 1094–1102
81. Wang, Y., and Prywes, R. (2000) *Oncogene* **19**, 1379–1385
82. Adiseshaiah, P., Li, J., Vaz, M., Kalvakolanu, D. V., and Reddy, S. P. (2008) *Biochem. Biophys. Res. Commun.* **371**, 304–308
83. Adiseshaiah, P., Papaiahgari, S. R., Vuong, H., Kalvakolanu, D. V., and Reddy, S. P. (2003) *J. Biol. Chem.* **278**, 47423–47433
84. Adiseshaiah, P., Peddakama, S., Zhang, Q., Kalvakolanu, D. V., and Reddy, S. P. (2005) *Oncogene* **24**, 4193–4205
85. Murakami, M., Ui, M., and Iba, H. (1999) *Cell Growth & Differ.* **10**, 333–342
86. Mayr, B., and Montminy, M. (2001) *Nat. Rev. Mol. Cell Biol.* **2**, 599–609
87. Lai, C. F., Chaudhary, L., Fausto, A., Halstead, L. R., Ory, D. S., Avioli, L. V., and Cheng, S. L. (2001) *J. Biol. Chem.* **276**, 14443–14450
88. Kapur, S., Baylink, D. J., and Lau, K. H. (2003) *Bone (NY)* **32**, 241–251
89. Shaywitz, A. J., and Greenberg, M. E. (1999) *Annu. Rev. Biochem.* **68**, 821–861
90. Sunters, A., Thomas, D. P., Yeudall, W. A., and Grigoriadis, A. E. (2004) *J. Biol. Chem.* **279**, 9882–9891
91. Demiralp, B., Chen, H. L., Koh, A. J., Keller, E. T., and McCauley, L. K. (2002) *Endocrinology* **143**, 4038–4047
92. McCabe, L. R., Banerjee, C., Kundu, R., Harrison, R. J., Dobner, P. R., Stein, J. L., Lian, J. B., and Stein, G. S. (1996) *Endocrinology* **137**, 4398–4408
93. Lian, J. B., Stein, G. S., Stein, J. L., and van Wijnen, A. J. (1998) *J. Cell Biochem.* **30**, S62–S72
94. D'Alonzo, R. C., Selvamurugan, N., Karsenty, G., and Partridge, N. C. (2002) *J. Biol. Chem.* **277**, 816–822
95. Ogasawara, A., Arakawa, T., Kaneda, T., Takuma, T., Sato, T., Kaneko, H., Kumegawa, M., and Hakeda, Y. (2001) *J. Biol. Chem.* **276**, 7048–7054

Supplemental Table I: PCR Primers Used for RT-PCR

| Gene	PCR Primers		Product Size (bp)
	Sense (5'-3')	Anti-Sense (5'-3')	
gapd (murine)	TGTCTTCΛCCΛCCΛTGGΛGΛΛCG	GTGGΛTGCΛGGGΛTGΛTGTTCTG	333
c-fos (murine)	CGCAGAGCATCGGCAGAAGG	TCTTGCAGGCAGGTCGGTGG	258
fra-1 (murine)	TGCGAGCAGATCAGCCCAGAG	CTGGAGAAAGGGAGATGCAAGG	347
fra-2 (murine)	GGAGGAGAAGCGTGCAATCC	GGGGCTGATTTTGCACACG	217
fosB (murine)	AAAAGGCAGAGCTGGAGTCGG	TGTACGAAGGGCTAACAACGG	324
pkg I (murine)	GTCACTAGGGATTCTGATGTATGA	AGAATTTCCAAAGAAGATTGCAAA	129
pkg II (murine)	GTGACACAGCGCGGTTGTT	TGGGAATGGAAAAGGACAAC	235
gapd (human)	AACGGATTTGGTCGTATTGGG	TGGAAGATGGTGATGGGATTTC	209
c-fos (human)	GTGCCAACTTCATTCCCACG	GAGATAACTGTTCCACCTTGCCC	231
fra-1 (human)	TGTGAACAGATCAGCCCGGAG	CTGGGGAAAGGGAGATACAAGG	331
fra-2 (human)	ATTATCCCGGGAACTTTGACAC	ATGTGTCCAGGGACAGAGGCC	274
fosB (human)	AAAAAGCAGAGCTGGAGTCGG	TGTACGAAGGGTTAACAACGG	323

Suppl. Fig. 1
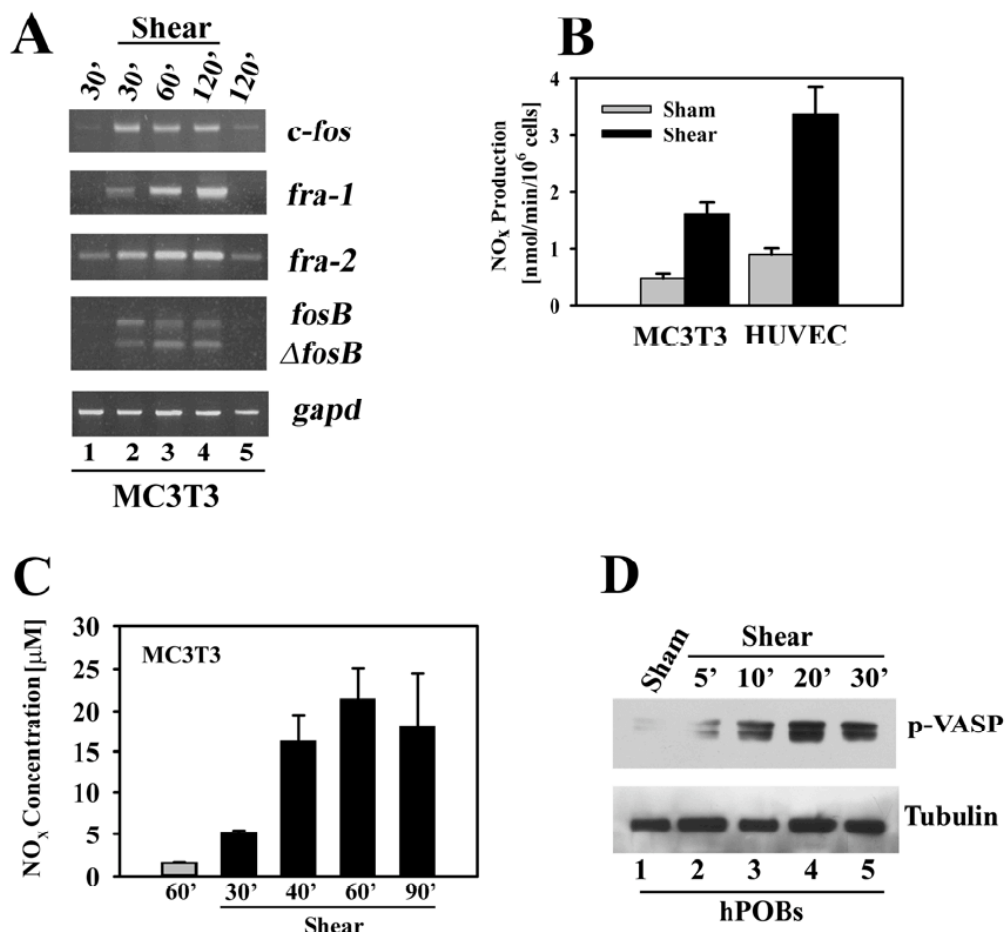
Supplemental Fig. 1:

A. Serum-deprived MC3T3 cells were incubated in a parallel plate flow chamber for the indicated times; cells were exposed to laminar flow for the first 20 min (lanes 2-4), or kept under static conditions (lanes 1 and 5). At the indicated times, *c-fos, fra-1, fra-2, fosB/ΔfosB,* or *gapd* mRNA levels were determined by semi-quantitative RT-PCR as described in Experimental Procedures.

B. In parallel experiments, MC3T3 cells and HUVEC cells were kept either under static conditions (grey bars) or were exposed to laminar flow (black bars) for 20 min. After that, cells were kept in the chamber for three additional minutes, and nitrate plus nitrite (NO_x) concentrations were measured in the media collected from the chamber. NO_x production was calculated as $nmol/min/10^6$ cells over the three min interval.

C. MC3T3 cells were kept under static conditions for 60 min (grey bar), or were exposed to laminar flow (black bars) for 20 min; media was harvested from the flow chamber at the indicated times after the onset of flow to measure NO_x concentrations (expressed in μM).

D. hPOBs were kept under static conditions (lane 1) or were exposed to laminar flow for up to 20 min (lanes 2-4); cells in lane 5 were exposed to 20 min of flow and harvested 10 min later. Cell lysates were analyzed by SDS-PAGE/Western blotting using antibodies specific for VASP phosphorylated on Ser[259] (upper panel), or for α-tubulin (lower panel).

Suppl. Fig. 2
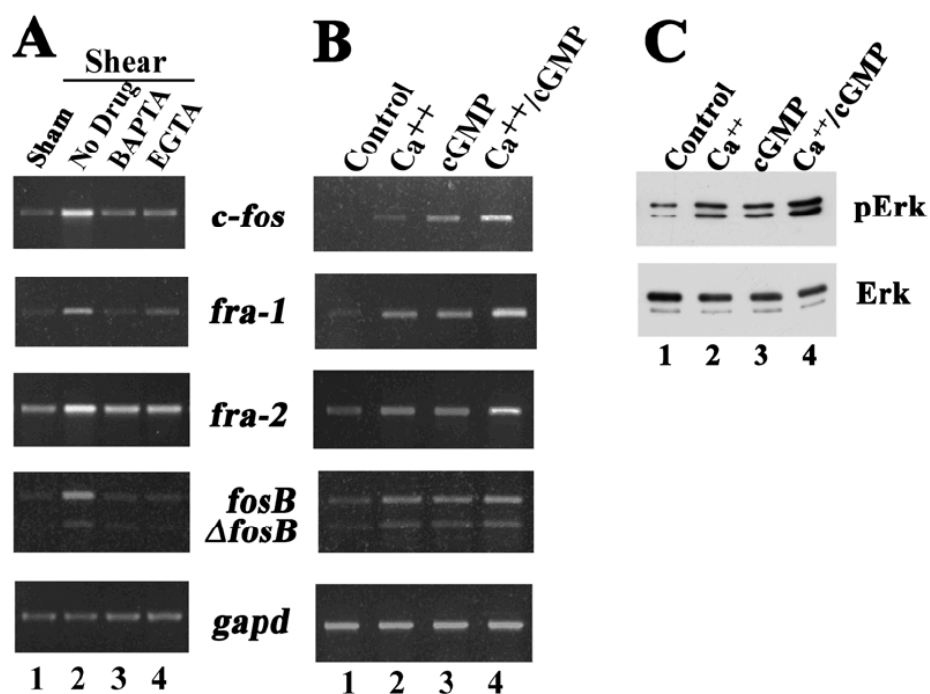
Supplemental Fig. 2:
A. MC3T3 cells were preincubated for 1 h in the presence of media alone (lanes 1 and 2), 10 μM BAPTA-AM (lane 3), or 5 mM EGTA (lane 4). After that, cells were either kept under static conditions (lane 1), or were exposed to laminar flow for 20 min (lanes 2-4), and 10 min later, *c-fos, fra-1, fra-2, fosB/ΔfosB* and *gapd* mRNA levels were determined by semi-quantitative RT-PCR as described in Experimental Procedures.
B. Cells were treated for 30 min with the calcium ionophore A23187 (0.3 μM, lanes 2 and 4) and/or 8-pCPT-cGMP (50 μM, lanes 3 and 4), and *c-fos, fra-1, fra-2, fosB/ΔfosB* and *gapd* mRNA levels were determined as in panel A.
C. Cells were incubated for 20 min with the calcium ionophore A23187 (0.3 μM, lanes 2 and 4) and/or 8-pCPT-cGMP (50 μM, lanes 3 and 4), and cell lysates were analyzed by Western blotting using a phospho-Erk1/2-specific antibody (upper panel); duplicate blots were probed with an antibody recognizing Erk1/2 irrespective of their phosphorylation state (lower panel).

Suppl. Fig. 3
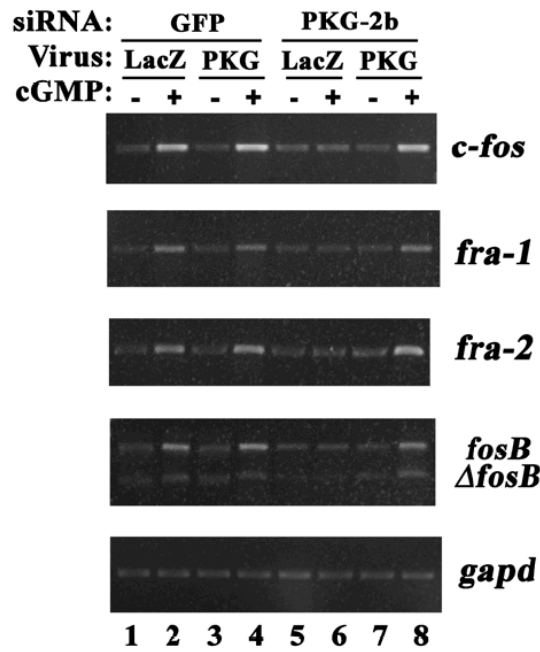
Supplemental Fig. 3:
MC3T3 cells were transfected with either GFP siRNA (lanes 1-4) or the mouse PKG II-specific siRNA PKG-2b (lanes 5-8); 8 h later, cells were infected with control virus encoding β-galactosidase (LacZ, lanes 1, 2, 5, and 6) or virus encoding siRNA-resistant rat PKG II (lanes 3, 4, 7, and 8). Forty-eight hours later, cells were treated with 8-pCPT-cGMP for 1 h, and *fos* family gene expression was determined by semiquantitative RT-PCR as described in Experimental Procedures.

Suppl. Fig. 4
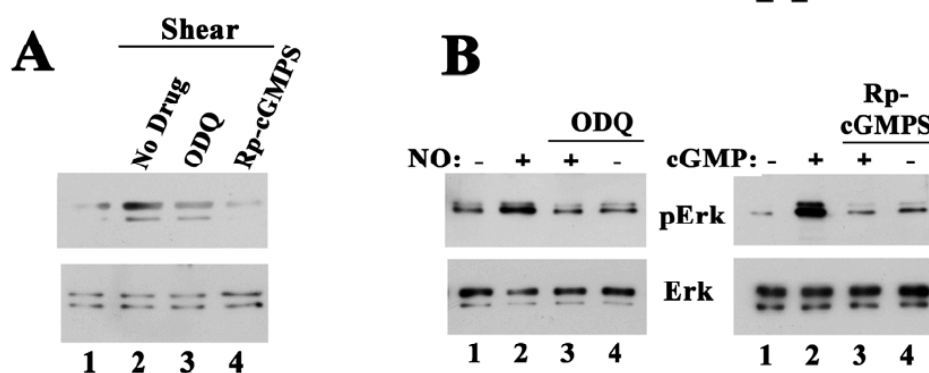
Supplemental Fig. 4:
A. Serum-deprived hPOBs were incubated for 1 h without drug, with 10 µM ODQ, or Rp-8-pCPT-PET-cGMPS as indicated, prior to a 10 min exposure to laminar flow (lanes 2-4); cells in lane 1 were kept under static conditions (sham-treated). Erk phosphorylation was assessed as described in Figs.7-10 and Supplemental Fig. 2C, using an antibody specific for Tyr-phosphorylated Erk1 (pTyr[204], clone E-4).
B. Serum-deprived hPOBs were incubated for 1 h with ODQ or Rp-8-pCPT-PET-cGMPS as indicated on top, prior to receiving 10 µM PAPA-NONOate (NO, left panels) or 50 µM 8-pCPT-cGMP (cGMP, right panels) for 10 min as indicated; cells in lane 1 were mock-treated. Erk phosphorylation was assessed using an antibody specific for dually-phosphorylated Erk1 (pThr[202]/pTyr[204]).

RESEARCH ARTICLE

MECHANOTRANSDUCTION

Cyclic GMP and Protein Kinase G Control a Src-Containing Mechanosome in Osteoblasts

Hema Rangaswami,[1] Raphaela Schwappacher,[1] Nisha Marathe,[1] Shunhui Zhuang,[1] Darren E. Casteel,[1] Bodo Haas,[2] Yong Chen,[2] Alexander Pfeifer,[2] Hisashi Kato,[1] Sanford Shattil,[1] Gerry R. Boss,[1] Renate B. Pilz[1]*

Mechanical stimulation is crucial for bone growth and remodeling, and fluid shear stress promotes anabolic responses in osteoblasts through multiple second messengers, including nitric oxide (NO). NO triggers production of cyclic guanosine $3',5'$-monophosphate (cGMP), which in turn activates protein kinase G (PKG). We found that the NO-cGMP-PKG signaling pathway activates Src in mechanically stimulated osteoblasts to initiate a proliferative response. PKGII was necessary for Src activation, a process that also required the interaction of Src with β_3 integrins and dephosphorylation of Src by a complex containing the phosphatases SHP-1 (Src homology 2 domain–containing tyrosine phosphatase 1) and SHP-2. PKGII directly phosphorylated and stimulated SHP-1 activity, and fluid shear stress triggered the recruitment of PKGII, Src, SHP-1, and SHP-2 to a mechanosome containing β_3 integrins. PKGII-null mice showed defective Src and ERK (extracellular signal–regulated kinase) signaling in osteoblasts and decreased ERK-dependent gene expression in bone. Our findings reveal a convergence of NO-cGMP-PKG and integrin signaling and establish a previously unknown mechanism of Src activation. These results support the use of PKG-activating drugs to mimic the anabolic effects of mechanical stimulation of bone in the treatment of osteoporosis.

INTRODUCTION

Mechanical stimulation induces bone growth and remodeling, which is critical for maintaining bone mass and strength (1). Compressive forces generated by weight bearing and locomotion induce small bone deformations and increase interstitial fluid flow. In response to these mechanical stimuli, osteoblasts lining endosteal and periosteal surfaces proliferate and differentiate, and osteocytes embedded in the canalicular bone network show enhanced survival (1, 2). Mechanoreceptors on osteoblasts and osteocytes include integrins associated with cytoskeletal proteins and mechanosensitive calcium channels (2). Mechanical stimulation rapidly and transiently increases intracellular calcium concentrations and production of nitric oxide (NO) and prostaglandin E_2 (3, 4). These second messengers activate various signal transduction pathways, including the Raf–MEK [mitogen-activated protein (MAP) kinase or extracellular signal–regulated kinase (ERK) kinase]–ERK1/2 cascade, which leads to changes in gene expression (3).

NO synthesis in mechanically stimulated osteoblasts and osteocytes occurs in part through activation of endothelial NO synthase (eNOS) and increased abundance of inducible NOS (iNOS) (5, 6). NO is important for bone modeling and remodeling, as evidenced by in vitro and in vivo studies. Low doses of NO donors promote osteoblast proliferation and differentiation in vitro and increase bone formation in response to mechanical stimulation (7, 8). Furthermore, young eNOS-deficient mice have reduced bone mass due to defects in osteoblast number and maturation, and adults show impaired bone adaptation to interstitial fluid flow (9, 10). Moreover, iNOS-deficient mice and rodents treated with NOS inhibitors fail to increase bone formation after mechanical stimulation (6, 7, 11).

[1]Department of Medicine, University of California, San Diego, La Jolla, CA 92093, USA. [2]Institute for Pharmacology and Toxicology and Biomedical Center, University of Bonn, 53105 Bonn, Germany.
*To whom correspondence should be addressed. E-mail: rpilz@ucsd.edu

NO produced in mechanically stimulated osteoblasts and osteocytes activates soluble guanylate cyclase, which produces cyclic guanosine $3',5'$-monophosphate (cGMP), which in turn activates both soluble type I and membrane-bound type II protein kinase G (PKG); other cGMP targets include phosphodiesterases and cyclic nucleotide–gated ion channels (5, 12). PKGII-deficient mice are dwarfs because of a block in chondrocyte differentiation in bone growth plates, whereas PKGI-deficient mice have no obvious skeletal abnormalities (13). We have shown that NO and cGMP cooperate with a calcium-dependent pathway to activate ERK in response to fluid shear stress, but the mechanism (or mechanisms) whereby shear stress activates ERK are unknown (5). Here, we establish that the NO-cGMP-PKG pathway activates ERK through SHP-1 [Src homology 2 (SH2) domain–containing tyrosine phosphatase 1], SHP-2, and Src in shear-stressed osteoblasts and show defective signaling in PKGII-deficient mice. We uncover a link between the NO-cGMP-PKG pathway and β_3 integrins, thereby explaining the requirement of both pathways for ERK activation in osteoblasts and osteocytes.

RESULTS

PKGII is necessary for fluid shear stress–induced osteoblast proliferation

Fluid shear stress stimulates osteoblast proliferation in an ERK-dependent fashion (14, 15), and this in vitro response correlates well with increased bone formation during mechanical stimulation in vivo, as shown by the differential osteogenic response to mechanical stress in different inbred strains of mice (16). Because we previously showed that the NO-cGMP-PKG signaling pathway is necessary for fluid shear stress–induced ERK activation (5), we examined the role of PKGII in early osteoblast proliferation with a small interfering RNA (siRNA) approach. We found that 15 min of laminar fluid shear stress (at 12 dynes/cm²) stimulated incorporation of bromodeoxyuridine (BrdU) in replicating DNA by a factor of
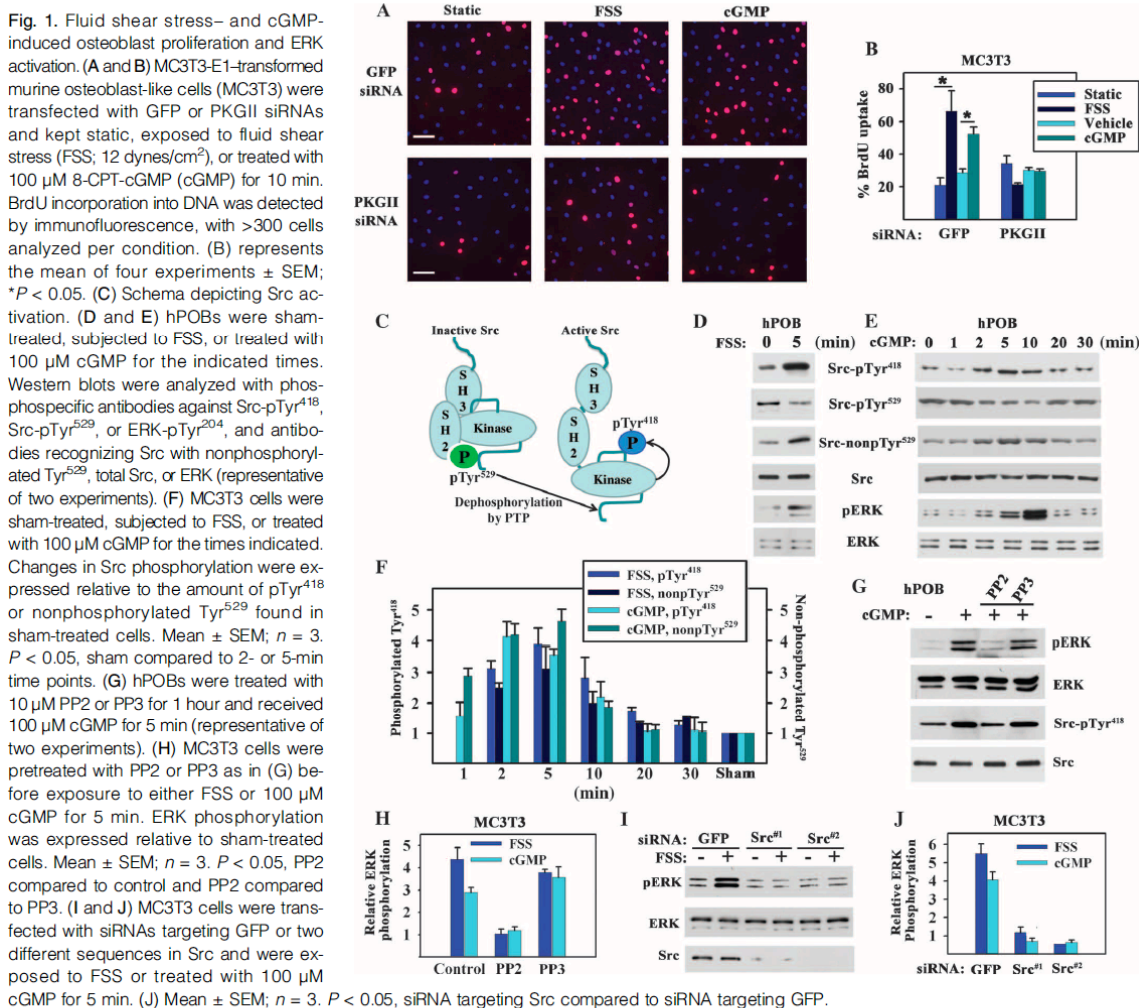
RESEARCH ARTICLE

~3 in MC3T3-E1 murine osteoblast-like cells (referred to as MC3T3), a response that was prevented by siRNA-mediated depletion of PKGII (Fig. 1, A and B, and fig. S1A). Treatment with 8-(4-chlorophenylthio)-cGMP (8-CPT-cGMP; referred to as cGMP) mimicked the effects of fluid shear stress on cell proliferation in cells transfected with an siRNA targeting green fluorescent protein (GFP) but had no effect in PKGII siRNA–transfected cells (Fig. 1, A and B). Thus, PKGII activity is required for shear- and cGMP-induced early osteoblast proliferation. However, fluid shear responses may vary with the degree of osteoblast differentiation (1).

Fluid shear stress– or cGMP-induced ERK activation requires Src

Src activity is regulated by phosphorylation. In unstimulated cells, the C-terminal Tyr^{529} is phosphorylated and interacts with the SH2 domain, keeping Src in a "closed" (inactive) conformation. Dephosphorylation of Tyr^{529} is a key event in Src activation because it changes the protein to an "open" conformation and enables autophosphorylation of Tyr^{418} in the kinase domain activation loop (Fig. 1C) (17). Exposing primary human osteoblasts (hPOBs), murine MC3T3 osteoblast-like cells, and MLO-Y4 osteocyte-like cells to fluid shear stress for up to 30 min rapidly induced Src dephosphorylation on Tyr^{529} and phosphorylation on Tyr^{418}, indicating Src activation. Src activation peaked slightly before ERK activation, and treatment of cells with an NO donor or cGMP mimicked the effects of fluid shear stress (Fig. 1, D to F, and fig. S1, B to D). Results obtained with an antibody specific for Src phosphorylated at Tyr^{529} (Src-pTyr^{529}) mirrored those obtained with antibody specific for Src that is not phosphorylated at Tyr^{529} (Src-nonpTyr^{529}). The Src family kinase inhibitor PP2, but not the inactive analog PP3, prevented fluid shear stress–

Fig. 1. Fluid shear stress– and cGMP-induced osteoblast proliferation and ERK activation. (A and B) MC3T3-E1–transformed murine osteoblast-like cells (MC3T3) were transfected with GFP or PKGII siRNAs and kept static, exposed to fluid shear stress (FSS; 12 dynes/cm^2), or treated with 100 µM 8-CPT-cGMP (cGMP) for 10 min. BrdU incorporation into DNA was detected by immunofluorescence, with >300 cells analyzed per condition. (B) represents the mean of four experiments ± SEM; *P < 0.05. (C) Schema depicting Src activation. (D and E) hPOBs were sham-treated, subjected to FSS, or treated with 100 µM cGMP for the indicated times. Western blots were analyzed with phosphospecific antibodies against Src-pTyr^{418}, Src-pTyr^{529}, or ERK-pTyr^{204}, and antibodies recognizing Src with nonphosphorylated Tyr^{529}, total Src, or ERK (representative of two experiments). (F) MC3T3 cells were sham-treated, subjected to FSS, or treated with 100 µM cGMP for the times indicated. Changes in Src phosphorylation were expressed relative to the amount of pTyr^{418} or nonphosphorylated Tyr^{529} found in sham-treated cells. Mean ± SEM; n = 3. P < 0.05, sham compared to 2- or 5-min time points. (G) hPOBs were treated with 10 µM PP2 or PP3 for 1 hour and received 100 µM cGMP for 5 min (representative of two experiments). (H) MC3T3 cells were pretreated with PP2 or PP3 as in (G) before exposure to either FSS or 100 µM cGMP for 5 min. ERK phosphorylation was expressed relative to sham-treated cells. Mean ± SEM; n = 3. P < 0.05, PP2 compared to control and PP2 compared to PP3. (I and J) MC3T3 cells were transfected with siRNAs targeting GFP or two different sequences in Src and were exposed to FSS or treated with 100 µM cGMP for 5 min. (J) Mean ± SEM; n = 3. P < 0.05, siRNA targeting Src compared to siRNA targeting GFP.

RESEARCH ARTICLE

induced Src autophosphorylation and ERK activation; similarly, PP2, but not PP3, prevented cGMP-induced ERK activation (Fig. 1, G and H, and fig. S1E). siRNA directed against Src, but not a control siRNA, blocked fluid shear stress– and cGMP-induced activation of ERK1/2 (Fig. 1, I and J, and fig. S1F). Thus, Src is required for ERK activation in fluid shear stress– or cGMP-stimulated osteoblasts.

Membrane-localized PKG mediates Src activation

To determine whether fluid shear stress–induced Src activation was mediated by the NO-cGMP-PKG pathway, we used pharmacologic inhibitors of NOS [L-N^G-nitroarginine methyl ester (L-NAME)], soluble guanylate cyclase (ODQ), or PKG [Rp-8-CPT-PET-cGMPS (Rp)] (Fig. 2A). Each of these agents almost completely prevented fluid shear stress–induced Src Tyr[418] autophosphorylation and Tyr[529] dephosphorylation in hPOBs and MC3T3 cells (Fig. 2, B and C). Thus, fluid shear stress–induced Src activation requires NO-cGMP-PKG signaling. To determine which PKG isoform mediated Src activation, we used siRNAs to selectively deplete cytosolic PKGI or membrane-bound PKGII (fig. S1A). siRNAs directed against PKGII, but not against PKGI, prevented fluid shear stress– and cGMP-induced Src activation (Fig. 2D).

To assess whether the differing ability of PKGI and PKGII to regulate Src activity was due to differences in subcellular localization or substrate recognition, we reconstituted PKGII-depleted MC3T3 cells with siRNA-resistant PKG constructs. Expression of wild-type PKGII, but not a membrane binding–deficient PKGII-G2A mutant, in PKGII-deficient cells restored cGMP-induced Src activation (Fig. 2, E to G). [The mutant PKGII-G2A is cytosolic because it lacks the N-terminal myristoylation signal that targets PKGII to the plasma membrane (18).] A membrane-targeted PKGI/II chimera containing the N-terminal 39 amino acids of PKGII fused to the N terminus of PKGI (PKGI-swap) restored cGMP-induced Src activation in PKGII siRNA–treated MC3T3 cells, whereas similar amounts of wild-type PKGI did not (Fig. 2, E to G). All four PKG constructs produce similar total cellular PKG activities, but in different subcellular compartments (18). We conclude that membrane targeting of PKG activity is essential for cGMP-induced Src activation and that it involves a substrate recognized by both PKGI and PKGII.

Src is not directly activated by PKGII

Cyclic adenosine 3′,5′-monophosphate (cAMP)–dependent protein kinase (PKA) activates Src directly by phosphorylating Ser[17], a site that could also be recognized by PKG (19). Purified PKGII did not affect Src phosphorylation or autophosphorylation and did not phosphorylate the PKA recognition site (or sites) in Src under conditions in which a known PKG and PKA substrate was efficiently phos-
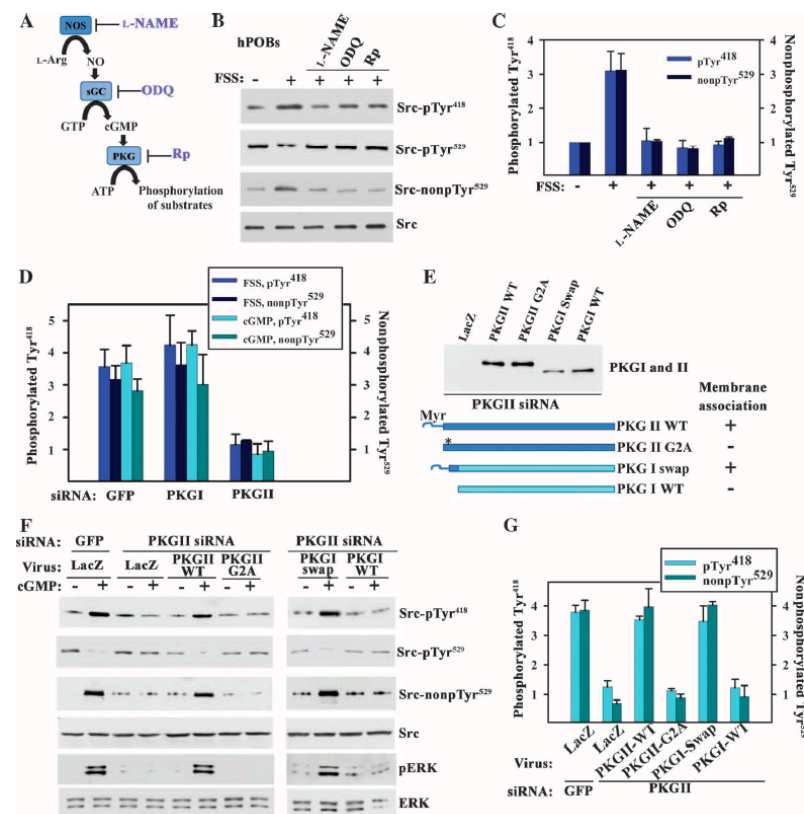

Fig. 2. Src activation by membrane-bound PKG. (A) Schema of the NO-cGMP-PKG signaling pathway with inhibitors of NOS, soluble guanylate cyclase (sGC), and PKG. (B) hPOBs were sham-treated or exposed for 5 min to fluid shear stress (FSS; 12 dynes/cm²); some cells were pretreated with 4 mM L-NAME, 10 μM ODQ, or 100 μM Rp-8-CPT-PET-cGMPS (Rp) for 1 hour. Src phosphorylation was determined as in Fig. 1D (representative of two experiments). (C) MC3T3 cells were pretreated as in (B) and exposed to FSS for 5 min. Mean ± SEM; $n = 3$. $P < 0.05$, drug-treated cells exposed to fluid shear compared to FSS alone. (D) MC3T3 cells were transfected with siRNAs specific for GFP, PKGI, or PKGII; exposed to either FSS or 100 μM cGMP for 5 min; and analyzed as in Fig. 1F. Mean ± SEM; $n = 3$. $P < 0.05$, PKGII siRNA compared to GFP siRNA. (E to G) MC3T3 cells were transfected with PKGII (or GFP) siRNA and infected with adenoviral vectors encoding LacZ (control), siRNA-resistant wild-type (WT) or myristoylation-deficient PKGII (PKGII G2A), and WT or membrane-targeted PKGI (PKGI swap). The Western blot in (E) shows expression of PKGI and PKGII constructs in PKGII siRNA–transfected MC3T3 cells (whole-cell lysates); membrane association is indicated as determined by subcellular fractionation. In (F), cells were treated with 100 μM cGMP for 5 min or left untreated, and cells were analyzed as in Fig. 1E. (G) shows the mean ± SEM for three experiments. $P < 0.05$, PKGII WT or PKGI swap compared to LacZ virus in PKGII siRNA–transfected cells.

phorylated (fig. S2, A to C). Some phosphorylation of the PKA recognition site (or sites) in Src was detectable in untreated MC3T3 cells; this phosphorylation was not increased in cGMP-treated cells, but was increased when PKA was activated with 8-Br-cAMP (fig. S2D). Thus, Src is not a PKGII substrate and is not activated by direct PKGII phosphorylation or interaction with PKGII.

Fig. 3. Fluid shear stress– and cGMP-induced Src activation mediated by SHP-1 and SHP-2. (**A**) MC3T3 cells were treated with 10 μM vanadate for 1 hour before a 5-min exposure to fluid shear stress (FSS; 12 dynes/cm^2) or 100 μM 8-CPT-cGMP (cGMP). Src phosphorylation was analyzed as in Fig. 1F. Mean ± SEM; $n = 3$. $P < 0.05$, vanadate compared to control. (**B**) hPOBs were treated with vanadate and cGMP as in (A) (images are representative of two experiments). (C and D) MC3T3 cells were transfected with siRNAs targeting GFP, SHP-1, SHP-2, RPTP-α, or PTP-1B, and phosphatase abundance was quantified by Western blotting (whole-cell lysates for SHP-1, SHP-2, and PTP-1B and membrane lysates for RPTP-α). In (D), cells were exposed to FSS or treated with 100 μM cGMP for 5 min, and Src phosphorylation was analyzed as in Fig. 1F. Mean ± SEM; $n = 3$. $P < 0.05$, SHP-1 or SHP-2 siRNA compared to GFP siRNA. (E and F) MC3T3 cells were transfected with siRNAs targeting GFP, SHP-1 (E), or SHP-2 (F). Cells were infected with adenovirus encoding LacZ, siRNA-resistant human SHP-1 (E), or SHP-2 (F), and received 100 μM cGMP for 5 min (representative of three experiments).

Fluid shear stress– and cGMP-induced Src activation is mediated by SHP-1 and SHP-2

Rapid dephosphorylation of Src pTyr^{529} in fluid shear stress– or cGMP-treated osteoblasts (Fig. 1, D to F) implies a role for a protein tyrosine phosphatase (PTP) (or phosphatases). The PTP inhibitor vanadate did not affect Src phosphorylation at Tyr^{529} in unstimulated osteoblasts, suggesting low activity of PTPs that catalyze Src pTyr^{529} dephosphorylation. However, vanadate blocked fluid shear stress– and cGMP-induced Src pTyr^{529} dephosphorylation and prevented Src Tyr^{418} autophosphorylation (Fig. 3, A and B, and fig. S3A). These results suggest that PKG regulates Src through activation or recruitment of a PTP (or PTPs) that catalyzes Src pTyr^{529} dephosphorylation (or both).

Several PTPs are present in osteoblasts that can dephosphorylate Src Tyr^{529} in vitro, including the tandem SH2 domain–containing PTPs SHP-1 and SHP-2, PTP-1B, and the receptor-type phosphatase RPTP-α. All four proteins contain potential PKG phosphorylation sites and may activate Src in cells (20, 21). Depleting either SHP-1 or SHP-2 by siRNAs prevented fluid shear stress– and cGMP-induced dephosphorylation of Src pTyr^{529} in MC3T3 cells, whereas depleting PTP-1B or RPTP-α had no effect (Fig. 3, C and D, and fig. S3, B and C). Reconstitution of siRNA-resistant human SHP-1 or SHP-2 in SHP-1– or SHP-2–depleted MC3T3 cells restored cGMP-induced Src pTyr^{529} dephosphorylation and Tyr^{418} autophosphorylation, as well as ERK activation (Fig. 3, E and F). These results indicate that SHP-1 and SHP-2 are both required for fluid shear stress– and cGMP-induced Src activation. SHP-1 and SHP-2 also cooperate in epidermal growth factor–induced ERK activation, with SHP-2 acting as a scaffold that recruits SHP-1 to the receptor (22).
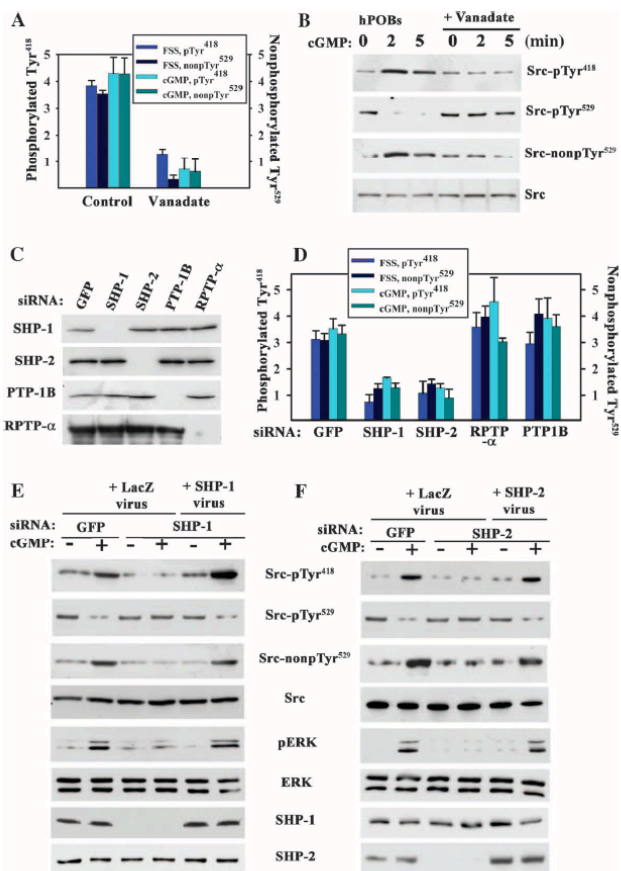
PKGII phosphorylates SHP-1 and stimulates PTP activity

The phosphatase activities of SHP-1 and SHP-2 are regulated by interactions between their SH2 and PTP domains and by phosphorylation of Tyr in the C termini, where the sequences of the two phosphatases diverge the most (21). We found that PKGII phosphorylated purified full-length SHP-1 wild-type and N-terminally truncated SHP-1 (ΔSH2, missing the two SH2 domains), but not the isolated catalytic domain (CAT); this localized the PKG phosphorylation site (or sites) to the C-terminal tail (Fig. 4, A and B). Under similar conditions, SHP-2 was not efficiently phosphorylated.

We measured SHP-1 phosphatase activity with a phospho-Tyr^{529}–containing Src peptide as a substrate. The specific activity of purified SHP-1ΔSH2 was similar to that of the isolated CAT domain and was higher than that of the full-length enzyme by a factor of ~5 (Fig. 4C), consistent with results reported for other substrates (21). PKGII phosphorylation of full-length SHP-1 or SHP-1ΔSH2 stimulated phosphatase activity, but PKGII did not stimulate SHP-1 CAT activity (Fig. 4C). Thus, PKGII phosphorylation of the SHP-1 C-terminal tail stimulates SHP-1 PTP activity toward Src phospho-Tyr^{529} in vitro.

Phosphorylation of Flag-tagged, full-length SHP-1 in human embryonic kidney (HEK) 293T cells was modestly enhanced by wild-type, but not kinase-dead PKGII, and SHP-1 phosphorylation occurred on a serine residue (or residues) (Fig. 4D and fig. S4A). An SHP-1 construct lacking the C-terminal 74 amino acids (SHP-1ΔCT) showed neither basal nor PKGII-stimulated

phosphorylation, and a construct containing alanines substituted for Ser[553], Ser[556], and Ser[557] in a potential PKG recognition sequence (SHP-1AAA) showed reduced basal phosphorylation, which was not increased in the presence of PKGII (Fig. 4E). Thus, PKGII targets at least one of these serines, which are conserved across species but are not present in SHP-2 (fig. S4B). Flag–SHP-1 isolated from HEK 293T cells expressing wild-type PKGII displayed about twice as much PTP activity as SHP-1 from cells cotransfected with empty vector or kinase-dead PKGII; in these experiments, wild-type PKGII expression did not alter the amount of Flag–

SHP-1 protein in the cell (Fig. 4F). The PTP activities of SHP-1ΔCT and SHP-1AAA were not affected by PKGII expression, consistent with their lack of PKG phosphorylation. Wild-type SHP-1, but not SHP-1ΔCT or SHP-1AAA, restored cGMP-induced Src activation in SHP-1 siRNA–treated MC3T3 cells (Fig. 4G). Thus, SHP-1 phosphorylation and activation by PKGII is necessary for Src activation.

SHP-1–specific antibodies did not immunoprecipitate sufficient SHP-1 from MC3T3 cells to measure PTP activity; however, we found that SHP-1 coimmunoprecipitated with SHP-2 (Fig. 4H), which suggests the possibility of direct interaction between the two proteins (22). We used SHP-2 antibodies to isolate a complex of endogenous SHP-1 and SHP-2 from MC3T3 cells and found that cGMP stimulated PTP activity (Fig. 4I and fig. S4C). cGMP stimulation neither altered the proportion of SHP-1 and SHP-2 in the complex (Fig. 4H) nor affected Tyr phosphorylation of endogenous SHP-1 and SHP-2 (fig. S4D).
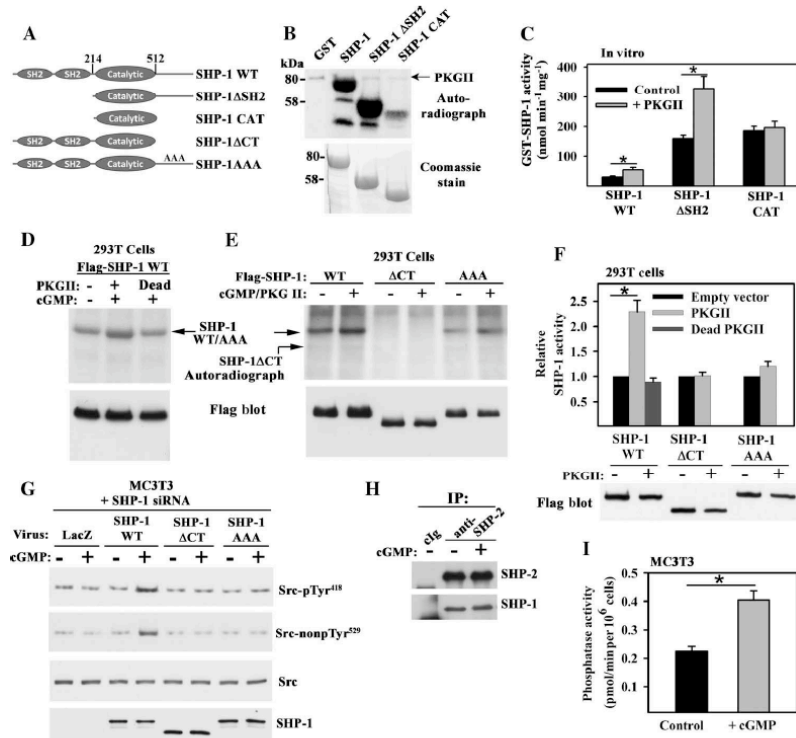

Fig. 4. PKGII phosphorylation of SHP-1 and SHP-2 and regulation of PTP activity. (A) SHP-1 constructs; AAA denotes alanine substitutions for Ser[553], Ser[556], and Ser[557]. (B) PKGII phosphorylation of bacterially expressed SHP-1 constructs in the presence of [γ-^{32}PO$_4$]ATP in vitro (representative of three experiments). (C) Effect of PKGII phosphorylation on SHP-1 PTPase activity in vitro (mean ± SEM, n = 3; *P < 0.05). (D and E) HEK 293T cells were cotransfected with Flag epitope–tagged SHP-1 constructs and empty vector, WT PKGII, or kinase-dead PKGII. Cells were labeled with ^{32}PO$_4$ for 4 hours and treated with 100 μM 8-CPT-cGMP (cGMP) for 10 min. Immunoprecipitates were analyzed by SDS-PAGE and autoradiography, and protein abundance was determined by Western blotting (representative of two experiments). (F) PTP activity of Flag-tagged SHP-1 constructs immunoprecipitated from HEK 293T cells transfected and treated as in (D) and (E). The activity of each construct was normalized to its activity in PKG-deficient cells (mean ± SEM, n = 4; *P < 0.05). (G) MC3T3 cells were transfected with SHP-1 siRNA and infected with adenovirus encoding LacZ or siRNA-resistant human SHP-1 WT, ΔCT, or AAA. Cells were exposed to 100 μM cGMP for 5 min, and Src phosphorylation or dephosphorylation was analyzed as in Fig. 1E (representative of three experiments). (H) Coimmunoprecipitation of SHP-1 and SHP-2 from MC3T3 cells treated with 100 μM cGMP for 5 min (representative of three experiments). (I) PTP activity in anti-SHP-2 immunoprecipitates (containing SHP-1 and -2) from control MC3T3 cells and from cells treated with 100 μM cGMP for 5 min. Mean ± SEM; n = 6. *P < 0.05.

Src and ERK activation by cGMP and PKGII requires α$_v$β$_3$ integrin ligation

Integrins link extracellular matrix proteins to the actin cytoskeleton, and anchoring of integrins to actin stress fibers is essential for fluid shear–induced c-*fos* induction (23). Osteoblasts express several integrins, including α$_v$β$_3$ (2). ERK activation in fluid shear– or stretch-stimulated osteoblasts is prevented by β$_3$ integrin–blocking antibodies and siRNAs directed against β$_3$ integrin (24, 25). We found that siRNA depletion of β$_3$ integrin prevented cGMP-induced Src and ERK activation in MC3T3 cells (Fig. 5, A and B) without affecting β$_1$ integrin abundance or MC3T3 cell adhesion, the latter effect likely because cells adhere to secreted extracellular matrix proteins through multiple integrins. cGMP-induced Src and ERK activation was restored by expressing siRNA-resistant human β$_3$ integrin in β$_3$ integrin–depleted cells, but not by a β$_3$ΔCT mutant [lacking the last three C-terminal amino acids (26)], which does not bind Src (Fig. 5, C and D). Thus, Src activation by PKGII requires Src interaction with the cytoplasmic tail of β$_3$ integrin.

To determine whether cGMP-PKGII activation of Src and ERK requires ligand binding to β$_3$ integrins, we either placed osteoblasts in suspension or allowed them to adhere to fibrinogen-coated plates for 1 hour (fibrinogen was used as a specific ligand for α$_v$β$_3$ integrin, and waiting 1 hour ensured that ERK activation triggered by cell spreading had subsided) (27). cGMP activated Src and ERK in cells plated on fibrinogen but had no effect on cells in suspension, unless MnCl$_2$ was added to di-

rectly activate $\alpha_v\beta_3$ integrin and enable binding to soluble fibrinogen (Fig. 5E and fig. S5). Similar results were obtained with fibronectin (fig. S5). Thus, cGMP-PKGII activation of Src and ERK in osteoblasts requires adhesive ligand (such as fibrinogen or fibronectin) binding to $\alpha_v\beta_3$ integrin.

Fluid shear stress triggers PKGII, SHP-2, and Src recruitment to β_3 integrin–containing focal adhesions

Osteoblast stimulation by fluid shear stress induces assembly of actin stress fibers and β_1 integrin–containing focal adhesions (23). We found that fluid shear stress promoted clustering of β_3 integrin with SHP-2 in the periphery of osteoblasts (fig. S6) and increased coimmunoprecipitation of SHP-2 and β_3 integrin (fig. S7A). Similarly, Kapur *et al.* reported that SHP-1 and SHP-2 association with β_3 integrin is enhanced by fluid shear stress in human osteosarcoma cells (28). Fluid shear stress increased the colocalization of PKGII and Src with SHP-2 in the plasma membrane (fig. S6) and the amount of PKGII and vinculin associated with a detergent-insoluble fraction containing cytoskeletal and focal adhesion proteins (Fig. 6, A and B); there was no change in the amount of β-actin or caveolin-1 associated with the detergent-insoluble fraction. With vinculin serving as a focal adhesion marker, triple immunofluorescence staining showed that the percentage of focal adhesions containing PKGII and SHP-2, or Src and SHP-2, increased from ~20% in static cells to ~40% in shear-stressed osteoblasts (Fig. 6, C and D). We also assessed the association of PKGII with β_3 integrin–containing integrins by bimolecular fluorescence complementation (BiFC). Two chimeras were cotransfected with human β_3 integrin into MC3T3 cells: PKGII-VN, with the N-terminal half of the Venus fluorophore between the N-terminal membrane localization signal and the leucine zipper of PKGII, and α_{IIb}-VC, with the C-terminal half of Venus fused to the C terminus of human α_{IIb} integrin (Fig. 6E). We observed Venus fluorescence in the periphery of cells coexpressing α_{IIb}-VC and β_3 integrin with wild-type

PKGII-VN, but not with mutant PKGII(G2A)-VN missing the N-terminal myristoylation signal, suggesting that membrane-bound PKGII directly or indirectly interacts with α_{IIb} or β_3 integrin (Fig. 6E and fig. S7B). We also demonstrated interactions among PKGII, β_3 integrin, SHP-2, and Src in reciprocal coimmunoprecipitation experiments (fig. S7C). On the basis of these data and the fact that SHP-1 and SHP-2 coimmunoprecipitate (Fig. 4H), we conclude that PKGII, β_3 integrin, Src, SHP-1, and SHP-2 may be present in a large complex and that fluid shear stress promotes assembly of this complex at focal adhesions. Because β_3 integrin–containing focal adhesion complexes have been implicated as mechanosensors in osteoblasts and osteocytes and other cells (27, 29), we propose that this PKGII-, β_3 integrin–, Src-, SHP-1–, and SHP-2–containing complex represents a mechanosome modulated by PKGII. The term "mechanosome" was previously coined to describe a hypothetical signaling complex composed of focal adhesion–associated proteins assembled and activated by mechanical stimulation (30).

Src and ERK signaling is impaired in osteoblasts from PKGII-null mice

PKGII-deficient mice ($Prkg2^{-/-}$) exhibit abnormalities in chondroblast differentiation, but osteoblasts from these mice were not previously examined (13). Primary osteoblasts from calvariae of $Prkg2^{-/-}$ mice and their wild-type littermates were morphologically similar; as expected, $Prkg2^{-/-}$ osteoblasts lacked messenger RNA (mRNA) encoding PKGII, but not PKGI (Fig. 7C). Src activation in response to fluid shear stress or cGMP was impaired in $Prkg2^{-/-}$ osteoblasts, whereas cells from wild-type littermates showed robust Src Tyr[418] autophosphorylation and phospho-Tyr[529] dephosphorylation (Fig. 7, A and B). A similar difference was seen in fluid shear stress– or cGMP-induced ERK phosphorylation. Because *fos* family genes are targets of PKGII and ERK (5), we assessed the effect of NO-cGMP-PKGII signaling in 1-week-old mice by measuring c-*fos* and
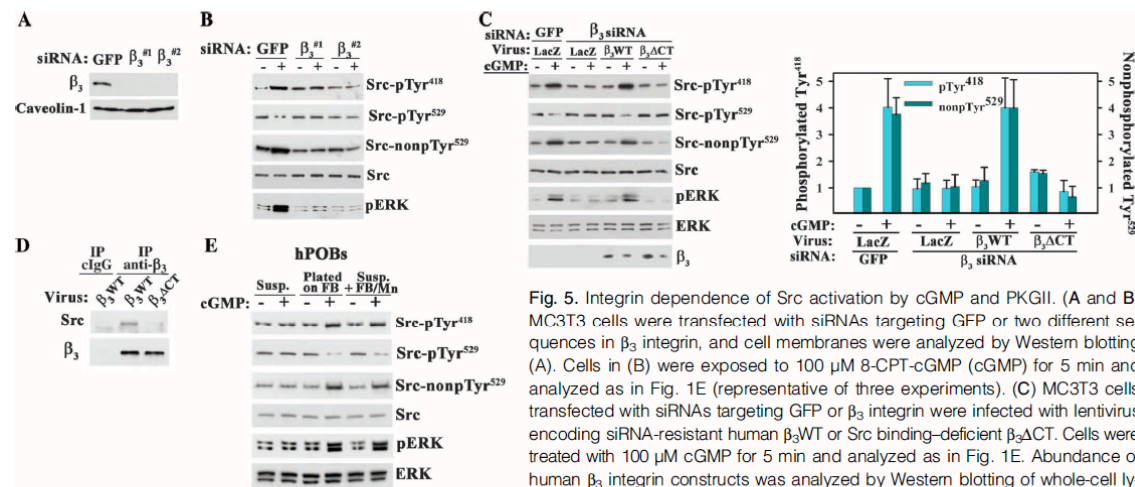

Fig. 5. Integrin dependence of Src activation by cGMP and PKGII. (**A** and **B**) MC3T3 cells were transfected with siRNAs targeting GFP or two different sequences in β_3 integrin, and cell membranes were analyzed by Western blotting (A). Cells in (B) were exposed to 100 µM 8-CPT-cGMP (cGMP) for 5 min and analyzed as in Fig. 1E (representative of three experiments). (**C**) MC3T3 cells transfected with siRNAs targeting GFP or β_3 integrin were infected with lentivirus encoding siRNA-resistant human β_3WT or Src binding–deficient $\beta_3\Delta$CT. Cells were treated with 100 µM cGMP for 5 min and analyzed as in Fig. 1E. Abundance of human β_3 integrin constructs was analyzed by Western blotting of whole-cell lysates; the amount of endogenous mouse β_3 integrin is below detection limits. The bar graph shows the mean ± SEM of three experiments. $P < 0.05$, for β_3WT compared to LacZ virus in β_3 siRNA–transfected, cGMP-treated cells. (**D**) Coimmunoprecipitation of Src with human β_3WT but not $\beta_3\Delta$CT from MC3T3 cells infected with β_3-expressing lentivirus (representative of two experiments). Endogenous murine β_3 is not efficiently immunoprecipitated. (**E**) hPOBs were kept in suspension (Susp.), allowed to attach to fibrinogen (FB)–coated dishes, or kept in suspension and stimulated with soluble FB (250 µg/ml) plus MnCl$_2$ (2 mM) (Susp. + FB/Mn). After 1 hour, some cells received 100 µM cGMP for 5 min. Cells were analyzed as in Fig. 1E (representative of three experiments).
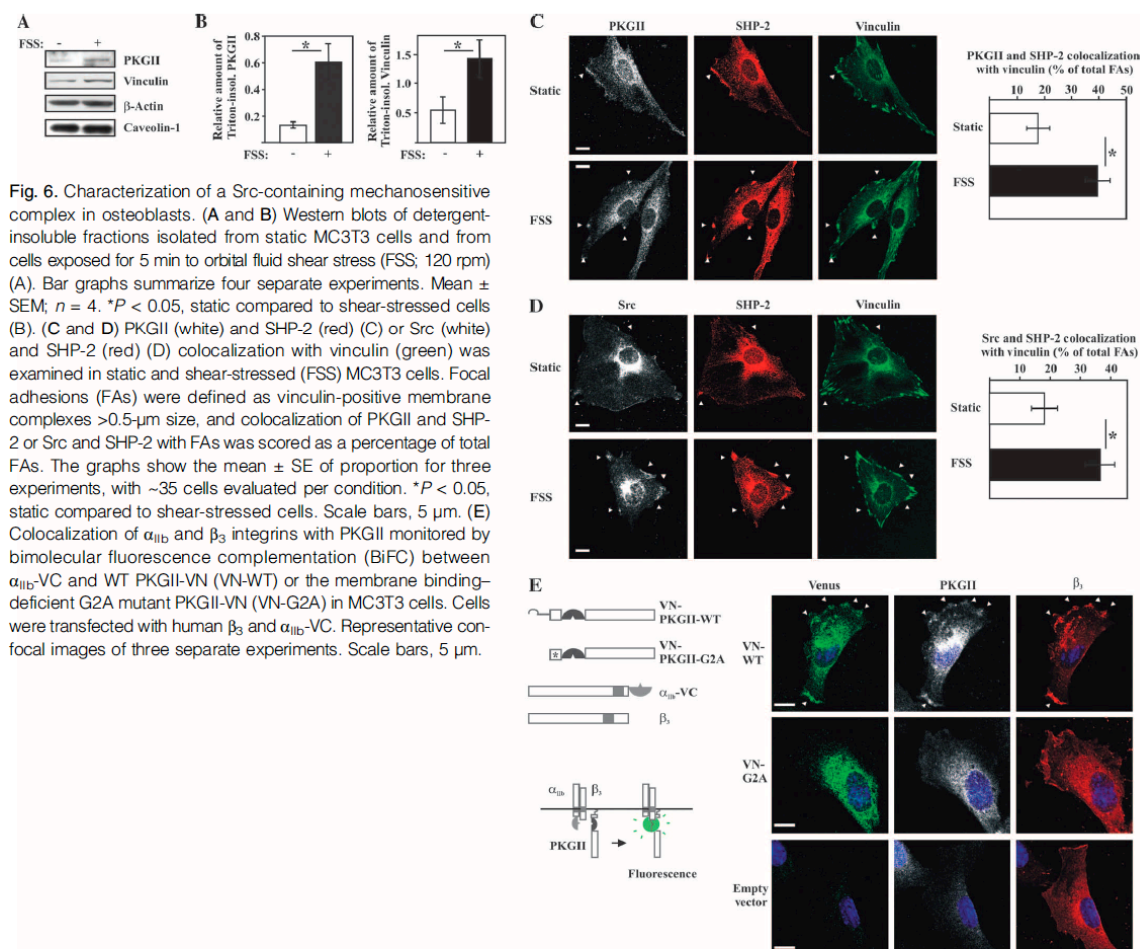
Fig. 6. Characterization of a Src-containing mechanosensitive complex in osteoblasts. (A and B) Western blots of detergent-insoluble fractions isolated from static MC3T3 cells and from cells exposed for 5 min to orbital fluid shear stress (FSS; 120 rpm) (A). Bar graphs summarize four separate experiments. Mean ± SEM; $n = 4$. *$P < 0.05$, static compared to shear-stressed cells (B). (C and D) PKGII (white) and SHP-2 (red) (C) or Src (white) and SHP-2 (red) (D) colocalization with vinculin (green) was examined in static and shear-stressed (FSS) MC3T3 cells. Focal adhesions (FAs) were defined as vinculin-positive membrane complexes >0.5-μm size, and colocalization of PKGII and SHP-2 or Src and SHP-2 with FAs was scored as a percentage of total FAs. The graphs show the mean ± SE of proportion for three experiments, with ~35 cells evaluated per condition. *$P < 0.05$, static compared to shear-stressed cells. Scale bars, 5 μm. (E) Colocalization of α_{IIb} and β_3 integrins with PKGII monitored by bimolecular fluorescence complementation (BiFC) between α_{IIb}-VC and WT PKGII-VN (VN-WT) or the membrane binding–deficient G2A mutant PKGII-VN (VN-G2A) in MC3T3 cells. Cells were transfected with human β_3 and α_{IIb}-VC. Representative confocal images of three separate experiments. Scale bars, 5 μm.

fra-2 mRNA abundance in tibial diaphyses. The amount of c-*fos* and *fra-2* transcripts was significantly lower in the tibial shafts of $Prkg2^{-/-}$ mice relative to those of wild-type mice (Fig. 7D). These results indicate that PKGII deficiency affects c-*fos* and *fra-2* expression in bones of intact animals. Fos family transcription factors play a key role in skeletal development and maintenance (*31*).

DISCUSSION

We have identified a previously unknown mechanosensitive signaling system in osteoblasts, defining the events leading from shear stress activation of eNOS to Src activation. β_3 Integrins function as mechanosensors (*29*), and the cytoplasmic tail of β_3 integrin serves as a scaffold for a signaling complex that includes Src, SHP-1, and SHP-2 (*26, 28, 32*). We discovered that PKGII is recruited to the β_3 integrin–SHP–Src complex in shear-stressed osteoblasts and that PKGII activated by cGMP phosphorylates

and thereby activates SHP-1; the latter dephosphorylates and activates Src (Fig. 7E). Activated Src phosphorylates and recruits the adaptor Shc, which leads to activation of Ras and the Raf-MEK-ERK pathway and stimulation of cell growth (*33, 34*). This signaling system fills a gap in our understanding of how mechanical forces sensed by cell-matrix adhesions are translated into cellular responses, such as osteoblast proliferation and osteocyte survival (*25*). Other mechanisms of ERK activation in shear-stressed osteoblasts include calcium- and focal adhesion kinase–dependent pathways (*5, 35*).

PKGII and integrins converge on the Src-ERK pathway
Current models for mechanotransduction propose that cells sense and respond to forces at their points of attachment to the extracellular matrix, for example, at integrin-containing focal adhesion complexes (*36*). Osteocytes are tethered to the canalicular wall through $\alpha_v\beta_3$ integrin (*29*). In response to mechanical stimulation, integrins cluster and initiate "outside-in" signaling, but the exact nature of force-induced conformational changes in integrins and integrin-associated proteins remains unclear (*2, 36*).

RESEARCH ARTICLE

Consistent with studies in other cell types (*26, 37*), we found that Src was associated with the cytoplasmic tail of β_3 integrins, and this association was necessary for Src activation by cGMP and PKGII. Clustering of
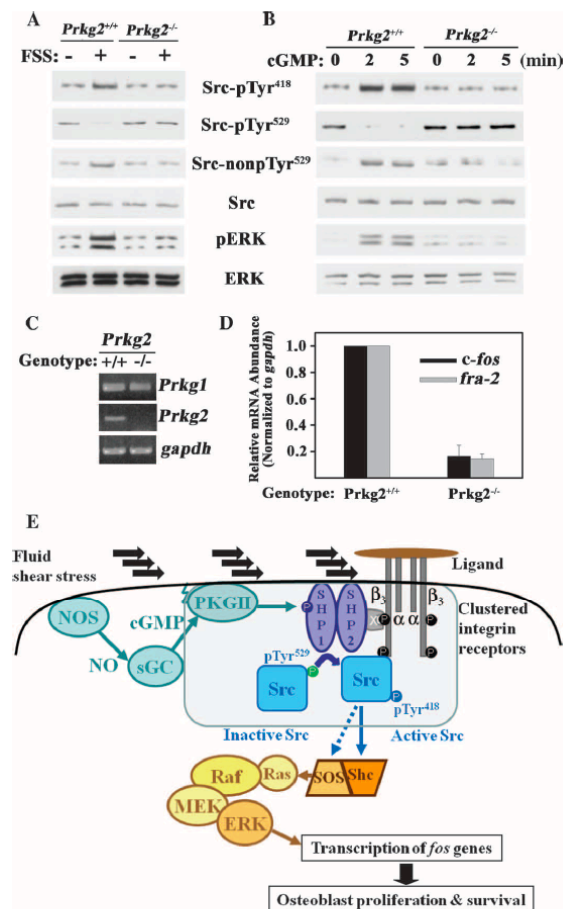

Fig. 7. Signaling defect in PKGII-null osteoblasts. (**A** and **B**) WT and PKGII-null primary osteoblasts were stimulated with either fluid shear stress (FSS; 12 dynes/cm^2) or 100 µM 8-CPT-cGMP (cGMP) for 5 min, and Src and ERK activation were analyzed as in Fig. 1E [representative of two (A) or three (B) experiments]. (**C**) Semiquantitative RT-PCR for PKGI and PKGII expression in primary calvarial osteoblasts isolated from 1-week-old *Prkg2*$^{-/-}$ mice and their WT littermates (representative of two experiments). (**D**) Tibial diaphyses were isolated from 1-week-old WT and *Prkg2*$^{-/-}$ mice, and c-*fos*, *fra-2*, and *gapdh* mRNA abundance was measured by quantitative RT-PCR. Mean ± SEM; $n = 5$. $P < 0.05$, WT compared to knockout mice. (**E**) Model of Src and ERK activation by FSS through NO-cGMP-PKGII, depicting the assembly of a mechanosensitive complex (shaded) containing PKGII, SHP-1, SHP-2, and Src bound to the cytoplasmic tail of β_3 integrin (x = docking protein). Activation of the Ras-Raf-MEK-ERK cascade by Src occurs through Shc-dependent and -independent pathways (*33*).

$\alpha_v\beta_3$ integrin in response to adhesive ligand binding (or shear stress, or both) may juxtapose Src molecules and allow partial activation through trans-autophosphorylation, but full Src activation downstream of integrins requires action of a protein tyrosine phosphatase, such as PTP-1B in platelets and RPTP-α in fibroblasts (*20*). We show that SHP-1 and SHP-2, as part of a larger complex, are necessary for fluid shear stress– and cGMP-induced Src activation. Consistent with our finding that Src and ERK activation by the cGMP-PKGII pathway required ligand binding to β_3 integrins, others found that ERK activation by fluid shear stress is prevented by β_3 integrin function–blocking antibodies (*24*). Some colocalization of SHP-2, Src, and PKGII with β_3 integrin–containing complexes was apparent in the plasma membrane of static osteoblasts, but fluid shear stress increased SHP-2, Src, and PKGII recruitment to focal adhesions. In contrast, NO and cGMP activation of PKG induces disassembly of focal adhesions in chondroblasts and endothelial cells (*38, 39*).

PKGII selectively targets SHP-1 and SHP-2 to activate Src and ERK

Src binds to the SH2 domains of SHP-1 and SHP-2 in vitro and is a substrate for both phosphatases (*34, 40*). SHP-1 and SHP-2 serve nonredundant functions in Src and ERK activation, and SHP-2 appears to function as a scaffold, coupling SHP-1 or Src (or both) to growth factor receptors (*22, 34*). Fibroblasts from SHP-2–deficient mice show defective Src and ERK activation in response to integrin ligation and growth factor stimulation (*41*), and SHP-1–deficient mice develop osteopenia due to combined effects of decreased bone formation and increased resorption (*42*).

We found that SHP-1 and SHP-2 associate and that SHP-2 binding to β_3 integrins is increased by fluid shear stress. The SHP-1–SHP-2 complex might bind to β_3 integrin indirectly, through SHP-2 binding to the Tyr-phosphorylated adaptor protein DOK-1 (*32*). SHP-1 and SHP-2 are autoinhibited by interaction between their SH2 and PTP domains, but interaction of the SH2 domains with other Tyr-phosphorylated proteins results in partial phosphatase activation (*21*). We found that PKGII activation of SHP-1 is mediated by phosphorylation of Ser[553], Ser[556], or Ser[557] in the C terminus of SHP-1; in contrast, protein kinase C phosphorylates SHP-1 on Ser[591] and appears to inhibit phosphatase activity, although reports are conflicting (*21*). Tyr phosphorylation of SHP-1 and SHP-2 increases phosphatase activity (*21*), but we found no effect of PKGII activation by cGMP on the Tyr phosphorylation of SHP-1 and SHP-2.

Our results suggest that the main mechanism of PKGII activation of Src is through SHP-1– and SHP-2–mediated Src pTyr[529] dephosphorylation, but additional mechanisms could exist, such as Src activation by interaction with other SH2 or SH3 domain–binding proteins or displacement of CSK (C-terminal Src kinase) (*17*). We did not find evidence for direct Src activation by PKGII, in contrast to Src activation by PKA (*19*). While this manuscript was in preparation, Leung *et al.* reported that Src activity in ovarian cancer cells depends on basal activity of PKGIα, with reciprocal phosphorylation between Src and PKGIα (*43*). We found no role of PKGI in Src activation in osteoblasts.

PKGII-deficient mice have skeletal defects

PKGII-deficient mice have no general metabolic disturbances and appear grossly normal at birth, but develop dwarfism because of abnormal endochondral ossification from defective chondroblast differentiation (*13*). In chondroblasts, PKGII promotes differentiation through regulation of Sox9 nuclear translocation and β-catenin stability (*12*) and antagonizes growth factor activation of the Raf-1–MEK–ERK cascade (*44*).

We found defective Src and ERK signaling in PKGII-deficient primary osteoblasts and decreased amounts of c-*fos* and *fra-2* mRNA in tibial diaphyses of *Prkg2*$^{-/-}$ mice relative to wild-type littermates. Be-

cause c-*fos* and *fra-2* are target genes of PKGII signaling, these data suggest that c-*fos* and *fra-2* mRNA abundance is regulated by PKGII activity in vivo. c-*fos* is involved in osteoblast cell cycle regulation (*45*), and induction of c-*fos* expression in bone by mechanical loading correlates with new bone formation (*7*). Because the global PKGII knockout phenotype is dominated by impaired endochondral ossification leading to abnormal architecture of long bones and vertebrae, we plan to generate osteoblast- and osteocyte-specific PKGII knockout mice to evaluate the in vivo consequences of defective osteoblast mechanotransduction.

NO-cGMP-PKGII signaling is important for osteoblast mechanotransduction

Skeletal maintenance requires continuous mechanical input, as evidenced by bone mass loss in unloaded limbs due to decreased osteoblastic bone formation and increased osteoclastic resorption (*1*, *2*). NO is crucial to the anabolic response to mechanical stimulation in vivo. In models of bone adaptation to loading, NOS inhibitors prevent loading-induced c-*fos* mRNA expression and impede osteogenesis (*7*, *11*). In a hindlimb suspension model, mice deficient in eNOS (*nos3*$^{-/-}$) or iNOS (*nos1*$^{-/-}$) exhibit the same bone loss in unloaded limbs as wild-type mice. However, interstitial fluid flow induced by venous ligation protects wild-type but not *nos3*$^{-/-}$ mice from bone loss in the suspended limb, and reloading induces new bone formation in wild-type but not *nos1*$^{-/-}$ mice (*6*, *10*).

We have identified a link between mechanical stimulation and activation of Src and ERK, establishing a central role of NO-cGMP-PKGII signaling in osteoblast mechanotransduction. Preclinical and clinical studies support osteogenic functions of NO, although optimal dosing of NO and the potential for NO-induced oxidative stress may be problematic (*46*). Our results suggest that agents that increase cGMP concentrations, such as NO-independent soluble guanylate cyclase activators and phosphodiesterase inhibitors, could have favorable "mechanomimetic" effects on bone.

MATERIALS AND METHODS

Reagents and DNA constructs

Sources of reagents, including antibodies, siRNAs, and plasmid and viral vectors, are described in the Supplementary Materials.

Cell culture, transfections, and exposure to drugs and fluid shear stress

MC3T3-E1–transformed murine osteoblast-like cells (from the American Type Culture Collection, used at <12 passages) and hPOBs (established from surgical specimens according to an institutionally approved protocol) were cultured, transfected with Lipofectamine 2000 (Invitrogen), and characterized by histochemical staining for the presence of alkaline phosphatase activity and reverse transcription polymerase chain reaction (RT-PCR) quantification of vitamin D–induced osteocalcin mRNA expression as described (*5*). Cells were plated on etched glass slides, serum-deprived (in 0.1% fetal bovine serum) for 24 hours, and exposed to laminar fluid shear stress (12 dynes/cm^2) in a parallel-plate flow chamber (Cytodyne Inc.) for 5 min unless noted otherwise. Sham-treated cells were grown under identical conditions and were placed in the flow chamber but not subjected to shear stress. Serum-deprived cells were preincubated with pharmacological inhibitors for 1 hour and treated with 100 μM 8-CPT-cGMP for 5 min unless noted otherwise.

Cell fractionation, immunoprecipitation, and immunoblotting

Detailed protocols for generation of membrane and cytosolic fractions, preparation of detergent-insoluble fractions containing focal adhesion proteins, immunoprecipitations, and Western blotting are provided in the Supplementary Materials.

Phosphorylation assays

Recombinant SHP-1 and SHP-2 were purified from bacteria as glutathione *S*-transferase (GST) fusion proteins bound to glutathione Sepharose; proteins were incubated for 15 min at 37°C in the presence of 10 μM [γ-^{32}PO$_4$]adenosine 5′-triphosphate (ATP), 10 μM cGMP, 10 mM MgCl$_2$, and 50 ng of Flag-tagged PKGII (purified from HEK 293T cells). To examine SHP-1 phosphorylation in intact cells, we transfected 293T cells with Flag-tagged SHP-1 constructs and incubated them with ^{32}PO$_4$ (100 μCi/ml) for 4 hours, with 100 μM 8-CPT-cGMP added for the last 10 min. Cell lysates were subjected to immunoprecipitation with anti–Flag antibody, and immunoprecipitates were analyzed by SDS–polyacrylamide gel electrophoresis (SDS-PAGE) and autoradiography.

PTP assays

Variable amounts of GST–SHP-1 constructs purified from bacteria, Flag–SHP-1 constructs immunoprecipitated from transfected HEK 293T cells, and anti–SHP-2 immunoprecipitates from MC3T3 cells were incubated for 15 to 60 min at 37°C with 100 μM C-terminal Src peptide (TSTEPQ-pY-QPGENL, from AnaSpec). Inorganic phosphate was measured by a colorimetric assay in a 96-well plate reader with malachite green and ammonium molybdate; the assay was linear with time and protein concentration.

Immunofluorescence staining, BrdU incorporation, and BiFC

Osteoblasts were either exposed to laminar fluid shear stress as described above or plated on glass coverslips in 24-well dishes and subjected to orbital fluid shear stress (120 rpm) for 5 min with similar results (Fig. 6 and fig. S6 show orbital fluid shear stress). A detailed description of BrdU treatment, transfection for BiFC, and sample preparation is provided in the Supplementary Materials. Cells were viewed with a confocal microscope (Olympus FV1000), a 40/1.3 oil-immersion objective, and 2× to 4× digital zoom. Images were analyzed with Fluoview (Olympus) and Photoshop (Adobe), and identical software settings were used for image acquisition of all samples in a given experiment.

RT-PCR

RNA was extracted in TRI Reagent, and 1 μg of total RNA was subjected to reverse transcription and real-time PCR using previously described primers; *gapd* served as an internal reference with the $2^{-\Delta\Delta Ct}$ method (*5*).

Prkg2$^{-/-}$ mice

Homozygous *Prkg2*$^{-/-}$ mice were generated as described (*13*); mice from each litter were genotyped by PCR, and tissues were harvested at the University of Bonn, Germany, with approval of the local Animal Welfare Committee. Osteoblast-like cells were extracted from the calvariae of 7-day-old mice by sequential collagenase digestion, and cells were characterized as described for hPOBs.

Statistical analyses

Pairwise comparisons were done by two-tailed Student's *t* test and comparison of multiple groups by analysis of variance (ANOVA) with Dunnett's posttest analysis to the control group; a *P* value of <0.05 was considered statistically significant. Where appropriate, such as for results of immunofluorescence staining and for normalized results, the Wilcoxon rank test was used for pairwise comparison and the Friedman test with Dunn's posttest analysis for comparison of multiple groups.

RESEARCH ARTICLE

REFERENCES AND NOTES

1. E. Ozcivici, Y. K. Luu, B. Adler, Y. X. Qin, J. Rubin, S. Judex, C. T. Rubin, Mechanical signals as anabolic agents in bone. *Nat. Rev. Rheumatol.* **6**, 50–59 (2010).
2. D. D. Bikle, Integrins, insulin like growth factors, and the skeletal response to load. *Osteoporos. Int.* **19**, 1237–1246 (2008).
3. K. K. Papachroni, D. N. Karatzas, K. A. Papavassiliou, E. K. Basdra, A. G. Papavassiliou, Mechanotransduction in osteoblast regulation and bone disease. *Trends Mol. Med.* **15**, 208–216 (2009).
4. T. N. McAllister, J. A. Frangos, Steady and transient fluid shear stress stimulate NO release in osteoblasts through distinct biochemical pathways. *J. Bone Miner. Res.* **14**, 930–936 (1999).
5. H. Rangaswami, N. Marathe, S. Zhuang, Y. Chen, J. C. Yeh, J. A. Frangos, G. R. Boss, R. B. Pilz, Type II cGMP-dependent protein kinase mediates osteoblast mechanotransduction. *J. Biol. Chem.* **284**, 14796–14808 (2009).
6. M. Watanuki, A. Sakai, T. Sakata, H. Tsurukami, M. Miwa, Y. Uchida, K. Watanabe, K. Ikeda, T. Nakamura, Role of inducible nitric oxide synthase in skeletal adaptation to acute increases in mechanical loading. *J. Bone Miner. Res.* **17**, 1015–1025 (2002).
7. J. W. Chow, S. W. Fox, J. M. Lean, T. J. Chambers, Role of nitric oxide and prostaglandins in mechanically induced bone formation. *J. Bone Miner. Res.* **13**, 1039–1044 (1998).
8. L. Mancini, N. Moradi-Bidhendi, L. Becherini, V. Martineti, I. MacIntyre, The biphasic effects of nitric oxide in primary rat osteoblasts are cGMP dependent. *Biochem. Biophys. Res. Commun.* **274**, 477–481 (2000).
9. K. E. Armour, K. J. Armour, M. E. Gallagher, A. Godecke, M. H. Helfrich, D. M. Reid, S. H. Ralston, Defective bone formation and anabolic response to exogenous estrogen in mice with targeted disruption of endothelial nitric oxide synthase. *Endocrinology* **142**, 760–766 (2001).
10. A. P. Bergula, M. A. Haidekker, W. Huang, H. Y. Stevens, J. A. Frangos, Venous ligation-mediated bone adaptation is *NOS 3* dependent. *Bone* **34**, 562–569 (2004).
11. C. H. Turner, Y. Takano, I. Owan, G. A. Murrell, Nitric oxide inhibitor L-NAME suppresses mechanically induced bone formation in rats. *Am. J. Physiol.* **270**, E634–E639 (1996).
12. F. Hofmann, D. Bernhard, R. Lukowski, P. Weinmeister, cGMP regulated protein kinases (cGK). *Handb. Exp. Pharmacol.* 137–162 (2009).
13. A. Pfeifer, A. Aszódi, U. Seidler, P. Ruth, F. Hofmann, R. Fässler, Intestinal secretory defects and dwarfism in mice lacking cGMP-dependent protein kinase II. *Science* **274**, 2082–2086 (1996).
14. S. Kapur, D. J. Baylink, K. H. Lau, Fluid flow shear stress stimulates human osteoblast proliferation and differentiation through multiple interacting and competing signal transduction pathways. *Bone* **32**, 241–251 (2003).
15. G. L. Jiang, C. R. White, H. Y. Stevens, J. A. Frangos, Temporal gradients in shear stimulate osteoblastic proliferation via ERK1/2 and retinoblastoma protein. *Am. J. Physiol. Endocrinol. Metab.* **283**, E383–E389 (2002).
16. K. H. Lau, S. Kapur, C. Kesavan, D. J. Baylink, Up-regulation of the Wnt, estrogen receptor, insulin-like growth factor-I, and bone morphogenetic protein pathways in C57BL/6J osteoblasts as opposed to C3H/HeJ osteoblasts in part contributes to the differential anabolic response to fluid shear. *J. Biol. Chem.* **281**, 9576–9588 (2006).
17. S. C. Harrison, Variation on an Src-like theme. *Cell* **112**, 737–740 (2003).
18. T. Gudi, G. K.-P. Hong, A. B. Vaandrager, S. M. Lohmann, R. B. Pilz, Nitric oxide and cGMP regulate gene expression in neuronal and glial cells by activating type II cGMP-dependent protein kinase. *FASEB J.* **13**, 2143–2152 (1999).
19. J. M. Schmitt, P. J. Stork, PKA phosphorylation of Src mediates cAMP's inhibition of cell growth via Rap1. *Mol. Cell* **9**, 85–94 (2002).
20. S. J. Shattil, Integrins and Src: Dynamic duo of adhesion signaling. *Trends Cell Biol.* **15**, 399–403 (2005).
21. A. W. Poole, M. L. Jones, A SHPing tale: Perspectives on the regulation of SHP-1 and SHP-2 tyrosine phosphatases by the C-terminal tail. *Cell. Signal.* **17**, 1323–1332 (2005).
22. N. Wang, Z. Li, R. Ding, G. D. Frank, T. Senbonmatsu, E. J. Landon, T. Inagami, Z. J. Zhao, Antagonism or synergism. Role of tyrosine phosphatases SHP-1 and SHP-2 in growth factor signaling. *J. Biol. Chem.* **281**, 21878–21883 (2006).
23. F. M. Pavalko, N. X. Chen, C. H. Turner, D. B. Burr, S. Atkinson, Y. F. Hsieh, J. Qiu, R. L. Duncan, Fluid shear-induced mechanical signaling in MC3T3-E1 osteoblasts requires cytoskeleton-integrin interactions. *Am. J. Physiol.* **275**, C1591–C1601 (1998).
24. D. Y. Lee, C. R. Yeh, S. F. Chang, P. L. Lee, S. Chien, C. K. Cheng, J. J. Chiu, Integrin-mediated expression of bone formation-related genes in osteoblast-like cells in response to fluid shear stress: Roles of extracellular matrix, Shc, and mitogen-activated protein kinase. *J. Bone Miner. Res.* **23**, 1140–1149 (2008).
25. L. I. Plotkin, I. Mathov, J. I. Aguirre, A. M. Parfitt, S. C. Manolagas, T. Bellido, Mechanical stimulation prevents osteocyte apoptosis: Requirement of integrins, Src kinases, and ERKs. *Am. J. Physiol. Cell Physiol.* **289**, C633–C643 (2005).
26. E. G. Arias-Salgado, S. Lizano, S. Sarkar, J. S. Brugge, M. H. Ginsberg, S. J. Shattil, Src kinase activation by direct interaction with the integrin β cytoplasmic domain. *Proc. Natl. Acad. Sci. U.S.A.* **100**, 13298–13302 (2003).
27. B. Geiger, J. P. Spatz, A. D. Bershadsky, Environmental sensing through focal adhesions. *Nat. Rev. Mol. Cell Biol.* **10**, 21–33 (2009).
28. S. Kapur, S. Mohan, D. J. Baylink, K. H. Lau, Fluid shear stress synergizes with insulin-like growth factor-I (IGF-I) on osteoblast proliferation through integrin-dependent activation of IGF-I mitogenic signaling pathway. *J. Biol. Chem.* **280**, 20163–20170 (2005).
29. Y. Wang, L. M. McNamara, M. B. Schaffler, S. Weinbaum, A model for the role of integrins in flow induced mechanotransduction in osteocytes. *Proc. Natl. Acad. Sci. U.S.A.* **104**, 15941–15946 (2007).
30. F. M. Pavalko, S. M. Norvell, D. B. Burr, C. H. Turner, R. L. Duncan, J. P. Bidwell, A model for mechanotransduction in bone cells: The load-bearing mechanosomes. *J. Cell. Biochem.* **88**, 104–112 (2003).
31. E. F. Wagner, R. Eferl, Fos/AP-1 proteins in bone and the immune system. *Immunol. Rev.* **208**, 126–140 (2005).
32. Y. Ling, L. A. Maile, J. Badley-Clarke, D. R. Clemmons, DOK1 mediates SHP-2 binding to the αvβ3 integrin and thereby regulates insulin-like growth factor I signaling in cultured vascular smooth muscle cells. *J. Biol. Chem.* **280**, 3151–3158 (2005).
33. K. D. Chen, Y. S. Li, M. Kim, S. Li, S. Yuan, S. Chien, J. Y. Shyy, Mechanotransduction in response to shear stress. Roles of receptor tyrosine kinases, integrins, and Shc. *J. Biol. Chem.* **274**, 18393–18400 (1999).
34. J. Lieskovska, Y. Ling, J. Badley-Clarke, D. R. Clemmons, The role of Src kinase in insulin-like growth factor-dependent mitogenic signaling in vascular smooth muscle cells. *J. Biol. Chem.* **281**, 25041–25053 (2006).
35. S. R. Young, R. Gerard-O'Riley, J. B. Kim, F. M. Pavalko, Focal adhesion kinase is important for fluid shear stress-induced mechanotransduction in osteoblasts. *J. Bone Miner. Res.* **24**, 411–424 (2009).
36. M. A. Schwartz, The force is with us. *Science* **323**, 588–589 (2009).
37. D. P. Felsenfeld, P. L. Schwartzberg, A. Venegas, R. Tse, M. P. Sheetz, Selective regulation of integrin–cytoskeleton interactions by the tyrosine kinase Src. *Nat. Cell Biol.* **1**, 200–206 (1999).
38. R. M. Clancy, J. Rediske, X. Tang, N. Nijher, S. Frenkel, M. Philips, S. B. Abramson, Outside-in signaling in the chondrocyte. Nitric oxide disrupts fibronectin-induced assembly of a subplasmalemmal actin/rho A/focal adhesion kinase signaling complex. *J. Clin. Invest.* **100**, 1789–1796 (1997).
39. A. Smolenski, W. Poller, U. Walter, S. M. Lohmann, Regulation of human endothelial cell focal adhesion sites and migration by cGMP-dependent protein kinase I. *J. Biol. Chem.* **275**, 25723–25732 (2000).
40. A. K. Somani, J. S. Bignon, G. B. Mills, K. A. Siminovitch, D. R. Branch, Src kinase activity is regulated by the SHP-1 protein-tyrosine phosphatase. *J. Biol. Chem.* **272**, 21113–21119 (1997).
41. S. Q. Zhang, W. Yang, M. I. Kontaridis, T. G. Bivona, G. Wen, T. Araki, J. Luo, J. A. Thompson, B. L. Schraven, M. R. Philips, B. G. Neel, Shp2 regulates SRC family kinase activity and Ras/Erk activation by controlling Csk recruitment. *Mol. Cell* **13**, 341–355 (2004).
42. K. Aoki, E. Didomenico, N. A. Sims, K. Mukhopadhyay, L. Neff, A. Houghton, M. Amling, J. B. Levy, W. C. Horne, R. Baron, The tyrosine phosphatase SHP-1 is a negative regulator of osteoclastogenesis and osteoclast resorbing activity: Increased resorption and osteopenia in *me^v/me^v* mutant mice. *Bone* **25**, 261–267 (1999).
43. E. L. Leung, J. C. Wong, M. G. Johlfs, B. K. Tsang, R. R. Fiscus, Protein kinase G type Iα activity in human ovarian cancer cells significantly contributes to enhanced Src activation and DNA synthesis/cell proliferation. *Mol. Cancer Res.* **8**, 578–591 (2010).
44. P. Krejci, B. Masri, V. Fontaine, P. B. Mekikian, M. Weis, H. Prats, W. R. Wilcox, Interaction of fibroblast growth factor and C-natriuretic peptide signaling in regulation of chondrocyte proliferation and extracellular matrix homeostasis. *J. Cell Sci.* **118**, 5089–5100 (2005).

45. A. Sunters, D. P. Thomas, W. A. Yeudall, A. E. Grigoriadis, Accelerated cell cycle progression in osteoblasts overexpressing the c-fos proto-oncogene: Induction of cyclin A and enhanced CDK2 activity. *J. Biol. Chem.* **279**, 9882–9891 (2004).

46. S. J. Wimalawansa, Rationale for using nitric oxide donor therapy for prevention of bone loss and treatment of osteoporosis in humans. *Ann. N. Y. Acad. Sci.* **1117**, 283–297 (2007).

MATERIALS AND METHODS

Reagents. Antibodies were obtained from the following sources: total Src, Src pTyr[418], Src pTyr[529], Src non-pTyr[529], and PKA/PKG substrate antibody (anti-RRXpS) from Cell Signaling; total ERK1, ERK1/2 phosphorylated on Tyr[204] (clone E-4), SHP-1 (SC287), SHP-2 (SC7384), β_3 integrin (SC6627), α-tubulin, and β-actin from Santa Cruz Biotechnology; rabbit monoclonal antibodies for SHP-2 and β_3 integrin from Epitomics; PTP-1B from Upstate Biotechnology Inc., RPTP-α and caveolin-1 from BD Transduction Laboratories; PKGI from Calbiochem/EMD; PKGII from Abgent; and BrdU from Sigma.

The cGMP agonist 8-(4-chlorophenylthio)-guano-sine-3',5'-cyclic monophosphate (8-CPT-cGMP, referred to as cGMP) and the cGMP antagonist 8-(4-chlorophenylthio)-β-phenyl-1,N^2-ethenoguanosine-3',5'-cyclic monophosphorothioate, Rp isomer (Rp-8-CPT-PET-cGMPS) were from Biolog. The NOS inhibitor *N*-nitro-L-arginine methyl ester (L-NAME), the soluble guanylate cyclase inhibitor 1H-[1,2,4]oxadiazolo[4,3-a]quinoxalin-1-one (ODQ), and 1-propanamine,3-(2-hydroxy-2-nitroso-propylhydrazino) (PAPA-NONOate) were from Cayman. The Src kinase family inhibitor PP2 and its inactive cogener PP3 were from Calbiochem/EMD. Human fibrinogen and fibronectin were from Enzyme Research Ltd.

DNA Constructs. Vectors encoding variants of human PKGI, rat PKGII, and human β_3 integrin were described previously (1,2). Bacterial expression vectors encoding glutathione-S-transferase (GST)-tagged human SHP-1 and SHP-2 were from Addgene; truncated versions were generated by PCR. For mammalian SHP-1 expression vectors, SHP-1 variants were fused in-frame with the N-terminal peptide DYKDDDDKG. Site-directed mutagenesis was performed using the QuickChange kit (Stratagene) as per the manufacturer's instructions. Venus vectors for bimolecular fluorescence complementation (BiFC) were provided by C.-D. Hu (Purdue University); α_{IIb}-VC integrin, containing the C-terminal half of Venus fused to the C-terminus of human α_{IIb} integrin, was described previously (3). The N-terminal half of Venus was inserted between amino acids 39 and 40 of PKGII to generate PKGII-VN. All PCR products were sequenced to assure absence of unwanted mutations.

siRNA Transfections and Viral Infections. Sequences targeted by siRNAs are summarized in Table S1; the oligoribonucleotides were produced by Qiagen. MC3T3 cells were plated at 1.3×10^5 cells per well of a 6-well dish or at 5×10^5 cells per glass slide, and were transfected 18 hours later (at ~40% confluency) with 100 pmol of siRNA and Lipofectamine 2000^{TM} (Invitrogen) in 1 ml of 10% FBS-containing media.

Adenoviral vectors encoding β-galactosidase (LacZ), PKGI, PKGII, and SHP-1 variants were produced using the pAd/CMV/V5-DEST^{TM} Gateway^R system (Invitrogen) (1,4). Lentiviral vectors

encoding human β_3 integrin variants were produced as described previously (3). At 24 hours after siRNA transfection, cells were infected in full growth medium at an MOI of ~10; 24 hours later cells were transferred to medium containing 0.1% FBS for an additional 24 hours until harvest.

Cell Fractionation. Cells were extracted in hypotonic buffer by Dounce homogenization, nuclei and cell debris were removed by centrifugation at 300 x g for 10 min, and the supernatant was subjected to centrifugation at 50,000 x g for 30 min to generate a "cytosolic" (supernatant) and a "membrane" (pellet) fraction. To isolate detergent-insoluble fractions, MC3T3 cells were plated on 150 mm dishes and infected with adenovirus encoding rat PKGII at an MOI of ~5 to increase PKGII expression by about 2-fold. Confluent cells were subjected to orbital flow for 5 min (120 rpm) or kept under static conditions. Triton-insoluble fractions were prepared as described (5). Lysates were concentrated to a minimal volume using trichloroacetic acid/acetone precipitation.

Immunoprecipitation and Western Blot Analyses. For Fig. 4H, MC3T3 cells were lysed in 50 mM Tris/HCl pH 7.5, 100 mM NaCl, 1 mM EDTA, 10 mM dithiotreitol, 0.5% NP-40, and a protease inhibitor cocktail (Calbiochem/EMD). Lysates were cleared by centrifugation (16,000 x g for 15 min) and subjected to immunoprecipitation using a SHP-2-specific monoclonal antibody on protein G agarose beads. For Fig. 5C and fig. S7A, MC3T3 cells were infected with lentivirus expressing wild-type or mutant human β_3 integrin; cells were lysed as above, and cleared lysates were subjected to immunoprecipitation with a rabbit monoclonal antibody which recognizes human β_3 integrin more efficiently than murine β_3 integrin. Western blots were generated using the indicated antibodies from a different species. Western blots were developed with horseradish peroxidase-coupled secondary antibodies or Clean-Blot IP Detection Reagent[TM] (Thermo Scientific) and enhanced chemiluminescence detection (6). For fig. S7C, HEK 293T cells were cotransfected with DNA vectors encoding human β_3 integrin and rat PKGII using Lipofectamine 2000[TM]. For immunoprecipitation of PKGII, cells were lysed in 1% Triton X-100, 50 mM Tris/HCl pH 7.4, 500 mM NaCl, 5 mM sodium vanadate, and protease inhibitor cocktail to solubilize PKGII (1). For immunoprecipitation of β_3 integrin, cells were lysed in 0.1% SDS, 0.1% sodium deoxycholate, 100 mM Tris/HCl pH 7.4, 150 mM NaCl, 5 mM sodium vanadate, 2 mM PMSF and protease inhibitors, which partly solubilizes PKGII.

PTP Assays. PTP assays were performed in 50 mM Tris/HCl pH 7.5, 100 mM NaCl, 1 mM EDTA, 10 mM dithiotreitol, 0.1% NP-40 using the C-terminal Src peptide TSTEPQ(pY)QPGENL as a substrate. Inorganic phosphate was measured with a modified malachite green/ ammonium molybdate method (7). Blank samples included HEK 293T cells transfected with empty vector (+/- PKGII) subjected to immunoprecipitation with anti-Flag antibody, and control IgG immunoprecipitates from MC3T3 cells.

Immunofluorescence Staining and BrdU Incorporation.   Cells were fixed in 4% paraformaldehyde and permeabilized in 0.5% Triton-X-100. After blocking with 3% BSA, cells were stained using the indicated primary antibodies, and FITC- and Texas Red-conjugated secondary antibodies (Jackson ImmunoResearch).   For triple staining, secondary antibodies conjugated to AlexaFluor 555 and 647 (Invitrogen), and a FITC-conjugated anti-vinculin antibody (Sigma-Aldrich) were used.   For BrdU incorporation, cells received 200 μM BrdU for 18 hours, were fixed, permeabilized, and incubated with 0.5 U/μl DNAse I (Sigma-Aldrich) for 30 min at 37ºC, prior to staining with anti-BrdU antibody (Sigma-Aldrich) and Hoechst 33342; cells were visualized with a Leica fluorescent microscope at 10-20x, and at least 300 cells were scored per condition.

BiFC assay. Cells were cotransfected with human α_{IIb} integrin-VC and β_3 integrin, and either wild-type PKGII-VN or PKGII (G2A)-VN. At 24 hours post transfection, cells were allowed to spread on fibrinogen-coated cover slips for 2 hours. After fixation and permeabilization, cells were stained for PKGII and human β_3 integrin using secondary antibodies conjugated to Alexa Fluor 555 and 647 (Invitrogen).

SUPPLEMENTAL FIGURES

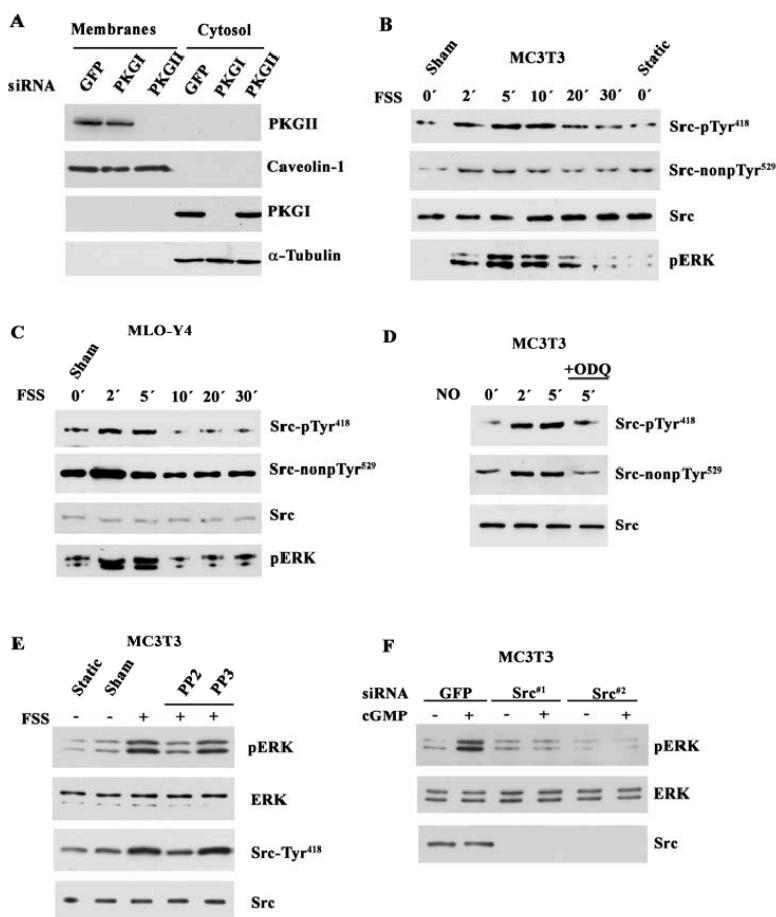**Figure S1: siRNA knockdown of PKGI or PKGII; effects of fluid shear stress and cGMP on Src and ERK phosphorylation in MLO-Y4 and MC3T3 cells.** (**A**) MC3T3 cells were transfected with siRNAs targeting GFP (control), PKGI, or PKGII, and cell membranes (top two panels) or cytosolic extracts (bottom two panels) were analyzed by Western blotting for the presence of PKGII and caveolin-1, or PKGI and α-tubulin, respectively. (**B** and **C**) Serum-starved MC3T3 osteoblast-like cells (B) and MLO-Y4 osteocyte-like cells (C, provided by Dr. L. Bonewald) were sham-treated or exposed to fluid shear stress (FSS; 12 dynes/cm^2) for the indicated times; some cells were kept static without being mounted into the flow chamber (B, last lane). Cell lysates were analyzed by Western blotting with antibodies specific for Src phosphorylated on Tyr^{418} (Src-pTyr^{418}), Src with unphosphorylated Tyr^{529} (Src-nonpTyr^{529}), total Src (Src), and ERK1/2 phosphorylated on Tyr^{204} (pERK). (**D**) MC3T3 cells were treated with the NO donor PAPA-NONOate (10 μM) for the indicated times; some cells were pre-treated for 1 hour with the soluble guanylate cyclase inhibitor ODQ (10 μM). (**E**) MC3T3 cells were treated as in (B); some cells were pre-treated for 1 hour with the Src family kinase inhibitor PP2 (10 μM) or the inactive analog PP3 (10 μM), prior to stimulation with fluid shear stress for 5 min. (**F**) MC3T3 cells were transfected with siRNAs targeting GFP or two different sequences in Src; after serum starvation for 24 hours, some cells were treated with 100 μM 8-CPT-cGMP (cGMP) for 5 min. Western blots shown in A to F are representative of at least two independent experiments.
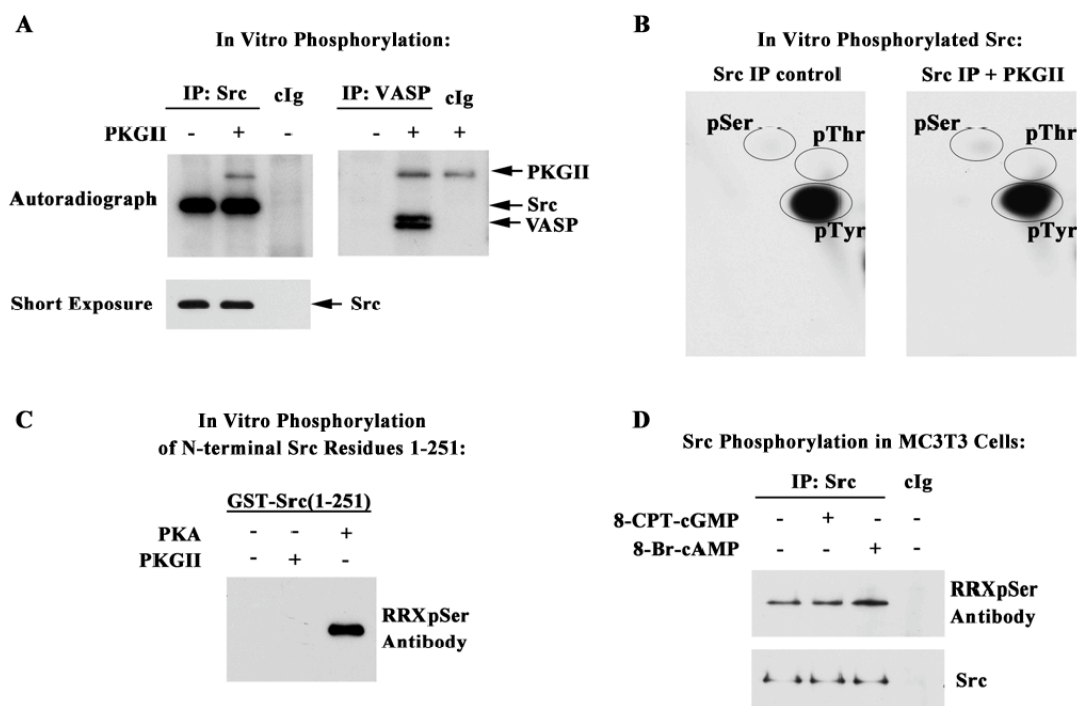
Figure S2: PKGII does not directly phosphorylate Src. (**A**) Src and VASP were immunoprecipitated from HEK 293T cells that were transfected with expression vectors encoding murine Src or human VASP, respectively. Washed immunoprecipitates were incubated for 15 min at 37ºC in kinase buffer containing 100 μM [γ-^{32}PO$_4$]ATP and 10 mM MgCl$_2$ in the absence or presence of 100 ng purified PKGII and 10 μM 8-CPT-cGMP; proteins were analyzed by SDS-PAGE/autoradiography (representative of three experiments). (**B**) Bands corresponding to in vitro phosphorylated Src in (A) were excised and subjected to acid hydrolysis followed by phospho-amino acid analysis using two-dimensional high voltage electrophoresis. Spots corresponding to ninhydrin-stained phospho-amino acid standards are circled (representative of two experiments). (**C**) GST-tagged Src (1-251), containing the first 251 amino acids of murine Src, was purified from bacteria and incubated for 15 min at 37ºC with kinase buffer containing 100 μM ATP and 10 mM MgCl$_2$ in the absence or presence of purified PKGII and cGMP or the catalytic subunit of PKA. Proteins were analyzed by Western blotting using a PKA/PKG substrate antibody which recognizes the sequence RRXpS (representative of two experiments). (**D**) Serum-deprived MC3T3 cells were treated for 5 min with 100 μM 8-CPT-cGMP (cGMP) or 1 mM 8-Br-cAMP (cAMP) as indicated. Cell lysates were subjected to immunoprecipitation with anti-Src antibody or control IgG, and immunoprecipitates were analyzed using the PKA/PKG substrate antibody described in (C) or rabbit anti-Src antibody (representative of two experiments).
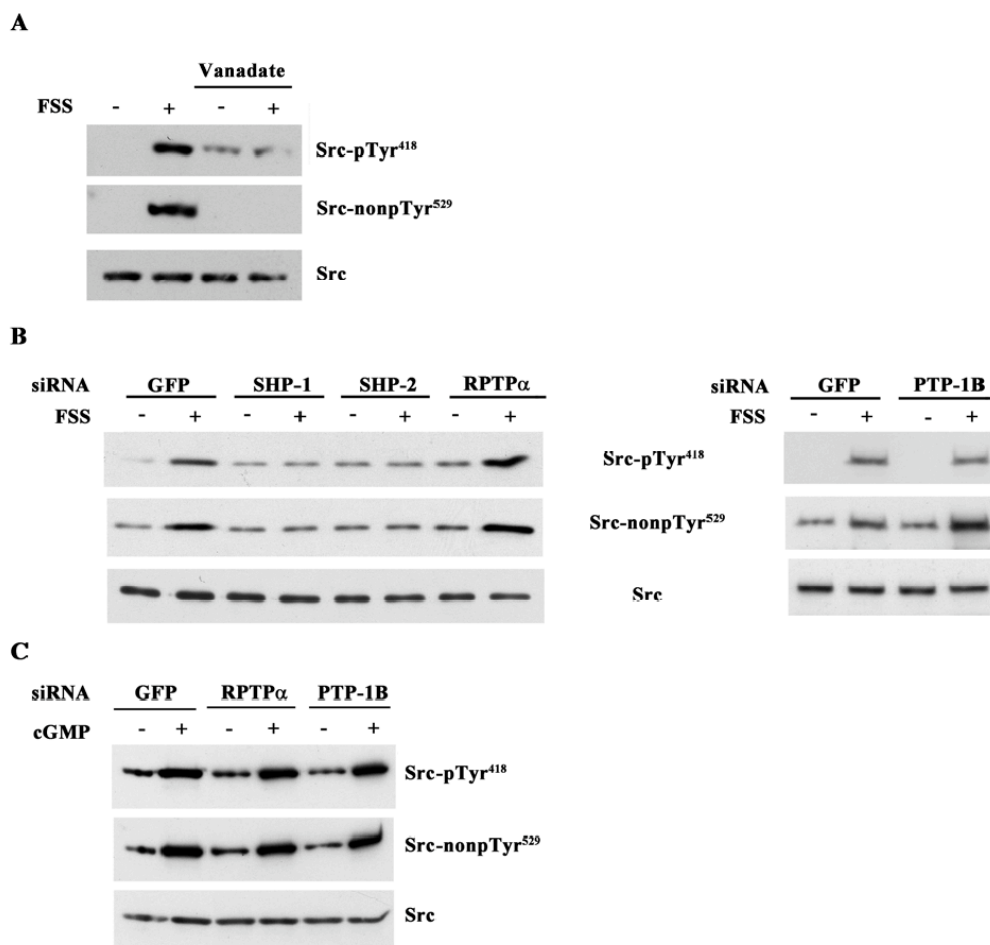
A

B

C

Figure S3: Effect of vanadate- and phosphatase-specific siRNAs on Src phosphorylation and dephosphorylation. (**A**) MC3T3 cells were pre-treated for 1 hour with 10 μM vanadate prior to stimulation with fluid shear stress (FSS; 12 dynes/cm^2) for 5 min. Src phosphorylation was assessed as in fig. S1B (representative of three experiments). (**B** and **C**) MC3T3 cells were transfected with the indicated siRNAs, serum-starved, and exposed to fluid shear stress (B) or treated with 100 μM 8-CPT-cGMP (cGMP; C) for 5 min (representative of three experiments).
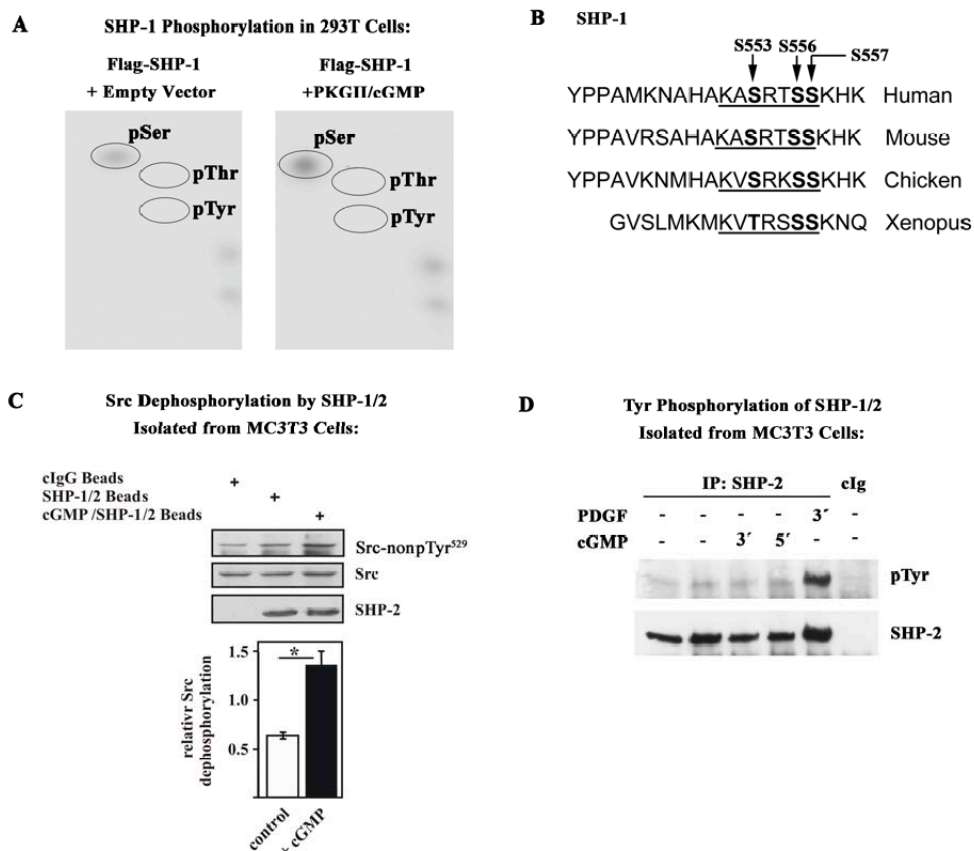
A SHP-1 Phosphorylation in 293T Cells:

Flag-SHP-1 + Empty Vector

Flag-SHP-1 +PKGII/cGMP

pSer / pThr / pTyr

B SHP-1

S553 S556 — S557

YPPAMKNAHAKASRTSSKHK Human
YPPAVRSAHAKASRTSSKHK Mouse
YPPAVKNMHAKVSRKSSKHK Chicken
GVSLMKMKVTRSSSKNQ Xenopus

C Src Dephosphorylation by SHP-1/2 Isolated from MC3T3 Cells:

cIgG Beads
SHP-1/2 Beads
cGMP /SHP-1/2 Beads

Src-nonpTyr^{529}
Src
SHP-2

relative Src dephosphorylation

D Tyr Phosphorylation of SHP-1/2 Isolated from MC3T3 Cells:

IP: SHP-2   cIg

PDGF   -   -   -   -   3′   -
cGMP   -   -   3′ 5′ -   -

pTyr
SHP-2

Figure S4: Analysis of SHP-1 phosphorylation and function in MC3T3 cells. (**A**) HEK 293T cells were cotransfected with Flag-tagged SHP-1 and empty vector or PKGII, and labeled with $^{32}PO_4$. Some cells were treated with 100 μM 8-CPT-cGMP (cGMP), and SHP-1 was isolated by immunoprecipitation as described in Fig. 4D. Bands corresponding to SHP-1 were excised, and subjected to phospho-amino acid analysis as described in fig. S2B. Migration of phospho-amino acid standards is indicated (representative of two experiments). (**B**) SHP-1 sequences from human, mouse, chicken, and *Xenopus* were aligned using BLAST (8), and a putative PKG consensus sequence is underlined. The indicated serine residues were mutated to alanines to generate SHP-1 AAA. (**C**) Serum-deprived MC3T3 cells were stimulated with 100 μM cGMP for 5 min or left untreated; cell lysates were subjected to immunoprecipitation using a SHP-2-specific antibody or control IgG as described in Fig. 4H. To examine SHP-mediated dephosphorylation of full-length Src, the immunoprecipitates containing SHP-1 and -2 (Fig. 4H) were incubated with MC3T3 cell lysates for 20 min at 37°C. The lysate and bead mixture was analyzed by Western blotting using an antibody specific for Src-nonpTyr^{529}, total Src, and SHP-2. The bar graph summarizes three experiments (mean +/- SEM, $p < 0.05$ for the comparison of immunoprecipitates obtained from control compared to cGMP-treated cells). (**D**) MC3T3 cells were mock-treated or treated with 100 μM cGMP for 3 or 5 min; some cells received 30 ng/ml platelet-derived growth factor (PDGF) for 3 min. Cell lysates were subjected to immunoprecipitation as in Fig. 4H, and immunoprecipitates were analyzed by Western blotting using a phospho-Tyr-specific antibody. Note that Tyr-phosphorylated SHP-2 in PDGF-treated cells migrates with a slightly higher apparent molecular weight (representative of two experiments).
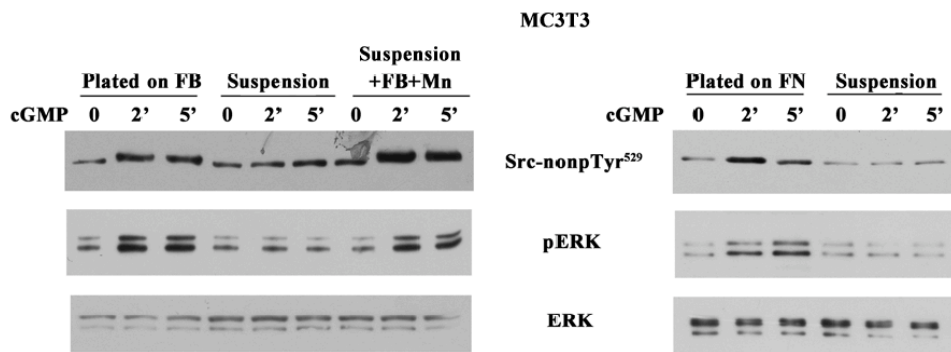
Figure S5: cGMP activation of Src requires ligation of β_3 integrins. MC3T3 cells were allowed to adhere to fibrinogen-coated dishes (FB, left panel) or fibronectin-coated dishes (FN, right panel); some cells were kept in suspension (on bovine serum albumin-coated dishes) or received soluble fibrinogen and $MnCl_2$ as described for hPOBs in Fig. 5E. After 1 hour, cells were stimulated with 100 μM 8-CPT-cGMP (cGMP) for the indicated times, and Src and ERK phosphorylation was assessed as in fig. S1B (representative of two experiments).
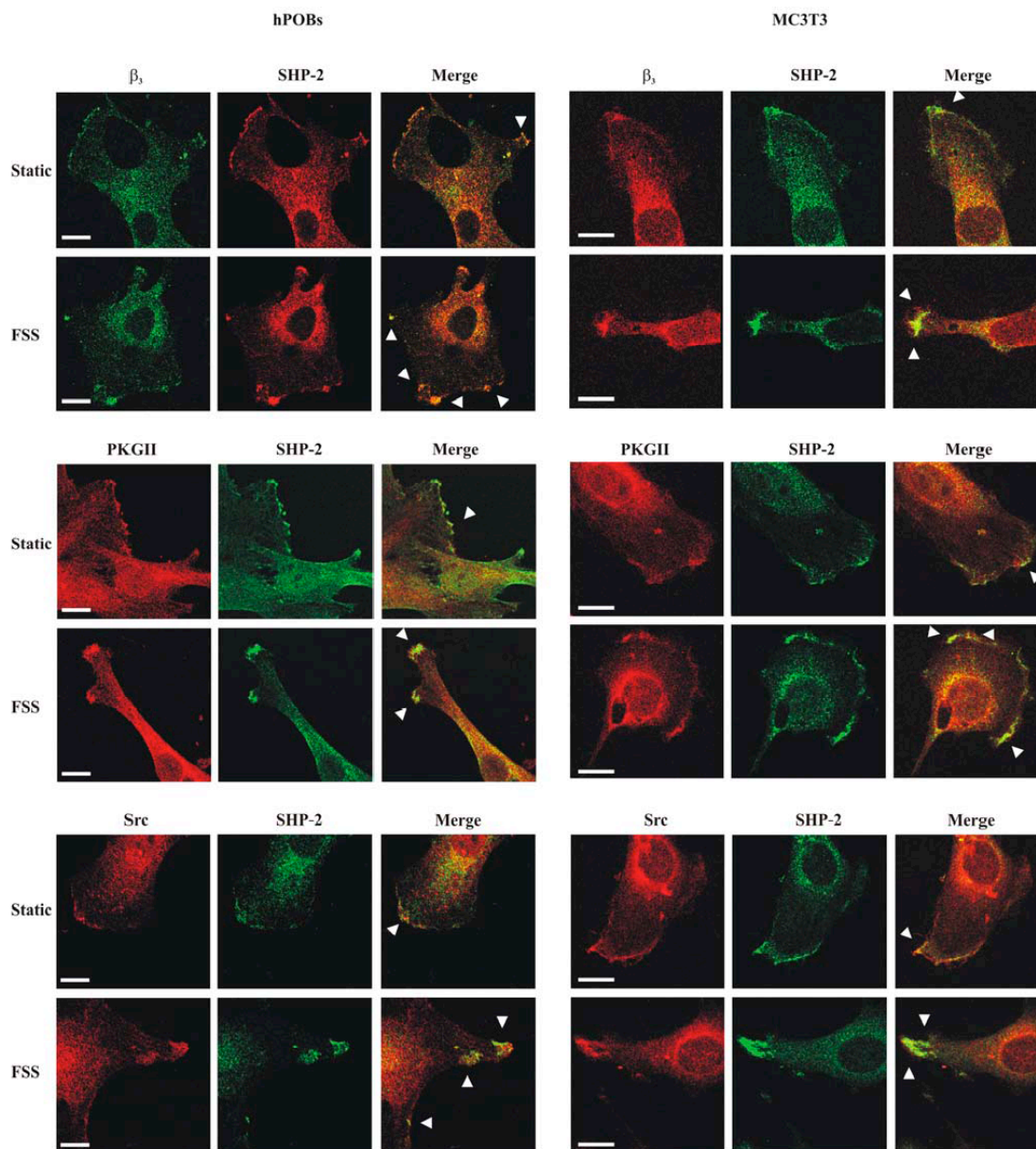
Figure S6: Colocalization of β₃ integrins, PKGII, and Src with SHP-2-containing membrane complexes. hPOBs (left) and MC3T3 cells (right) were infected with PKGII adenovirus to increase PKGII expression by about 2-fold; cells were held static or exposed to orbital fluid shear stress (FSS; 120 rpm) for 5 min, and PKGII, SHP-2, Src, and β₃ integrin were detected by immunofluorescence staining using rabbit antibodies specific for PKGII, Src, or β₃ integrin, and mouse antibodies for SHP-2. Representative confocal images of three experiments are shown; the bar represents 5 μm.
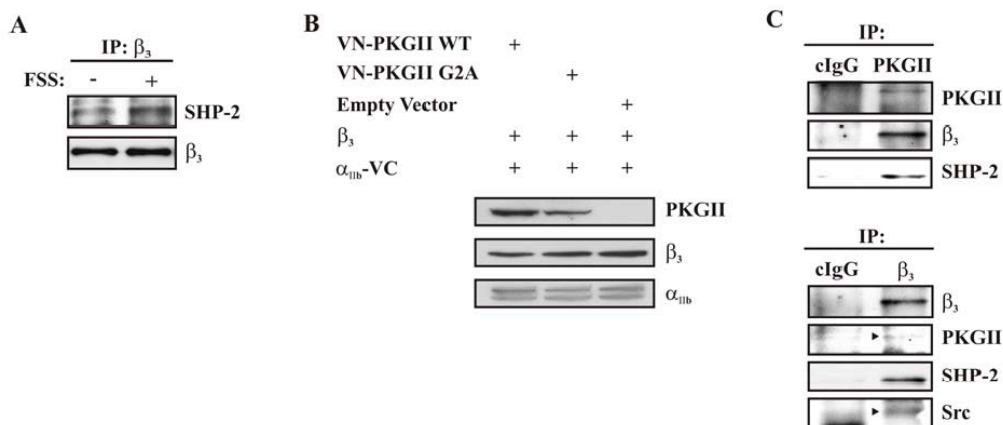
Figure S7: Interactions among PKGII, SHP-2, Src, and β₃ integrins **(A)** MC3T3 cells infected with lentivirus expressing human β₃ integrin were exposed to orbital fluid shear stress (FSS; 120 rpm) for 5 min or held static. β₃ integrin was immunoprecipitated, and precipitates were analyzed by Western blotting for the presence of SHP-2 (representative of two experiments). **(B)** MC3T3 cells were transfected with vectors encoding VN-PKGII and α_{IIb}-VC chimeras, and human β₃ integrin, as indicated, and cell lysates were analyzed by Western blotting for the presence of PKGII-fusion proteins, β₃ integrin, and α_{IIb} integrin. **(C)** Coimmunoprecipitation of β₃ integrin and SHP-2 with PKGII, and of PKGII, SHP-2, and Src with β₃ integrin (representative of two experiments). Note that under conditions allowing coimmunoprecipitation, the amount of solubilized PKGII is low.

Gene:	siRNA Target Sequence (5'-3')	Comments
PKGI	CCGGACAUUUAAAGACAGCAA	Target sequence in the C-terminus of PKG Iα and β
PKGII[#1]	CTGCTTGGAAGTGGAATACTA	
PKGII[#2]	CCGGGTTTCTTGGGTAGTCAA	Mismatched with rat
β₃ Integrin[#1]	CCGCTTCAATGAAGAAGTGAA	
β₃ Integrin[#2]	CACGGTGAGCTTTAGTATCGA	Mismatched with human
SHP-1[#1]	CTGGACATTTCTTGTGCGTGA	
SHP-1[#2]	CTGGATCAGATCAACCAGCGA	Mismatched with human
SHP-2[#1]	CAGAAGCACAGTACCGGTTTA	
SHP-2[#2]	AAGGACATGAATATACCAATA	Mismatched with human
PTP-1B	TCGGATTAAATTGCACCAGGA	
RPTP-α	TTCACGGATGCCATAACAGAA	
GFP	AAGCTGACCCTGAAGTTCATC	
Src[#1]	TTCCCTTGTGTCCATATTTAA	
Src[#2]	CCCAGACTTGTTGTACATATT	

Table S1. siRNA target sequences.

REFERENCES

1. T.Gudi, G.K.P.Hong, A.B.Vaandrager, S.M.Lohmann, and R.B.Pilz. Nitric oxide and cGMP regulate gene expression in neuronal and glial cells by activating type II cGMP-dependent protein kinase. *FASEB J.* **13**, 2143-2152 (1999).

2. E.G.Arias-Salgado, S.Lizano, S.Sarkar, J.S.Brugge, M.H.Ginsberg, and S.J.Shattil. Src kinase activation by direct interaction with the integrin β cytoplasmic domain. *Proc.Natl.Acad.Sci.U.S.A* **100**, 13298-13302 (2003).

3. N.Watanabe, L.Bodin, M.Pandey, M.Krause, S.Coughlin, V.A.Boussiotis, M.H.Ginsberg, and S.J.Shattil. Mechanisms and consequences of agonist-induced talin recruitment to platelet integrin $\alpha_{IIb}\beta_3$. *J.Cell Biol.* **181**, 1211-1222 (2008).

4. H.Rangaswami, N.Marathe, S.Zhuang, Y.Chen, J.C.Yeh, J.A.Frangos, G.R.Boss, and R.B.Pilz. Type II cGMP-dependent protein kinase mediates osteoblast mechanotransduction. *J.Biol.Chem.* **284**, 14796-14808 (2009).

5. K.B.Kaplan, K.B.Bibbins, J.R.Swedlow, M.Arnaud, D.O.Morgan, and H.E.Varmus. Association of the amino-terminal half of c-Src with focal adhesions alters their properties and is regulated by phosphorylation of tyrosine 527. *EMBO J.* **13**, 4745-4756 (1994).

6. T.Gudi, S.M.Lohmann, and R.B.Pilz. Regulation of gene expression by cGMP-dependent protein kinase requires nuclear translocation of the kinase: Identification of a nuclear localization signal. *Mol.Cell.Biol.* **17**, 5244-5254 (1997).

7. P.A.Lanzetta, L.J.Alvarez, P.S.Reinach, and O.A.Candia. An improved assay for nanomole amounts of inorganic phosphate. *Anal.Biochem.* **100**, 95-97 (1979).

8. S.F.Altschul, W.Gish, W.Miller, E.W.Myers, and D.J.Lipman. Basic local alignment search tool. *J.Mol.Biol.* **215**, 403-410 (1990).

Chapter 5:

Discussion

This dissertation has investigated the molecular mechanisms whereby cGMP-dependent protein kinases regulate cell survival and proliferation in osteoblasts and osteocytes. We found that PKGIα and PKGII are essential for estradiol-mediated cell survival and the PKGII is responsible for Src activation in response to fluid shear stress. Estrogens and load-bearing exercise have long been known to help support healthy bone function but the mechanisms by which they act were incompletely understood [1]. Here, we fill a gap in knowledge of osteoporosis prevention.

In the second chapter, we analyzed the role of PKGs in extragenomic estrogen signaling. cGMP was shown to mimic the estradiol-protective effects on osteocyte survival and the protection was abolished using NO/cGMP/PKG pathway inhibitors. This indicated a role for the pathway in estrogen signaling. We additionally identified PKGII and PKGIα as having differential effects on osteocyte survival; PKGII stimulated the Akt and ERK pro-survival pathways while PKGIα inhibited BAD through direct phosphorylation at Ser^{155}. Interestingly, PKGIβ was unable to phosphorylate BAD in intact cells, most likely due to lack of proper subcellular localization.

In future studies in our laboratory, this finding may be further investigated to identify one or more binding partners which allow for the association of PKGIα with BAD or prevent the interaction of PKGIβ with BAD. These interacting proteins may influence the subcellular localization allowing for PKGIα to be in the optimal placement for BAD phosphorylation. Alternately, PKGIβ may be sequestered away from active BAD or it may be otherwise inhibited by associated proteins. By purifying PKGIα and PKGIβ from intact cells and identifying unique interacting proteins with mass

spectrometry, we may determine novel binding partners of PKGIα versus PKGIβ. This will allow a better understanding of how PKGIα, and not PKGIβ, is able to regulate BAD phosphorylation.

Characterization of the bone phenotype in PKGI knockout mice would provide further evidence of the importance of PKGI in osteocyte cell survival. However, total PKGI knockout mice have a severely shortened life span due to intestinal dysfunction and their bone phenotype has not yet been characterized [2]. Therefore, generation of osteoblast-specific PKGI or PKGIα knockout mice would be crucial to examine bone characteristics. The PKGIα osteoblast-specific knockout would also determine if the observed differential effects of PKGIα and PKGIβ from cultured osteocytes translate into physiological significance.

In Chapter 4, we investigated the role of PKGII in mechanotransduction. We characterized a novel complex containing PKGII, Src, SHP-1, SHP-2, and $\alpha_v\beta_3$ integrins required to translate the mechanical energy of external fluid shear stress into internal biochemical signals. PKGII, through its indirect activation of Src via SHP-1, controlled downstream ERK activation and *fos* family gene expression.

In light of these findings, it would be of value to examine the bone characterization of PKGII-deficient mice. In preliminary studies, we show that PKGII-deficient primary osteoblasts isolated from calvariae are unable to activate Src or ERK in response to fluid shear stress or cGMP. Additionally, mRNA examined from the tibial diaphyses showed reduced levels of *c-fos* and *fra-2* mRNA, as compared to wildtype littermates. This indicates that PKGII is required for *c-fos* and *fra-2* expression in resting cells as well as fluid shear-stimulated cells. Further characterization of bone morphology,

including calcein labeling of calvariae to determine the rate of new bone formation and mRNA expression of other osteoblast specific genes, is currently being examined in the laboratory.

Furthermore, osteoblast-specific PKGII knockout mice will help evaluate the physiological role of PKGII in a mechanical loading model. Mechanical loading is imperative to retaining bone mass as evidenced by both weightlessness and bed rest [3-5]. Unloaded limbs lose bone mass due to a decrease in osteoblast bone formation and increased osteoclast resorption [3]. Hindlimb suspension studies could demonstrate the role of PKGII in osteoblast mechanotransduction.

Taken together, the results of this dissertation help understand the role of PKGs in estradiol- and fluid shear stress-mediated signaling pathways in osteocytes and osteoblasts. Further exploration of the roles of these proteins in skeletal biology will advance our knowledge of the genesis and progression of osteoporosis. Ultimately, research in this area may lead to improved therapeutics for the increasing number of individuals affected by these disorder.

REFERENCES

1.   **National Osteoporosis Foundation**

2.   Pfeifer A, Klatt P, Massberg S, Ny L, Sausbier M, Hirneiss C, Wang GX, Korth M, Aszodi A, Andersson KE, et al: **Defective smooth muscle regulation in cGMP kinase I-deficient mice.** *EMBO J* 1998, **17:**3045-3051.

3.   Aguirre JI, Plotkin LI, Stewart SA, Weinstein RS, Parfitt AM, Manolagas SC, Bellido T: **Osteocyte apoptosis is induced by weightlessness in mice and precedes osteoclast recruitment and bone loss.** *J Bone Miner Res* 2006, **21:**605-615.

4.   LeBlanc A, Schneider V, Shackelford L, West S, Oganov V, Bakulin A, Voronin L: **Bone mineral and lean tissue loss after long duration space flight.** *J Musculoskelet Neuronal Interact* 2000, **1:**157-160.

5.   Sievanen H: **Immobilization and bone structure in humans.** *Arch Biochem Biophys* 2010, **503:**146-152.